Gas-phase selective oxidation of C3-C4 hydrocarbon using only molecular oxygen

Zheng-Qian Xuan

Thesis submitted to Cardiff University for degree of Doctor of Philosophy

October 2009

ProQuest LLC
789 East Eisenhower Parkway
P.O. Box 1346
Ann Arbor, MI 48106-1346

Declaration

DECLARATION

This work has not previously been accepted in substance for any degree and is not concurrently submitted in candidature for any degree.

Signed ..... (candidate) Date 26/10/2009

STATEMENT 1

This thesis is being submitted in partial fulfillment of the requirements for the degree of PhD

Signed ..... (candidate) Date 26/10/2009

STATEMENT 2

This thesis is the result of my own independent work/investigation, except where otherwise stated. Other sources are acknowledged by explicit references.

Signed ..... (candidate) Date 26/10/2009

STATEMENT 3

I hereby give consent for my thesis, if accepted, to be available for photocopying and for inter-library loan, and for the title and summary to be made available to outside organizations.

Signed ..... (candidate) Date 26/10/2009

STATEMENT 4: PREVIOUSLY APPROVED BAR ON ACCESS

I hereby give consent for my thesis, if accepted, to be available for photocopying and for inter-library loans **after expiry of a bar on access previously approved by the Graduate Development Committee.**

Signed ..... (candidate) Date 26/10/2009

Acknowledgements

I would like to express my cordial gratitude to my supervisors, Professor Graham J. Hutchings, for his great encouragement and advice during my PhD career. It is my great honor that I could learn a lot from him, not only his broad knowledge and sharp scientific instinct on heterogeneous catalysis, but his kind and optimistic personality.

Particularly, I would like to thank Dr. Philip Landon and Dr. David Morgan for their valuable and warmhearted suggestions on my thesis and PhD research. I would like to thank Dr. Stuart Taylor and Dr. Albert Carley for their kind help and encouragement during my PhD career. I also wish to thank Dr. Nianxue Song for his initial work and help at the beginning of my PhD research. Additionally, I wish to thank Dr. Kieran Cole for his comments and helpful advice for the final revision of the thesis. Thanks all the member of Professor Hutchings' research group and the technical staff in the School of Chemistry.

I would like to thank the Committee of Vice-Chancellors and Principals of the Universities of United Kingdom for offering me with an ORS Award during my PhD career in Cardiff University. I would also like to thank Professor Hutchings and Dr. Taylor for the funding from the School of Chemistry and their help with my application for ORS Award. I would like to thank my parents for their financial support and warm encouragement.

Finally, I hope to express my earnest thank to my mother, Professor Fu-Zheng Xu, although she could not witness what I have achieved. I would like to say: "Mother, I believe that you would watch me attentively in the Paradise."

Abstract

The gas-phase epoxidation of propylene to propylene oxide (PO) has been investigated over a series of supported copper-based bimetallic (Cu-Ni, Cu-Ag and Cu-Au) or even trimetallic (Cu-Ag-Ni) alloy catalysts using only molecular oxygen as oxidant. Supported single metal (Cu, Ag and Au) catalysts have been tested for contrast. Zinc oxide and nano powder of silica have been applied as two main supports. It has been found that support has a significant effect on the catalytic performances of final catalysts.

For the single metal support on zinc oxide, Cu presents better selectivity than that of Ag or Au. Cu-Ag supported on zinc oxide pre-treated in 5% H_2/Ar has exhibited very high selectivity to PO (*ca.* 81%) propylene conversion (*ca.* 0.011%) at comparatively low temperature, 210°C. The observation of high selectivity to PO only at low temperature correlates to the intrinsic instability of PO. However, other alloys supported on zinc oxide did not show better selectivity than Cu-Ag. Particularly for Cu-Ni catalysts, the addition of nickel poisons the catalysts so that poor selectivity is obtained.

For the support of nano-SiO_2, the copper catalyst can offer both better selectivity (63%) and higher conversion (0.014%) than that supported on zinc oxide (selectivity to PO, *ca.* 60%, at propylene conversion, *ca.* 0.007%). A variety of alloy catalysts have shown very good reactivity and selectivity to PO. Typically, Cu-Ni pre-treated in 5% H_2/Ar can give high selectivity to PO, *ca.* 78%, as a propylene conversion, *ca.* 0.018%, at low temperature, 210°C. Cu-Ag catalysts have also shown stable performance with high selectivity to PO above 70% and propylene conversion of 0.020% at low temperature. On the other hand, gold plays the similar role in Cu-Au/nano-SiO_2 as nickel in Cu-Ni/ZnO catalyst. Cu-Au/nano-SiO_2 is even worse than copper only supported nano-SiO_2. The XPS analysis of Cu-Ag catalysts implies that Cu^0 should be active in propylene epoxidation to PO over catalysts not only on nano-SiO_2 but also zinc oxide. These results suggest that there is a great potential to develop copper-based materials as an inexpensive catalyst for propylene epoxidation.

The gas-phase selective oxidation of *n*-butane to maleic anhydride has also been studied and performed in a gas-gas periodic flow reactor under aerobic and anaerobic environments. Under anaerobic conditions, the catalytic performances of VPD and phase E are worse than that in aerobic conditions. Some vanadia supported on alumina have been loaded in both aerobic and anaerobic flow. The high loading (3.5%) vanadia supported on alumina is more reactive than the lower one (1%).

Table of Contents

Chapter 1: Introduction

Chapter 2: Exprimental Techniques

Chapter 4: Gas-phase selective epoxidation of propylene to propylene oxide over catalysts supported on zinc oxide

Chapter 6: Summary, Conclusion and Future work

Chapter 1.
Introduction

1.1 Catalysis history and definition

The term "catalysis" was first referred by Berzelius [1] in 1835 to describe reactions that are accelerated by substances that remain unchanged after the reaction. At the same time, Mitscherlich introduced the term "contact action" for a similar group of phenomena. Ideas of how a catalyst works have undergone continuous refinement by enormous industrial practice and the development of modern petroleum chemical refineries. An understanding of catalysis from both theoretical and practical viewpoint is significant to chemists and chemical engineers.

Later, Ostwald studied a series of reactions catalyzed by acids and bases and found that the chemical reaction took place at finite rates that could be used to determine the strengths of acids and bases. Owing to this pioneering work, he was awarded the Nobel Prize in Chemistry in 1909 [2]. In the theoretical field, Sabatier emphasized the chemical approach. Under the impact of Balandin's multiplet hypothesis [3], geometrical factors drew much attention in the following decades although it is obvious that most variations of catalytic activity cannot be explained by geometrical factors alone. In fact, both physical and chemical viewpoints could provide insight. It is desirable to relate catalytic activity to specific properties of the catalyst. Thereafter, an understanding of the reaction mechanism and catalytic behaviour could proceed predominantly through the chemical approach. The activity of a catalyst usually refers to the rate at which the reaction reaches to chemical equilibrium. It indicates the reactivity of catalytic systems. The selectivity, usually defined as the percentage of the consumed reactant that forms the desired product, is a measure of the extent to which it accelerates the reaction. The selectivity, often a function of degree of conversion, varies

with pressure, temperature, reactant composition and extent conversion as well as with the nature of the catalyst. Yield is an industrially engineering term which denotes the quantity of product formed per quantity of reactant consumed in the overall process. Additionally, stability indicates how long a catalyst is able to remain its activity.

Nowadays, catalysis, as an academically and commercially significant process, plays an essential role in the manufacture of a wide rage of products, from plastics to fertilizers and herbicides. A catalyst is a substance that accelerates the rate of chemical reaction without being consumed in the process. Catalysis is the acceleration of a chemical process by a catalyst, which can lower the activation energy of the reaction. A profile of the activation energies in an exothermic reaction has been shown in Figure 1.1.

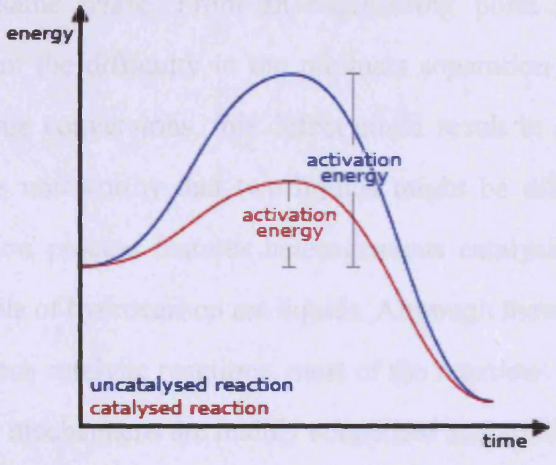

Figure 1.1. Potential energy profile for a catalyzed and uncatalyzed exothermic reaction.

A catalyst may lose its activity or selectivity for many reasons which mainly include poisoning, fouling, reduction of active sites, loss of active species. A catalyst poison is an impurity that lowers catalyst activity. The term "fouling" generally describes a physical blockage such as the deposition of dust or fine powder or carbonaceous deposits (coke). The coke can be removed by burning to reactivate the catalyst. Sintering, as an irreversible physical process, is one of the main reasons leading to the reduction of active sites. A supported metal catalyst could be reduced in activity or selectivity by amalgamating with a metallic impurity or the support.

1.2 Type of catalysis

Catalytic systems can be divided into two distinct types based on the physical state where the reaction takes place. They are named homogeneous and heterogeneous catalysis, respectively. Additionally, biocatalysis is a significant category in the biological field. There are large differences in the above-mentioned characteristic features (e.g. activity, selectivity or stability) with different catalytic systems.

1.2.1 Homogeneous catalysis

Homogeneous catalysis denotes that a reaction occurs with catalysts and the reactants being present in the same phase. From an engineering point of view, a major disadvantage arises from the difficulty in the products separation from the catalyst. Particularly in large-scale conversions, this defect could result in many problems in commercialization. It is noteworthy that two liquids might be different phases. For example, some alkylation process features heterogeneous catalysis despite both the acid catalyst and reactants of hydrocarbon are liquids. Although there are some gaseous examples of homogeneous catalytic reactions, most of the reactions occur in the liquid phase, during which the mechanisms are mainly concerned and studied by chemists. In homogeneous catalytic reactions, the active species are often formed in the reaction mixture through a number of pre-catalytic reactions with an induction period being required before conversions. In some cases such as transition metal complex reactions, homogenous catalysis could offer enhanced selectivity compared with heterogeneous catalytic reactions. However, the separation of products and reactants often involving distillation is the unavoidable issue to be solved as some catalysts are destroyed at high temperature and can hardly be recovered.

1.2.2 Heterogeneous catalysis

Opposite to homogeneous catalysis, heterogeneous catalytic reactions take place on the surface of the catalyst where it is in a different phase to the reactants. There is no difficulty in separating the catalyst between reactants and products for recycling. In fact, the majority of large-scale processes in chemical and refinery industries are based on heterogeneous catalytic reactions.

Most of heterogeneous catalytic reactions can be described according to the following processes:

(i) Diffusion of the reactants to the active site of the catalyst surface
(ii) Adsorption of the reactants on the surface
(iii) Reaction on the surface
(iv) Desorption of products from the surface
(v) Diffusion of products away from the active site of the surface

The first two steps can be understood in terms of the chaotic kinetic motion of molecules. Adsorption and surface reactions are processes in series. A detailed understanding of surface reactions needs information about the active sites on the catalyst and the structure of the surface complexes during conversion of reactants to products. It is not an easy job to identify the active sites because of their low concentration on the surface area. In the case of solid catalysts, the selectivity is often analyzed in terms of electronic and geometric factors. In considering surface interactions between the catalyst and reactants on a molecular level, Sachtler [4] summarized four main factors, such as bond strength and coordination which have to be fulfilled in order for catalysis among a number of thermodynamically feasible reactions. When applied in practical reactions, catalysts must usually be activated to display the desired activity and selectivity or even be deactivated after reaction. The activity and

selectivity depends not only on the activation procedure but also the whole preparation process. It is rather difficult to obtain some catalysts with the same activity and selectivity for different preparations. Thus, to develop highly active and selective catalysts with great stability, has been a challenge faced by chemists and chemical engineers.

1.2.3 Biocatalysis

Biocatalysis usually referred to as reactions performed using protein, enzyme or some natural organic compounds as catalysts. Enzymes are a type of protein. Enzymatic catalysis is an important area in this field. The most striking feature of these biocatalysts is their exceptional selectivity and activity, which can be understood from protein structure [5]. The primary structure of a protein is made up of covalent peptide bonds. Furthermore, non-covalent interactions such as electrostatic and van der Waals attractions, π-electron stacking and hydrogen bonding are also involved to determine the spatial structure of a protein. Enzyme catalysts are not classified with respect to their chemical nature but catalytic behaviour. There are many applications in food industry, pharmaceutics and the disposal of industrial and urban waste, which have great prospects in green chemistry.

1.3 Heterogeneous selective oxidation of hydrocarbon

Heterogeneous catalytic oxidation, as one of the most important oxidation processes, is usually divided into selective and total oxidations. The latter products normally carbon dioxide and water in the case of hydrocarbon are the most thermodynamically stable. The oxidation of ethylene using a silver catalyst [6] and the oxidation of carbon monoxide using a copper oxide catalyst [7] are two typical examples of selective and total oxidations, respectively. All selective oxidations have to compete with the more exothermic and thermodynamically favored total oxidation reactions. To favor the

formation of the selective oxidation over total oxidation has been the major challenge in catalyst design of organic chemicals productions.

The catalytic synthesis of oxygenated derivatives from hydrocarbon offers a convenient method of controlling hydrocarbon oxidation. Margolis [8,9] discussed catalytic oxidations of hydrocarbon where one of the features is the possibility involving the interaction of surface radicals with oxygen in these reactions. Shooter [10] also attempted to correlate certain properties of the catalysts with their performance in reactions by qualitative classification of oxide catalysts. Later, the catalytic oxidation of lower olefins have been reviewed by Voge and Adams [11] as well as Sachtler [12].

Some heterogeneous selective oxidation processes of hydrocarbons have been summarized in Table 1.1.

Table 1.1. Major heterogeneous selective oxidation processes of hydrocarbon [13].

Reactants	Products	Conversion, %	Selectivity, %
Ethene	Ethene oxide	90	80
Propylene	Acrolein	>90	80-85
n-Butane	Maleic anhydride	70-80	65-70
Isobutene	Methacrolein	>97	85-90
Benzene	Maleic anhydride	98	75
o-Xylene	Phthalic anhydride	100	79
Naphthalene	Phthalic anhydride	100	84

A large part of hydrocarbons, functionalized by selective oxidation, serve as the feedstocks for plastic and polymer production. Selective oxidation has been one of the most significant processes in modern chemical industry, which is also the main goal of the work in this thesis. The products such as alcohols, aldehydes, ketones, epoxides and acids are usually applied to manufacture plastics, dyes, detergents and food

additives. Thus, to study and produce high effective catalysts for selective oxidation has been a great challenge in chemical engineering, food industry, medical science and pharmaceutics.

1.3.1 Selective oxidation of alkanes

The direct utilization of natural gas, consisting mainly of C_1–C_4 alkanes, has received extensive attention due to the increasing shortage of crude oil [14]. The catalytic conversion of light alkane feedstock is one of the promising routes to prepare valuable chemical products [15-18].

Methane, as one of the simplest hydrocarbons, can be used to produce a lot of compounds with high added value since it is the main component of natural gas. The selective oxidation of methane for producing valuable C_1-oxygenates, such as methanol [19] and formaldehyde [20-24], has been a potentially important process. The challenge faced by chemists is particularly difficult because of the low reactivity of the starting alkane molecule. The conversion of methane into higher hydrocarbons such as ethane and ethylene is also of commercial importance [25]. The direct conversion of methane to aromatic products (benzene, naphthalene) has been also investigated in the past few years [26-31]. These processes can contribute to find other sources of hydrocarbons and preserve crude oil stocks, providing cleaner processes that lead to better environmental preservation.

Selective oxidation of ethane to ethylene and acetic acid was reported by Thorsteinson et al [32]. Compared with the processes of naphtha oxidation and methanol carbonylation (currently used to obtain acetic acid), the direct selective oxidation of ethane is attractive because of the easier separation of products and the cheapness of ethane. Recently, some studies of the ethane conversion to acetaldehyde or even acrolein have been reported as well [33-40]. In the case of propane oxidation, a series of

products such as propylene, acrylic acid, acetone, 2-propanol or acrolein can be obtained when using different catalysts [41-50].

Among C_4 alkanes, selective oxidation of *n*-butane to maleic anhydride is one of the most significant reactions, which is the only commercial oxidation process involving light alkane. Maleic anhydride serves as a very important source material towards the polymer industry, the main use of which is the production of unsaturated polyesters [51]. There are also widely industrial applications in lubricant additive, corrosion inhibitor, detergents and herbicides production. Although maleic anhydride was previously manufactured by the oxidation of benzene, *n*-butane has currently been used as the primary feedstock because of its lower price [52, 53]. The original plant designed for the selective oxidation of *n*-butane to maleic anhydride involved in the use of multitubular fixed bed reactors, which still dominate the production of maleic anhydride [54]. Vanadium–phosphorus oxide species have been one of the most important catalysts for selective oxidation of *n*-butane [55-70]. Some further introduction will be detailed later and in Chapter 3.

1.3.2 Selective oxidation of alkenes

Ethylene, as a very important industrial material, can be partially oxidized to ethylene oxide, acetaldehyde and acetic acid, while treated with different catalysts in a variety of conditions. Epoxides such as ethylene oxide are very valuable industrial organic intermediates and their uses include the manufacture of solvents, plasticizers, explosives, epoxide homopolymers and polyesters [71]. It has long been known that ethylene oxide can be obtained by ethylene oxidation over silver catalysts [72]. Most commercial catalysts consist of silver (up to 35%) usually supported on carriers of low surface area such as silica, aluminosilicates or silicon carbide. The oxidation of ethylene over silver gives ethylene oxide, carbon oxides and water. There is also evidence that formaldehyde is formed in some cases [73]. The most widely accepted

mechanism for ethylene oxidation over silver was owing to Twigg [74, 75]. It was concluded that ethylene oxide and carbon dioxide were formed by a parallel-consecutive mechanism with short contact times between 200 and 350°C in a flow system. In 1962, Kemball and Patterson reported that ethylene could be oxidized to acetic anhydride and acetic acid over evaporated palladium films [76], during which these products accounted for only 3% of the total products. Cant and Hall extended their investigation to the metals such as Pt, Pd, Ir, Ru and Rh supported on high surface area silica [77]. Other studies of noble metal catalysts have been made by Moss and Thomas [78, 79] who studied mainly catalysts of palladium-silver alloy films. Other supports such as active carbon and alumina were also investigated [80, 81]. However, selective oxidation of ethylene to ethylene oxide still attracts the most attention due to its industrial importance.

Similarly to the case of ethylene, selective oxidation of propylene is a significant industrial process. The products include propylene oxide, acrolein, acrylic acid, acrylonitrile. Like ethylene oxide, propylene oxide is an important industrial intermediate and its manufacture by the direct oxidation of propylene is highly desirable. To find better catalysts for direct epoxidation of propylene is one of the aims in this work. Silver, the catalyst so effective for ethylene epoxidation, was not active and selective to propylene oxide any more [82]. It was thought [83] that the low yields of propylene oxide on silver catalysts, are owing to isomerization and decomposition. The use of other supported metals such as rhodium and ruthenium has also been investigated but numerous products obtained [77, 84]. Later, the most satisfactory process for propylene epoxidation was developed by Halcon International Inc. Based on Halcon's original discovery, hydroperoxides such as ethylbenzene hydroperoxide can be made to react with olefins in the liquid phase to produce both epoxides and alcohols at high yields in the presence of selected catalysts. Further investigations related to direct epoxidation of propylene will be reviewed in Chapter 4.

Hearne and Adams also discovered that propylene could be selectively oxidized to acrolein over cuprous oxide [85]. It was the milestone that aldehydes can be obtained by catalytic oxidation of olefin over metal oxide catalysts. Evidences suggested this process proceeds via π-bonded allyl surface intermediate [86-88]. Other studies have aimed to identify the active phase in selective copper oxide catalysts [89, 90] and to develop a variety of catalysts [91-113]. Additionally, propylene could undergo a very different type of oxidation to give acetone and acetic acid under certain conditions [97, 114]. However, the oxidation to acetone only occurred at low temperatures (100-300°C).

1.4 Selective oxidation of *n*-butane to maleic anhydride

In the activation of light alkanes by high-temperature contact with a redox catalyst, the selective oxidation of *n*-butane to maleic anhydride (MA) by VPO catalysts is the most successful example which has been replacing in part the commercial synthesis from benzene. Maleic anhydride is widely used as a chemical intermediate in the synthesis of fumaric and tartaric acids, certain agricultural chemicals, resins in numerous products, dye intermediates and pharmaceuticals [115]. It is mainly used in the production of unsaturated polyesters and butanediols. The world consumption exceeds 1.3 million metric tons per year [116]. Approximately 70% MA has been manufactured by *n*-butane oxidation as the route from benzene is environmentally unfriendly and more expensive than the cost of *n*-butane. There are several reactor technologies available, including fixed-bed (Scientific Design, Huntsman, BASF, Pantochim), fluidised-bed (Lonza, BP, Mitsubishi), and transported-bed (DuPont). Best process performances reported in patent literature range from 53 to 65% molar yield to MA [117–122], with a conversion of the hydrocarbon not higher than 85–86%. An excellent result of more than 70% yield is reported [123], which refers to a recycle process. In laboratory reactors best yields reported are lower than 50%.

The n-butane selective oxidation process involves in the cleavage of eight C-H bonds and the introduction of three oxygen atoms, which is a fourteen electron oxidation in comparison to other selective oxidation processes. Although many V^{5+} vanadyl orthophosphates and V^{4+} vanadyl hydrogen phosphates, vanadyl pyrophosphate and vanadyl metaphosphate were studied, $VOHPO_4 \cdot 1/2H_2O$ (vanadyl hydrogen phosphate hemihydrate) has been attracting more attention as a catalyst precursor, which gives a final catalyst mainly composed of $(VO)_2P_2O_7$ (vanadyl pyrophosphate, VPP) after activation.

The best performance for a fixed-bed reactor does not exceed 65% per-pass yield, while that in a fluidised-bed is typically somewhat lower; in fact, back-mixing phenomena are responsible for the consecutive combustion of MA [124]. The yield of MA is usually affected by following factors:

(a) The presence of competitive reactions of n-butane combustion and of oxidative degradation to acetic and acrylic acids. These are characterized by higher activation energies with respect to the main reaction.

(b) The presence of consecutive reactions of combustion decreases the selectivity to MA as the alkane conversion is increased. However, while up to 60–70% n-butane conversion the extent of the consecutive combustion, although present, is not considerable, the decrease in selectivity becomes dramatic over 70–80% conversion. This problem has been attributed to the development of local catalyst overheating, owing to the high reaction exothermicity, and to the poor heat-transfer properties of the catalytic material, which is obviously more significant in fixed-bed than in other reactor configurations characterized by better heat-transfer properties.

Based on above-mentioned problems, some proposed options are as following:

(a) Novel procedures for preparation of catalysts need be developed to allow the modification of morphological features of either precursors or final catalysts.

(b) Highly heat-conductive supports could be applied for better attribution of reaction heat.

(c) Operation at low n-butane conversion using pure oxygen or oxygen enriched air, together with recycling of unconverted hydrocarbon can improve the efficiency of oxygen and the selectivity to MA. However, it is possible that the low productivity be obtained.

The structure of VPO species catalysts depends upon a lot of factors such as P/V stioichiometry, thermal treatment, activation temperature and gas phase composition. Generally, $(VO)_2P_2O_7$ (vanadyl pyrophosphate, VPP) has been accepted to play a key role in the selective oxidation of *n*-butane to maleic anhydride and most of hypotheses are based on the (100) face. The catalytic behavior of the different crystal faces was studied by Inumaru [117] by exposing individual planes. Transient studies [118] showed that the active surface of equilibrated catalysts different depending upon the reaction conditions and the P/V ratio of the catalysts. There is a debate as to whether VPP is the only active phase or other phases are responsible for the reaction as well. Ballarini [118] argued that $VO(H_2PO_4)_2$ could be the main component of the active phases at T>380°C.

Due to the amount of V^{5+}, the final oxidation state usually varies between +4.00 and +4.40. Guliants [120] prepared a series of vanadium phosphate catalysts containing different phases and showed VOPO4 phases to be detrimental to the performance of the catalyst, which was also confirmed by Cavani and Trifiro [121] who suggested that V^{5+} sites are responsible for the over-oxidation of maleic anhydride to carbon oxides. Many groups involves in the discussion of this one-phase hypothesis. They agree that V^{5+} phases are significant in the active catalyst and a redox mechanism is suggested [122, 125, 126]. V^{4+} attributes a very active catalyst poor selectivity, while V^{5+} offers a very selective catalyst low activity. This mechanism has been supported by the X-ray Photoelectron Spectroscopy (XPS) [127] and Temporal Analysis of Products studies [128-130]. No maleic anhydride but furan as the main product was formed in the absence of V^{5+} sites.

The P/V ratio is proposed to be a key factor in determining the activity and selectivity of the catalyst as well [131, 132]. Garbassi [133] observed that a P/V ratio of 1.05-1.1 is necessary for a high catalytic performance. Satsuma [134] proposed that a number of vanadium sites at P/V ratio less than 1.0 remain inactive but at higher P/V ratios all surface sites are active. However, the study by Coulston [127] has shown contradictory findings. Based upon this conclusion, the claim that phosphorous enrichment reported by other groups was due to incorrect calibration of XPS instrumentation.

The selective oxidation of *n*-butane to maleic anhydride involves in the abstraction of eight hydrogen atoms and the insertion of three oxygen atoms. Although several mechanisms were proposed, no intermediates have been observed under standard continuous flow conditions. A consecutive alkenyl mechanism has been widely supported in literatures [135-143]. Once butane is adsorbed onto the surface of the VPO species, it will be transformed via adsorbed alkenyl intermediates to maleic anhydride. Zhang-Lin [144, 145] suggested a consecutive mechanism based on kinetic calculation for the oxidation of butane, 1-butene, 1,3-butadiene and furan over $(VO)_2P_2O_7$ and $VOPO_4$ phases. The studies have shown that furan is not as the intermediate in butane oxidation as in butadiene oxidation. Ziolkowski [146, 147] also proposed a concerted mechanism based on theoretical calculation on the (100) plane of $(VO)_2P_2O_7$. According to this mechanism, the butane is adsorbed onto the active site by hydrogen bonds. Redox couple mechanism is another route shown by Centi [148]. Based on experimental data at high butane concentration and total oxygen conversions, the reaction proceeds a series of redox couples which will be clarified in Chapter 3.

Although there is a great deal of debate concerned with vanadium phosphate catalysts, Hodnett [149] summarized some generally accepted statements as following:

(a) The most active and selective catalysts mainly consists of $(VO)_2P_2O_7$

(b) The oxidation state of the catalyst is close to +4 in *n*-butane lean conditions

(c) The rate determing step is butane activation by hydrogen abstraction

(d) Only the surface layers are involved in catalysis directly and the surface has some phosphorous enrichment.

1.5 Catalytic selective epoxidation

The epoxidation of olefins has been playing a more important role in the industrial manufacture than before. In the last decade, great advances have been made in this field as many novel catalysts, reactions and processes are discovered and developed. Ethylene oxide and propylene oxide are the major chemicals in the field of catalytic epoxidation.

Ethylene oxide (EO) as an important chemical is mainly applied for production of ethylene glycol and surface active agents. Several dozen of chemical intermediates and industrial fine petroleum derive from EO, which is widely used in applications of oil manufacture and refining, pharmaceuticals, pesticides, dyeing, electronics and textiles. EO is primarily produced by the direct oxidation of ethylene using air or oxygen in a packed-bed, multi-tubular reactor with recycle. Catalysts for EO manufacture are usually composed of silver (10-20 wt%) supported on a low surface area with alkali metal promoters particularly Cs and fluoride or many other promoters. Typical reaction conditions are 10-35 atm, 230-280 °C with gas hourly space velocity (GHSV) 1,500-10,000 h^{-1}, and contact time 0.1-5s.

Propylene oxide is even more valuable product than ethylene oxide, which is the significant chemical intermediate whose manufacture accounts for about 10% of total consumption of propylene in Europe. Two thirds of that is used for the production of polyether polyols, whereas the rest being converted to propylene glycols, glycol ethers and other materials. But there are more and tougher problems to be solved in the heterogeneous epoxidation of propylene. For example, Ag catalysts only deliver

very low selectivity over a wide range of conditions and catalyst formulations [150, 151]. As a result, the old chlorohydrin process [152] and Halcon method are still the dominant commercial processes for manufacture of propylene epoxide. However, the former is environmentally unfriendly because of the use of chlorine while the latter [153] usually involves co-production of propene epoxide and styrene. It has been proposed, and seems to be generally agreed, [150, 151, 154–157] that the difficulty with propene epoxidation resides in the ease with which an allylic hydrogen atom may be stripped from the molecule, a process that presumably shuts off the epoxidation channel and results in combustion.

The source of oxygen is a significant aspect in the epoxidation of olefins. Obviously, the most desirable oxidant is molecular oxygen, which is an economical and plentiful resource in nature. However, except for silver, other catalysts also employed activated forms of oxygen, which involve the use of sacrificial reductant for their production. Therefore, hydrogen peroxide has emerged as the most attractive oxidant and intermediate at laboratory and commercial scale for epoxidation.

1.5.1 Catalysis by gold

Traditionally, it was long been thought that gold was regarded as noble and catalytically unreactive. However, in the same group of the periodic table as gold, both copper and silver are applied in lots of large scale processes. Therefore, it is not surprising that the same chemistry is observed on gold. With the development of nano-chemistry, it has been found that nanocrystalline gold supported on some metal oxides to be most reactive in many reactions [158-162]. Haruta [158] discovered the high activity of gold for CO oxidation at sub ambient temperature. In early studies, Bond and co-workers [163] demonstrated that very small gold particles supported on silica could offer interesting catalytic performance for hydrogenation, but until recently the use of gold as selective hydrogenation catalyst has received little attention while most

of effort and interest have been focused on selective catalytic oxidation over supported gold [164].

In the 1980s, the general perception was changed by two significant observations as follows, which highlighted the particular attributes of gold as a heterogeneous catalyst.

1) Supported gold catalyst was discovered very reactive for low temperature CO oxidation [158].

2) Hutchings [165] predicted that gold would be the best catalyst for acetylene hydrochlorination.

The selective epoxidation of propylene represents another type of reaction catalyzed by gold. Owing to the facile abstraction of labile allylic H atoms resulting in combustion rather than selective oxidation, the heterogeneous epoxidation of alkenes other than ethylene is very difficult. Subsequently, the commercial manufacture of propylene oxide (PO) usually proceeds by one of two homogeneous processes. However, the heterogeneous catalytic process using molecular oxygen still received extensive attention by many chemists.

In 1998, Haruta reported that gold supported on TiO_2 can give propene epoxide with a selectivity up to 100% in the presence of a mixture of hydrogen and oxygen under very mild conditions (323K-373K and atmospheric pressure), although at very low reactant conversion *ca.* 1.1% [166]. This finding uncovers that nano-sized gold particles are very sensitive to the selective epoxidation of propylene to PO. Haruta suggested that spherical nano-sized gold particles loaded onto TiO_2 required higher temperatures to promote the epoxidation of propene, resulting in complete combustion to produce only CO_2 and H_2O, the yield of H_2O is higher than that of CO_2 [167]. On the other hand, hemispherical Au particles, strongly attached to the TiO_2 support, generate PO with almost 100% selectivity at a lower temperature, 323K. The consumption of H_2 is about three times that of propylene conversion and appreciably less than that over spherical

supported Au particles catalysts. These findings imply that the reaction occurs at the perimeter interfaces around the gold nano-particles. Consequently, Liu and Haruta have confirmed the hypothesis [167].

Additionally, selection of the support, catalyst preparation and the control of gold nano-particle size are three key factors for propylene epoxidation for non-promoted gold catalyst [166, 168]. Haruta also proved that highly dispersed gold nanoparticles supported on 3D mesoporous, silylated titanosilicates with large pores in the presence of a promoter, $Ba(NO_3)_2$, are effective for the epoxidation of propene to PO with molecular O_2 and H_2. Conversions of up to 10% with 93% PO selectivity have been achieved, however the H_2 efficiency is still low, typically 30% [169]. Although the operation mode of supported gold catalysts in propylene epoxidatoin is unclear, the fact that both hydrogen and oxygen are necessary in epoxidation conjectures that some peroxide species could be a key reaction intermediate for the reaction. However, no evidence has suggested the peroxide mechanism feasible during propylene epoxidation. Nijhuis disclosed the role of supported gold nano-particles in the epoxidation of propylene, which takes place on the titania sites [170]. In the proposed reaction mechanism, the bidentate propoxy species adsorbed on titania are obtained. The peroxide species produced by hydrogen and oxygen on gold help to desorb the bidentate propoxy species from the catalyst, generating propylene oxide and water and recovering the titania back to its original state.

For Au/TiO_2 catalysts, water production and propylene epoxidation have a strong influence on each other. Nijhuis also concluded that water plays a significant role [171], which is similar to the observation that moisture enhances the catalytic activities of CO oxidation using supported gold catalysts [172]. Water addition to the feed gas stream was preferred as it prevented the catalyst deactivation by lowering the concentration of propylene oxide adsorbed on the titania through competitive adsorption [171].

1.5.2 Catalysis by silver

Traditionally, silver has been most widely and maturely [173] used as a catalyst in the selective epoxidation of ethylene to ethylene oxide using molecular oxygen, which shows an environmentally benign application [174]. Ethylene oxide is an important source material for manufacture of ethylene glycol.

Two main mechanisms have been proposed for the selective epoxidation to ethylene oxide over silver catalysts, which involve in the adsorption of atomic oxygen and molecular oxygen, respectively. Based on early viewpoint [12], adsorbed molecular oxygens rather than adsorbed oxygen atoms (O_{ads}) are responsible for epoxidation as the latter prefer combustion. Another hypothesis [175] was that either epoxidation or combustion is owing to adsorbed oxygen atoms (O_{ads}) which undergo either Eley-Rideal or Langmuir-Hinshelwood reactions, separatively. Campbell and Koel [176] implied that dioxygen was actually the selective oxidant; whereas Grant and Lambert [177] claimed that O_{ads} reacted with adsorbed ethene to generate both the epoxide and combustion products. However, most of researchers now agree that selective oxidation is due to oxygen adatoms (O_{ads}).

For the atomic mechanism, atomic oxygen is active in both epoxidation and combustion, molecular oxygen plays no role. On one hand, epoxidation takes place when an oxygen atom reacts with the double bond of one adsorbed ethylene molecule; on the other hand, combustion occurs when another oxygen atom abstracts the hydrogen atom of one adsorbed ethylene molecule. Based on this mechanism, it would be favourable to utilize inhibitors or promoters to activate the atomic oxygen towards epoxidation rather than combustion.

The molecular mechanism states that molecular oxygen is active in epoxidation, while atomic oxygen is reactive in combustion. According to the mechanism, it would

desirable to use inhibitors to prevent the adsorption of atomic oxygen.

Industrial processes usually improve selectivity to ethylene oxide by using inhibitor and promoters [178]. The silver catalyst is widely used, promoted by alkali metals, which is further altered by the addition of small amounts of chlorinated hydrocarbons to the reaction feed. Chlorine is normally used being adsorbed onto the silver as an inhibitor, and alkali metals are dispersed in the bulk of silver as promoters. The appropriate amount of inhibitors could improve the selectivity by modifying the electron properties of the adsorbed oxygen atom in epoxidation. However, the chlorine amount has to be controlled since over-coverage of chlorine can deactivate the catalyst. In fact, the presence of chlorine on the silver surface affects the coverage by different oxygen species differently [179]. Generally speaking, adsorbed chlorine increases the amount of oxygen that participates in the epoxidation reaction although it decreases the gross amount of adsorbed oxygen. Electrophilic oxygen prefers to attack the C=C double bond in ethylene whereas the electon-withdrawing species, such as adsorbed chlorine, plays a role of decreasing the electron density of the oxygen atom. Currently, most researchers prefer the atomic oxygen mechanism to molecular oxygen mechanism as the former is more persuasive. The primary defect of silver catalyst is that there are no applicable methods of generation although the initial selectivity ranges 79-85%.

1.5.3 Catalysis by copper

Copper is traditionally applied in methanol synthesis and the water gas shift reaction, which is also well known to be reactive for steam reforming of methanol [180, 181]. The catalysts are usually prepared by co-precipitation of Cu, Zn and Al as hydroxides or carbonates, which are decomposed to mixed oxides (e.g. $Cu/ZnO/Al_2O_3$) by pre-treating in air or H_2.

Methanol steam reforming (MSR) is an alternative path of hydrogen production, which is considered as a component of a hydrogen fuel cell-powered vehicle. The main advantage of a vehicle with a reformer is that it does not need a pressurized gas tank to store hydrogen fuel; instead methanol is stored as a liquid. Only low concentration of carbon monoxide is generated via the MSR process in the absence of other harmful gases.

$$CH_3OH + H_2O \rightarrow CO_2 + 3H_2$$

Copper alloy catalysts, such as Cu-Ni, Cu-Pd, Cu-Ir and Cu-Pt, are also widely used in selective hydrogenation of oils and a series of hydrocarbons [180]. Recently, it has been discovered that copper could be considered as a potential catalyst for alkene epoxidation. Lambert [182, 183] has elucidated that copper may be more effective and selective than silver, especially in propylene epoxidation. Theoretical and experimental researches have also proved that Cu-Ag bimetallic catalysts can improve selectivity to ethylene oxide in the epoxidation of ethylene using oxygen [184, 185]. There could be a great prospect to develop catalysts of Cu, Ag and their alloys in the direct epoxidation using molecular oxygen.

1.6 Aims of the thesis

This work in the thesis is a part of the ATHENA project, which is an EPSRC/Johnson Matthey sponsored project involving University Departments at Birmingham, Cambridge, Cardiff, Glasgow and Surrey in the UK together with Fritz-Haber-Institute in Germany and Northwester University in the USA. Cardiff is the central organization for selective oxidation section. This work aims to find and develop novel catalysts for the selective oxidation of hydrocarbons.

In the C-4 section in ATHENA project, the selective oxidation of *n*-butane, 1-butene

or iso-butene has been included to explore novel and inexpensive catalysts. In the selective oxidation of *n*-butane, a gas-gas periodic flow reactor has been introduced to study the catalytic performances between rosette and platelet structures under both aerobic and anaerobic environments.

Propylene epoxidation to propylene oxide is an important part in the C-3 section of this project. The aim is to compare the catalytic performances of different supported noble metals and alloys and to find more selective and active catalysts. The initial work also includes to compare different supports in common usage.

1.7 References

[1] Laidler, K.J., Meiser, J.H., *Physical Chemistry*, Benjamin/Cummings **1982**, p.423

[2] Roberts, M. W., *Catal. Lett.* **2000**, *67(1)*, 1.

[3] Balandin, A. A., *Adv. Catal.* **1969**, *19*, 1.

[4] Sachtler, W. M. H., *Faraday Disc. Chem. Soc.* **1981**, *72*, 8.

[5] Hammes, G. G., *Enzyme Catalysis and Regulation*, Academic Press, New York, **1982**.

[6] Twigg, G. H., *Proc. R. Soc.* **1946**, *A88*, 92.

[7] Stone, F. S., *Adv. Catal.* **1962**, *13*, 1.

[8] Margolis, L. Y., *Adv. Catal.* **1963**, *14*, 429.

[9] Margolis, L. Y., *Usp. Khim.* **1959**, *28*, 615.

[10] Sampson, R. J., Shooter, D., *Oxid. Combust. Rev.* **1965**, *1*, 225.

[11] Voge, H. H., Adams, C. R., *Adv. Catal.* **1967**, *17*, 151.

[12] Sachtler, W. M., *Catal. Rev.* **1970**, *4*, 27.

[13] Cavani, F., Trifirò, F., *Appl. Catal.* **1992**, *A88*, 115.

[14] Lunsford, J. H., *Catal. Today* **2000**, *63*, 165.

[15] Mamedov, E. A., Corberán, V. C., *Appl. Catal. A: Gen.* **1995**, *127*, 1.

[16] Weckhuysen, B. M., Schoonheydt, R. A., *Catal. Today* **1999**, *51*, 223.

[17] Bettahar, M. M., Costentin, G., Savary, L., Lavalley, J. C., *Appl. Catal. A: Gen.* **1996**, *145*, 1.

[18] Jia, M.J., Valenzuela, R.X., Amorós, P., Beltrán-Porter, D., El-Haskouri, J., Marcos, M.D., Corberán, V. C., *Catal. Today* **2004**, *91*, 43.

[19] Tabata, K., Teng, Y., Takemoto, T., *Catal. Rev.* **2002**, *44(1)*, 1.

[20] Herman, R. G., Sun, Q., Shi, C., Klier, K., Wang, C.-B., Hu, H., Wachs, I. E., Bashin, M. M., *Catal. Today* **1997**, *37*, 1.

[21] Spencer, N. D., Pareira, C. J., *J. Catal.* **1989**, *116*, 399.

[22] Fornes, V., Lopez, C., Lopez, H. H., Martinez, A., *Appl. Catal. A: Gen.* **2003**, *249*, 345.

[23] Ruddy, D. A., Ohler, N. L., Bell, A. T., Tilley, T. D., *J. Catal.* **2006**, *238*, 277.

[24] Berndt, H., Martin, A., Brückner, A., Schreier, E., Müller, D., Kosslick, H., Wolf, G.-U., Lücke, B., *J. Catal.* **2000**, *191*, 384.

[25] Lapeña-Rey, N., Middleton, P. H., *Appl. Catal.* **2002**, *A240*, 207.

[26] Wang, L., Tao, L., Xie, M., Xu, G., Huang, J., Xu, Y., *Catal. Lett.* **1993**, *21*, 35.

[27] Weckhuysen, B. M., Wang, D., Rosynek, M. P., Lunsford, J. H., *J. Catal.* **1998**, *175*, 347.

[28] Shu, Y., Xu, Y., Wong, S. T., Wang, L., Guo, X., *J. Catal.* **1997**, *170*, 11.

[29] Borry, R. W., Lu, E. C., Kim, Y., Iglesia, E., *Stud Surf* Sci. *Catal,* **1998**, *119*, 403.

[30] Xiong, Z. T., Chen, L. L., Zhang, H. B., Zeng, J. L., Lin, G. D., *Catal Lett.* **2001**, *74*, 227.

[31] Shu, Y., Ohnishi, R., Ichikawa, M., *Appl. Catal. A* **2003**, *252*, 315.

[32] Thorsteinson, E. M., Wilson, T. P., Young, F. G., Kasai, P. H., *J. Catal.* **1978**, *52*, 116.

[33] Teng, Y., Kobayashi, T., *Chem. Lett.* **1998**, *4*, 327.

[34] Teng, Y., Kobayashi, T., *Catal. Lett.* **1998**, *55*, 33.

[35] Nakagawa, K., Teng, Y., Zhao, Z., Yamada, Y., Ueda, A., Suzuki, T., Kobayashi, T., *Catal. Lett.* **1999**, *63*, 79.

[36] Zhao, Z., Yamada, Y., Ueda, A., Sakurai, H., Kobayashi, T., *Appl. Catal. A* **2000**,

196, 37.

[37] Zhao, Z., Yamada, Y., Ueda, A., Kobayashi, T., *Shokubai (Catal. Catal.)* **1999**, *41*, 435.

[38] Zhao, Z., Yamada, Y., Teng, Y., Ueda, A., Nakagawa, K., Kobayashi, T., *J. Catal.* **2000**, *190*, 215.

[39] Zhao, Z., Kobayashi, T., *Appl. Catal. A* **2001**, *207*, 139.

[40] Kobayashi, T., *Catal. Today* **2001**, *71*, 69.

[41] Bravo-Suárez, J. J., Bando, K. K., Lu, J. Q., Fujitani, T., Oyama, S. T., *J. Catal.* **2008**, *255*, 114.

[42] Vitry, D., Dubois, J. L., Ueda, W., *J. Mol. Catal. A: Chem.* **2004**, *220*, 67.

[43] Mizuno, N., Tateishi, M., Iwamoto, M., *Appl Cata A: Gen*, **1995**, *128(2-3)*, L165.

[44] Wang, Z. X., Wu, W., Liu, G. S., Mao, G. L., Kuang, D. T., *Shiyou Xuebao(Acta Petrol Sin)*, **1998**, *14(3)*, 21.

[45] Ueda, W., Oshihara, K., *Appl Catal A: Gen*, **2000**, *200(1-2)*, 135.

[46] Zheng, W., Yu, Z. X., Zhang, P., Zhang, Y. H., Fu, H. Y., Zhang, X. L., Sun, Q. Q., Hu, X. G., *J. Nat. Gas Chem.* **2008**, *17(2)*, 191.

[47] Bravo-Suárez, J. J., Bando, K. K., Fujitani, T., Oyama, S. T., *Chem. Commun.* **2008**, in press.

[48] Yang, H. P., Fan, Y, N., Lin, M., Xu, B. L., Chen, Y., *Chinese J. Catal.* **2001**, *22(6)*, 515.

[49] Yang, H. P., Fan, Y. N., Feng, L. Y., Qiu, J. H., Lin, M., Xu, B. L., Chen, Y., *Acta Chim. Sinica* **2002**, *60(6)*, 1006−1010.

[50] Yang, H., Fan, Y., Wu, J., Chen, Y., *J. Mol. Catal. A* **2005**, *227(2)*, 279.

[51] Culbertson, B. M., *Catal. Today* **1987**, *1*, 609.

[52] Dmuchovsky, B., Franz, J. E., "Maleic Anhydride", *Kirk-Othmer Encyclopedia of ChemicalTechnology, Volume 12*, John Wiley and Sons, Inc., New York, NY, **1967**, pp. 819-837.

[53] Emig, G., Martin, F., *Catal. Today* **1987**, *11*, 477.

[54] Burnett, J. C., Keppal, R. A., Robinson, W. D., *Catal. Today* **1987**, *1*, 537.

[55] Nakamura, M., Kawai, K., Fujiwara, Y., *J. Catal.* **1974**, *34*, 345.

[56] Zazhigalov, V. A., Zaitsev, Y. P., Belousov, V. M., Parlitz, B., Hanke, W., Öhlman, G., *React. Kinet. Catal. Lett.* **1989**, *32*, 209.

[57] Ramstetter, A., Baerns, M., *J. Catal.* **1988**, *109*, 303.

[58] Varma, R. L., Saraf, D. N., *Ind. Chem. Eng.* **1978**, *20*, 42.

[59] Kuo, P. S., Yang, B. L., *J. Catal.* **1989**, *117*, 301.

[60] Martinez-Lara, M., Moreno-Real, L., Pozas-Tormo, R., Jimenez-Lopez, A., Bruque, S., Ruiz, P., Poncelet, G., *Can. J. Chem.* **1992**, *70*, 5.

[61] Derewinski, M., Haber, J., Kozlowski, R., Zazhigalov, W. A., Zajtsev, J. P., Bacherikowa, I. W., Belousov, W. M., *Bull. Polish Acad. Sci. Chem.* **1991**, *39*, 403.

[62] Ruitenbeek, M., Overbeek, R. A., van Dillen, A. J., Koningsberger, D. C., Geus, J. W., *Recl. Trav. Chim. Pays-Bas* **1996**, *115*, 519.

[63] Overbeek, R. A., Warringa, P. A., Crombag, M. J. D., Visser, L. M., van Dillen, A. J., Geus, J. W., *Appl. Catal. A* **1996**, *135*, 209.

[64] Overbeek, R. A., Pekelharing, A. R. C. J., van Dillen, A. J., Geus, J. W., *Appl. Catal. A* **1996**, *135*, 231.

[65] Wachs, I. E., Jehng, J.-M., Deo, G., Weckhuysen, B. M., Guliants, V. V., Benziger, J. B., *Catal. Today* **1996**, *32*, 47.

[66] Ruitenbeek, M., Overbeek, R. A., Koningsberger, D. C., Geus, J. W., in: Derouane E.G. et al. (Eds.), Catalytic Activation and Functionalization of Light Alkanes, Kluwer Academic Publishers, Dordrecht, **1998**.

[67] Harding, W. D., Birkeland, K. E., Kung, H. H., *Catal. Lett.* **1994**, *28*, 1.

[68] Birkeland, K. E., Babitz, S. M., Bethke, G. K., Kung, H. H., Coulston, G. W., Bare, S. R., *J. Phys. Chem. B* **1997**, *101*, 6895.

[69] Bethke, G. K., Wang, D., Bueno, J. M. C., Kung, M. C., Kung, H. H., *The Third World Congress on Oxidation Catalysis*, Elsevier, Amsterdam, **1997**, 453.

[70] Wachs, I. E., Jehng, J.-M., Deo, G., Weckhuysen, B. M., Guliants, V. V., Benziger, J. B., Sundaresan, S., *J. Catal.* **1997**, *170*, 75.

[71] Landau, R., Brown, D., Russell, J. L., Kollar, J., *Proc. 7th World Petrol. Cong.* **1967**, *5*, 67.

[72] Lefort, T. E., *U.S. Pat.* **1935**, 1,998,878.

[73] MacDonald, R. W., Hayes, J. E., *J. Catal.* **1969**, *15*, 301.

[74] Twigg, G. H., *Proc. R. Soc.* **1946**, *A188*, 92.

[75] Twigg, G. H., *Trans. Faraday Soc.* **1946**, *42*, 284.

[76] Kemball, C., Patterson, W. R., *Proc. R. Soc.* **1962**, *A270*, 219.

[77] Cant, N. W., Hall, W. K., *J. Catal.* **1970**, *16*, 220.

[78] Moss, R. L., Thomas, D. H., *J. Catal.* **1967**, *8*, 151.

[79] Moss, R. L., Thomas, D. H., *J. Catal.* **1967**, *8*, 162.

[80] Mitsutani, A., Tanaka, K., Yano, M., *Kogyo Kagaku Zasshi* **1965**, *68*, 1219. *Chem. Abstr.* 65, 3732e.

[81] Ishii, Y., Matsuura, I., *Technol. Rep. Kansai Univ.* **1969**, *No. 10*, 47.

[82] Murray, K. E., *Aust. J. Sci. Res.* **1950**, *A3*, 443.

[83] Kaliberdo, L. M., Vaabel, A. S., Torgasheva, A. A., *Kinet. Katal.* **1967**, *8*, 105. *Chem. Abstr.* 67, 64122g.

[84] Cant, N. W., Hall, W. K., *J. Catal.* **1971**, *22*, 310.

[85] Hearne, G. W., Adams, M. L., *U. S. Pat.* **1948**, 2,451,485.

[86] Voge, H. H., Wagner, C. C., Stevenson, D. P., *J. Catal.* **1963**, *2*, 58.

[87] Adams, C. R., Jennings, T. J., *J. Catal.* **1963**, *2*, 63.

[88] Zhdanova, K. P., Filippova, A. A., Popova, N. I. *Probl. Kinet. Katal.* **1968**, *12*, 211.

[89] Ghorokhovatskii, Ya. B., Vovyanko, I. I., Rubanik, M. Ya., *Kinet. Katal. (Eng. Transl.)* **1966**, *7*, 65.

[90] Wood, B. J., Wise, H., Yolles, R. S., *J. Catal.* **1969**, *15*, 355.

[91] Adams, C. R., *Chem. Ind.* **1970**, *52*, 1644.

[92] Callahan, J. L., Grasselli, R. K., Milberger, E. C., Strecker, H. A., Ind. Eng. Chem. Prod. Res. Dev. 1970, 9, 134.

[93] Gorshkov, A. P., Kolchin, I. K., Gribov, I. M., Margolis, L. Ya., *Kinet. Katal.* **1968**, *9*, 1068.

[94] Gorshkov, A. P., Kolchin, I. K., Gribov, I. M., Margolis, L. Ya., *Neftekh.* **1968**, *8*, 370.

[95] Tan, S., Moro-oka, Y., Ozaki, A., *J. Catal.* **1970**, *17*, 125.

[96] Tan, S., Moro-oka, Y., Ozaki, A., *J. Catal.* **1970**, *17*, 132.

[97] Buiten, J., *J. Catal.* **1968**, *10*, 188.

[98] Lazukin, V. I., Rubanik, M. Ya., Zhigailo, Ya. V., Kurganov, A. A., Buteiko, Zh. F., *Katal. Katal., Akad. Nauk SSR, Resp. Mezhvedom. Sb.* **1966**, No. 2, 50. Chem. Abstr. 66, 75620y.

[99] Barclay, J. L., Bethell, J. R., Bream, J. B., Hadley, D. J., Jenkins, R. H., Stewart, D. G., Wood, B., *Br. Pat.* **1960**, 864,666.

[100] Bream, J. B., Hadley, D. J., Barclay, J. L., Stewart, D. G., *Br. Pat.* **1961**, 876,446.

[101] Barclay, J. L., Hadley, D. J., *Br. Pat.* **1962**, 902,952.

[102] Bethell, J. R., Hadley, D. J., *U.S. Pat.* **1963**, 3,094,565.

[103] Callahan, J. L., Gertisser, B., *U.S. Pat.* **1965**, 3,198,750.

[104] Callahan, J. L., Gertisser, B., *U.S. Pat.* **1967**, 3,308,151.

[105] Lazukin, V. I., Rubanik, M. Ya., Zhighailo, Ya. V., Kurganov, A. A., *Katal. Katal.* **1968**, *4*, 70.

[106] Ohdan, K., Umemura, S., Yamada, K., *Kogyo Kagaku Zasshi* **1969**, *72*, 2373.

[107] Ohdan, K., Umemura, S., Yamada, K., *Kogyo Kagaku Zasshi* **1969**, *72*, 2495.

[108] Zhiznevskii, V. M., Tolopko, D. K., Fedevich, E. V., *Neftekh.* **1968**, *8*, 68. *Chem. Abstr.* 69, 66646w.

[109] Wakabayashi, K., Kamiya, Y., *Bull. Chem. Soc. Japan* **1967**, *40*, 401.

[110] Golodets, G. I., Pyatnitskii, Yu. I., Il'chenko, N. I., *Dokl. Adad. Nauk SSSR (Engl. Transl.)* **1971**, *196*, 70.

[111] Ohdan, K., Umemura, S., Yamada, K., *Kogyo Kagaku Zasshi* **1970**, *73*, 441.

[112] Kuchmii, S. Ya., Gerei, S. V., Ghorokhovatskii, Ya. B., *Dopv. Adad. Nauk Ukr.* SSR, Ser. B, **1970**, *33*, 1100. *Chem. Abstr.* 76, 85316z.

[113] Ishikawa, T., Nishimura, T., Hayakawa, T., Takehira, K., *Bull. Japan Petrol. Inst.* **1971**, *13*, 67.

[114] Moro-oka, Y., Takita, Y., Ozaki, A., *J. Catal.* **1971**, *23*, 183.

[115] Trivedi, B. C., Culbertson, B. M., *Maleic Anhydride*, Plenum, New York, 1982.

[116] *Chemical Week*, May **2003**, *7*, 33.

[117] Inumaru, K., Misono, M., Okuhara, T., *Appl. Catal. A:General* **1997**, *149*, 133.

[118] Ballarini, N., Cavani, F., Cortelli, C., Ricotta, M., Rodeghiero, F., Trifiro, F.,

Fumagalli, C., Mazzoni, G., *Catal. Today* **2006**, *117*, 174.

[119] Ebner, J. R., Thompson, M. R., *Catal. Today* **1993**, *16*, 51.

[120] Guliants, V. V., Benziger, J. B., Sundaresan, S., Wachs, J. E., Jehng, J. M., Roberts, J. E., *Catal. Today* **1996**, *28*, 275.

[121] Cavani, F., Trifiro, F., *Appl. Catal. A:Gerneral* **1997**, *157*, 195.

[122] Volta, J.-C., *Catal. Today* **1996**, *32*, 29.

[123] Bertola, A., Cassarino, S., Nsunda, V., *US Patent* **2001**, 6,174,833.

[124] Ballarini, N., Cavani, F., Cortelli, C., Ligi, S., Pierelli, F., Trifiro, F., Fumagalli, C., Mazzoni, G., Monti, T., *Topics in Catal.* **2006**, *38(1-3)*, 147.

[125] Okuhara, T., Misono, M., *Catal. Today* **1993**, *16*, 61.

[126] Schuurman, Y., Gleaves, J. T., *Ind. Eng. Chem. Res.* **1994**, *33*, 2935.

[127] Coulston, G. W., Thompson, E. A., Herron, N., *J. Catal.* **1996**, *163*, 122.

[128] Rodemerck, U., Kubias, B., Zanthoff, H. W., Wolf, G. U., Baerns, M., *Appl. Catal. A:General* **1997**, *153*, 217.

[129] Rodemerck, U., Kubias, B., Zanthoff, H. W., Baerns, M., *Appl. Catal. A:General* **1997**, *153*, 203.

[130] Lorences, M. J., Patience, G. S., Cenni, R., Diez, F., Coca, J., *Catal. Today* **2006**, *112*, 45.

[131] Trifiro, F., *Catal. Today* **1993**, *16*, 91.

[132] Ruiz, P., Bastians, P., Caussin, L., Reuse, R., Daza, L., Acosta, D., Delmon, B., *Catal. Today* **1993**, *16*, 99.

[133] Garbassi, F., Bart, J. C. J., Montino, F., Petrini, G., *Appl. Catal.* **1985**, *16*, 271.

[134] Satsuma, A., Hattori, A., Mizutani, K., Furuta, A., Miyamoto, A., Hattori, T., Murakami, Y., *J. Phys. Chem.* **1989**, *93*, 1484.

[135] Schiott, B., Jorgensen, K. A., *Catal. Today* **1993**, *16*, 79.

[136] Schiott, B., Jorgensen, K. A., Hoffmann, R., *J. Phys. Chem.* **1991**, *95*, 2297.

[137] Gleaves, J. T., Ebner, J. R., Kuechler, T. C., *Catal. Rev. – Sci. Eng.* **1988**, *30*, 49.

[138] Gleaves, J. T., Centi, G., *Catal. Today* **1993**, *16*, 69.

[139] Gleaves, J. T., Yablonskii, G. S., Phanawadee, P., Schuurman, Y., *Appl. Catal.*

A:General **1997**, *160*, 55.

[140] Miyamoto, K., Nitadori, T., Mizuno, N., Okuhara, T., Misono, M., *Chem. Lett.* **1988**, 303.

[141] Taufiq-Yap, Y. H., Sakakini, B. H., Waugh, K. C., *Catal. Lett.* **1997**, *48*, 105.

[142] Abon, M., Volta, J.-C., *Appl. Catal. A:General* **1997**, *157*, 173.

[143] Busca, G., Centi, G., *J. Am. Chem. Soc.* **1989**, *111*, 46.

[144] Zhang-Lin, Y., Forissier, M., Sneeden, R. P., Vedrine, J. C., Volta, J.-C., *J. Catal.* **1994**, *145*, 256.

[145] Zhang-Lin, Y., Forissier, M., Vedrine, J. C., Volta, J.-C., *J. Catal.* **1994**, *145*, 267.

[146] Ziolkowski, J., Bordes, E., Courtine, P., *J. Mol. Catal.* **1993**, *84*, 307.

[147] Ziolkowski, J., Bordes, E., Courtine, P., *J. Catal.* **1990**, *122*, 126.

[148] Centi, G., Fornasari, G., Trifiro, F., *J. Catal.* **1984**, *89*, 44.

[149] Hodnett, B. K., *Catal. Today* **1993**, *16*, 131.

[150] Akimoto, M., Ichikawa, K., Echigoya, E., *J. Catal.* **1982**, *74*, 266.

[151] Geenen, P. V., Boss, H. J., Pott, G. T., *J. Catal.* **1982**, *77*, 499.

[152] Trent, D. L., Propylene Oxide, in: *Kirk-Othmer Encyclopedia of Chemical Technology*, vol. 20, John Wiley and Sons, New York, 1996.

[153] Mimoun, H., Mignard, M., Brechot, P., Saussine, L., *J. Am. Chem. Soc.* **1986**, *108*, 3711.

[154] Barteau, M. A., Madix, R. J., *J. Am. Chem. Soc.* **1983**, *105*, 344.

[155] Carter, E. A., Goddard III, W. A., *J. Catal.* **1988**, *112*, 80.

[156] Roberts, J. T., Madix, R. J., Crew, W. W., *J. Catal.* **1993**, *141*, 300.

[157] Imachi, M., Egashiri, M., Kuczkowski, R. L., Cant, N. W., *J. Catal.* **1981**, *70*, 177.

[158] Haruta, M., Kobayashi, T., Sano, H., Yamada, N., *Chem. Lett.* **1987**, *4*, 405.

[159] Bond, G. C., Thompson, D. T., *Catal. Rev. Sci. Eng.* **1999**, *41*, 319.

[160] Bond, G. C., Thompson, D. T., *Gold Bull.* **2000**, *33*, 41.

[161] Hutchings, G. J., *Gold Bull.* **1996**, *29*, 123.

[162] Hutchings, G. J., Scurrell, M. S., *CATTECH* **2003**, *7*, 90.

[163] Sermon, P. A., Bond, G. C., Wells, P. B., *J. Chem. Soc., Faraday Trans.* **1979**, *1(75)*, 385.

[164] Bailie, J. E., Hutchings, G. J., *Chem. Commun.* **1999**, 2151.

[165] Hutchings, G. J., J. Catal. **1985**, *96*, 292.

[166] Hayashi, T.; Tanaka, K.; Haruta, M. *J. Catal.* **1998**, *178*, 566.

[167] Haruta, M. *CATTECH* **2002**, *6*, 102.

[168] Sinha, A. K.; Seelan, S.; Tsubota, S.; Haruta, M. *Top. Catal.* **2004**, *29*, 95.

[169] Sinha, A. K.; Seelan, S.; Tsubota, S.; Haruta, M. *Angew. Chem., Int. Ed.* **2004**, *43*, 1546.

[170] Nijhuis, T. A.; Visser, T.; Weckhuysen, B. M. *Angew. Chem., Int. Ed.* **2005**, *44*, 1115.

[171] Nijhuis, T. A.; Weckhuysen, B. M. *Chem. Commun.* **2005**, *48*, 6002.

[172] Daté, M.; Okumuta, M.; Tsubota, S.; Haruta, M. *Angew. Chem., Int. Ed.* **2004**, *43*, 2129.

[173] Serafin, J. G., Liu, A.C., Seyedmonir, S.R.J., *Mol. Catal.* A **1998**, *131*, 157.

[174] Veriykios, X. E.; Stein, F. P.; Coughlin, R. W. *Catal. Rev. Sci. Eng.* **1980**, *22*, 197.

[175] Force, E. L., Bell, A. T., *J. Catal.* **1975**, *40*, 356.

[176] Campbell, C.T., Koel, B. E., *J. Catal.* **1985**, *92*, 272.

[177] Grant, R. B., Lambert, R. M., *J. Catal.* **1985**, *92*, 364.

[178] Grant, R. B., Lambert, R. M., *J. Catal.* **1985**, *93*, 92.

[179] Kilty P. A., Rol, N. C., Sachtler, W. M. H., *Proc. 5th Int. Congr. Catalysis*, Hightower J. W. (Ed.). North-Holland, Amsterdam, **1973**, pp929.

[180] Chinchen, G. C.; Waugh, K. C., *J. Catal.* **1986**, *97*, 280.

[181] Vaughan, O. P. H., Kyriakou, G., Macleod, N., Tikhov, M., Lambert, R. M., *J. Catal.* **2005**, *236*, 401.

[182] Cropley, R. L., Williams, F. J., Vaughan, O. P. H., Urquhart, A. J., Tikhov, M. S., Lambert, R. M., *Surf. Sci.* **2005**, *578*, L85.

[183] Vaughan, O. P. H., Kyriakou, G., Macleod, N., Tikhov, M., Lambert, R. M., *J. Catal.* **2005**, *236*, 401.

[184] Linic, S., Jankowiak, J. T., Barteau, M. A., *J. Catal.* **2004**, *224*, 489.

[185] Jankowiak, J. T., Barteau, M. A., *J. Catal.* **2005**, *236*, 366.

Chapter 2.
Experimental Techniques

2.1 Introduction

Catalysts are highly complicated materials. Characterization techniques are designed to correlate catalyst behaviour with physical and chemical structure. The basic principles and operations of some characterization techniques which are concerned with the research work are being introduced in this chapter.

2.2 X-ray powder diffraction (XRD)

2.2.1 Introduction

Since X-ray was discovered by Röentgen in 1895 [1], it has been found many applications in the fields of medical science, physics and chemistry. X-ray powder diffraction (XRD) is one of the most widely used techniques especially in such fields as metallurgy, mineralogy, condensed matter physics and pharmaceutical sciences. It has been a standard powerful tool for phase identification, determination of crystallinity, lattice parameters and crystal structures. Crystalline materials can be identified by their diffraction patterns since the pattern is regarded as the fingerprint of the pure substance. Nowadays, crystallographic databases have been built, in which more than 700,000 crystal structures have been published and stored. The publishing rate has reached over 50,000 crystal structures per year. XRD data can be obtained for identification of some compounds by a search procedure. However, there are no phase diffraction patterns for pure amorphous materials in XRD analysis.

2.2.2 Theoretical principles

Crystallites of most solid materials will behave as three-dimensional gratings toward X-ray. The X-ray pattern of a powder will depend upon the size of the crystallites in the solid. In an X-ray powder diffractometer, the powder sample is filled in a small disc like container and its surface carefully flattened. X-rays are generated by a sealed tube under vacuum where the filament was heated by a high voltage current. The sample is irradiated with monochromatic X-ray light and the stray radiation is collected by the detector. Then a profile of XRD pattern is obtained. The apparatus of XRD is shown in Figure 2.1 where the incident angle θ is defined as the angle between the incident beam and the sample, and 2θ is defined as the angle between the incident and diffracted beams.

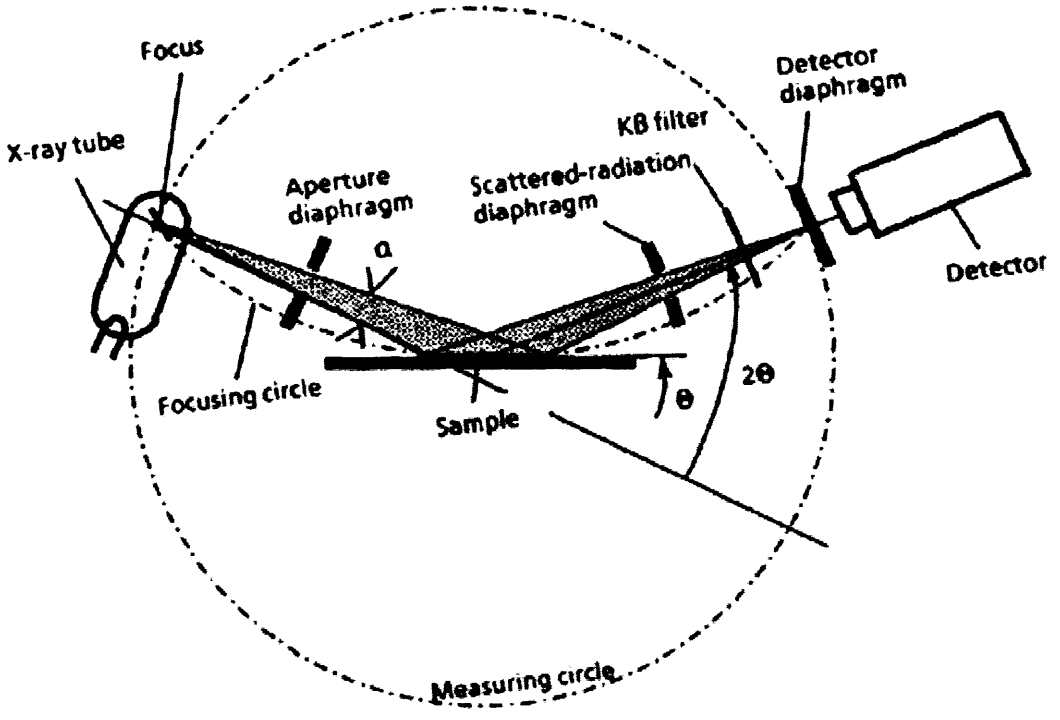

Figure 2.1. Scheme of X-ray powder diffraction apparatus.

X-ray diffraction analysis uses the property of crystal lattices to diffract monochromatic X-ray light. This involves the occurrence of interferences of the waves scattered at the

successive planes, which are described by following Bragg's equation [1, 2] and Figure 2.2.

$$\mathbf{n\,\lambda = 2d\,\sin\theta}$$

Where n is an integer that represents the order of reflections, λ is the the wavelength of the X-rays, d is the interplanar spacing generating the diffraction and θ is the diffraction angle. The greater the wavelength, the larger the glancing angle for reflection on the same plane; the greater the spacing, the smaller is the glancing angle for a given wavelength.

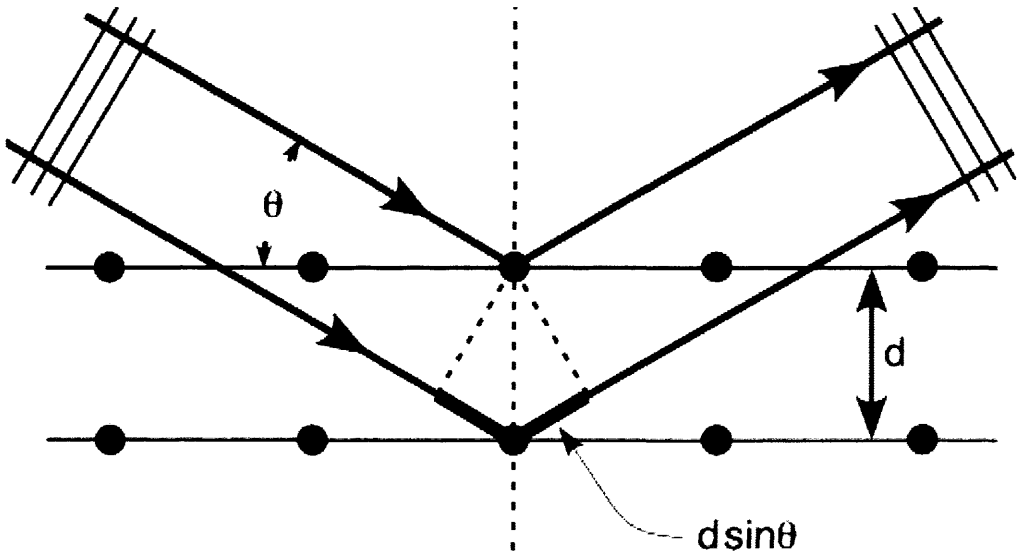

Figure 2.2. Bragg's diffraction.

Subsequently, the X-ray diffraction pattern has been obtained as a fingerprint of the specimen since λ, θ and d-spacings can be calculated. In the profile of an XRD pattern, the number of observed peaks is related to the symmetry of the unit cell in the crystal structure. The d-spacings of the peaks depend upon the repeating distances between planes of atoms in the structure. The intensities of peaks correlate with the atoms in the repeating planes.

X-ray patterns were obtained using an Enraf Nonius FR590 generator, with a $CuK_{\alpha 1}$ source. X-rays were detected using a curved position sensitive scintillater X-ray operated at 1.2kW (40mA and 30kV). The sample was spun to ensure a random arrangement of crystallites. A sample was run for 0.5 h and the diffractogram was compared to known patterns on the JCPDS database.

2.3 Raman spectroscopy

When light is scattered from a molecule, most photons are elastically scattered. The scattered photons have the same frequency as the incident ones. But a small fraction of the scattered light is scattered by an excitation, with the scattered photons having a frequency different from, and usually lower than, the frequency of the incident photons [3]. The process leading to the inelastic scatter and the variation of photos frequency is named Raman effect. Raman scattering can result in a change of vibrational, rotational or electronic energy of a molecule. The vibrational Raman effect attracts the most attention by chemists. So the "Raman effect" usually denotes the vibrational Raman effect in chemistry.

Raman spectroscopy is commonly used for vibrational and rotational information of chemical bonds since the Raman effect was discovered by Sir Raman [4]. A monochromatic light source, currently laser, is required for illumination, and a spectrogram of the scattered light then shows the deviations caused by state changes in the molecule. The frequency of light scattered from a molecule may be changed due to the structural characteristics of the molecular bonds. The difference in energy between the incident photon and the Raman scattered photon is equal to the energy correlated with a vibration of the scattering molecule. Raman spectrum can be obtained by plotting the intensity of scattered light versus energy difference. The energy of a vibrational mode depends upon many factors such as molecular structure atomic mass, bond order, molecular substituents, molecular geometry and hydrogen bonding etc.

However, Vibrational Raman spectroscopy is not limited to intramolecular vibrations. Crystal lattice vibrations and other motions of extended solids are Raman-active.

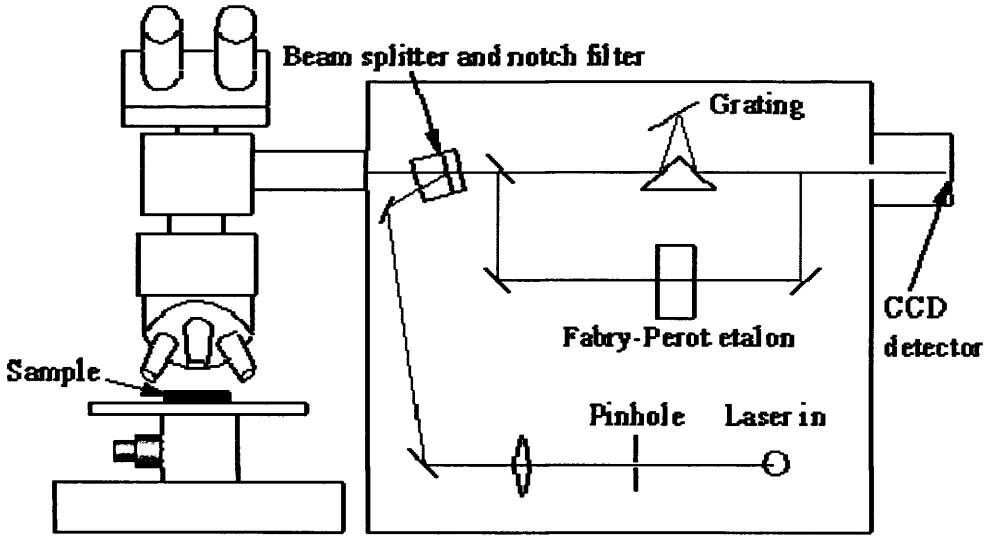

Figure 2.3. Scheme of a Raman spectrometer

In a typical laser Raman system, the laser beam pass through a filter to remove some plasma emission line after it is adjusted parallel by a telescope. Then the beam is focused on the sample area, which is controlled by an optical microscope. The scatter light collected passes by spectrometer through a notch filter to remove light at laser wavelength. After passing by a slit, the light is scattered by a diffraction grating and focused on a cooled charge coupled device followed by data analysis controlled by a computer.

In this work, Raman spectra were obtained by Renishaw Ramascope and BH-2 microscope using 514.5 nm laser excitation wavelength.

2.4 Brunauer-Emmett-Teller (BET) method

The process that gas molecules become attached to a solid surface is known as adsorption [5]. The former is named adsorbate while the latter being adsorbent. Surface area is a significant parameter of adsorbent in the study of adsorption. The most

common method of measuring surface area, now a routine analysis technique in most of catalyst researches, was developed by Brunauer, Emmett and Teller in 1938 [6]. This method is normally applied while molecules form multi-layers. In this case, the rate of adsorption is taken to be proportional to both the amount present in that layer. The heat of adsorption for all layers except the first layer is assumed to be equal to the heat of liquefaction of the adsorbed gas. These assumptions are mainly made for mathematical convenience. A final equation is given as follows:

$$\frac{P}{V(P_0 - P)} = \frac{1}{V_m C} + \frac{(C-1)P}{V_m C P_0}$$

Where V = volume of gas adsorbed at pressure P

V_m = volume of gas adsorbed in monolayer, same units as V

P = equilibrium pressure of adsorbates gas at the experimental temperature

P_0 = saturation pressure of adsorbates gas at the experimental temperature

C = a constant related exponentially to the heats of adsorption and liquefaction of the gas

$$C = e^{(q_1 - q_L)/RT}$$

Where q_1 = heat of adsorption on the first layer

q_L = heat of liquefaction of adsorbed gas on all other layers

The larger the value of C, the more accurately the surface area can be determined.

The total surface area S_{total} and specific surface area S_{BET} are evaluated as following equations:

$$S_{total} = \frac{V_m N s}{V}$$

$$S_{BET} = \frac{S_{total}}{a}$$

Where N = Avogadro's number

s = adsorption cross section

V = molar volume of adsorbent gas

a = molar weight of adsorbed species

In the practical operation, the powder sample is placed in a sample vessel connected to a gas inlet, a vacuum pump and an electronic barometer where liquid nitrogen is used to cool the vessel all the time. After degassing between 30 minutes and 2 hours, the system will be evacuated in order to remove adsorbed molecules from the sample surface. Then N_2 is introduced in the deposition step while the pressure being measured. According to above-mentioned equation, the surface area of the sample is calculated automatically.

In this work, BET was performed using Micromeritics Gemini 2360 at about 77K while samples were degassed on Micromeritics Flowprep 060 prior to analysis.

2.5 Scanning electron microscope (SEM)

Scanning electron microscope (SEM) is a kind of microscope to generate high-solution images of a sample surface using a high-energy beam of electrons rather than light [7]. A three-dimensional photo containing information about sample's surface topography, composition and other properties can be obtained while the electrons interact with the atoms of the sample. Nowadays, SEM has been used mainly for examination of the topology of material surfaces.

A typical scheme of a SEM apparatus is shown in Figure 2.4. A high vacuum normally with pressures of less than 10-6 torr is necessary for SEM analysis. The electron beam is usually emitted by a tungsten filament cathode and is accelerated towards an anode. Tungsten is applied for thermionic electron gun to produce high-energy electrons.

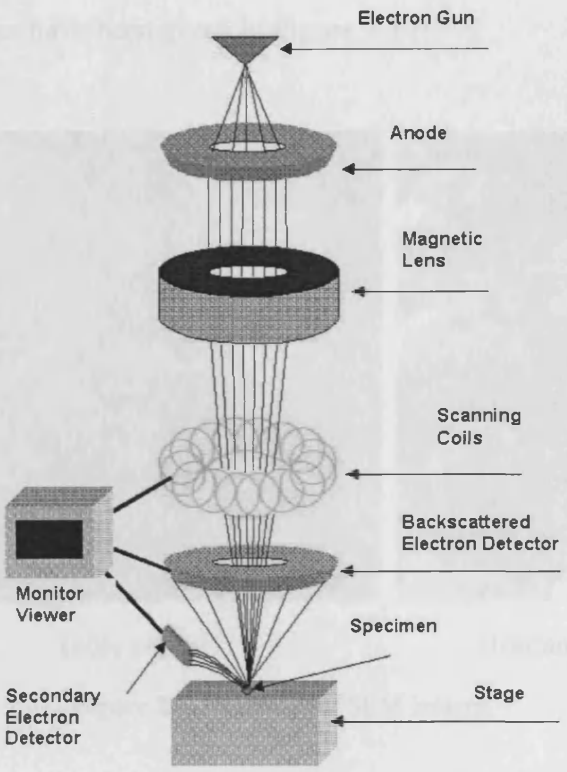

Figure 2.4. Scheme of scanning electron microscopy (SEM).

The beam is focused by condenser lenses toward the sample. When the primary electron beam interacts with the sample, two kinds of electrons, namely secondary electrons and backscatter electrons, are generated by repeated scattering and absorption due to energy loss. Secondary electrons generated as ionization products are so-called since they are produced by other radiation (not primary radiation) which can be in the form of ions, electrons or photons with high energy. The resulting signal is the major means of viewing image in the SEM. The range of secondary electrons depends greatly upon the topographic features of given surface area. Backscatter electrons are high-energy electrons originating in the beam, which are reflected or scattered back out of the specimen. The strong topographic contrast is mainly owing to the backscatter electrons, the intensity of which is related to the mean atomic number in the interaction area. Both of them, together with characteristic X-rays and light, are converted to a digital signal that can be viewed on screen. The resolution of SEM images depends upon wavelength of the electrons and the magnetic electron-optical system, which is

also limited by the interaction volume between the material and the electron beam. Some image examples have been given in Figure 2.5.

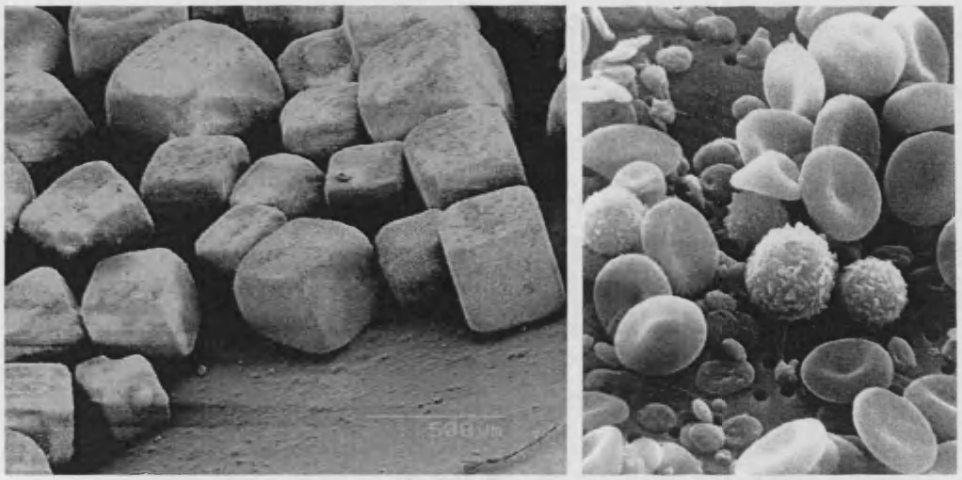

Table salt Human blood cell

Figure 2.5. Examples of SEM images.

The analysis was performed using a Zeiss Evo-40 Series scanning electron microscope. The energy dispersive X-ray spectroscopy (EDX) is connected with SEM so that the chemical composition of the sample can be determined.

2.6 Temperature-programmed reduction (TPR)

Temperature-programmed reduction (TPR), one of temperature programmed gas chromatography techniques (TPGC), involves in heating a catalyst in a flow of hydrogen with a linear temperature ramp while controlling the hydrogen consumption. Temperature programming has been used to accelerate the elution rate of peaks. In a linear program, the rate of increasing temperature with time is constant. A fingerprint profile can be obtained to analyze the influences of supports or promoters on reducibility. This technique has been proved a powerful tool for studying reduction kinetics of oxidized catalyst precursors. Robertson et al. used TPR first to study the

reducibility in hydrogen of copper-nickel on silica catalysts and to evaluate the metal support interaction [8, 9]. Moreover, the amount and the reduction degree of reducible species can be derived from the integrated hydrogen consumption while an appropriated model of the reduction process exists. Usually, it is impossible to correlate the reducibility in hydrogen with the catalytic performance in selective oxidation with hydrocarbon as reducing agents.

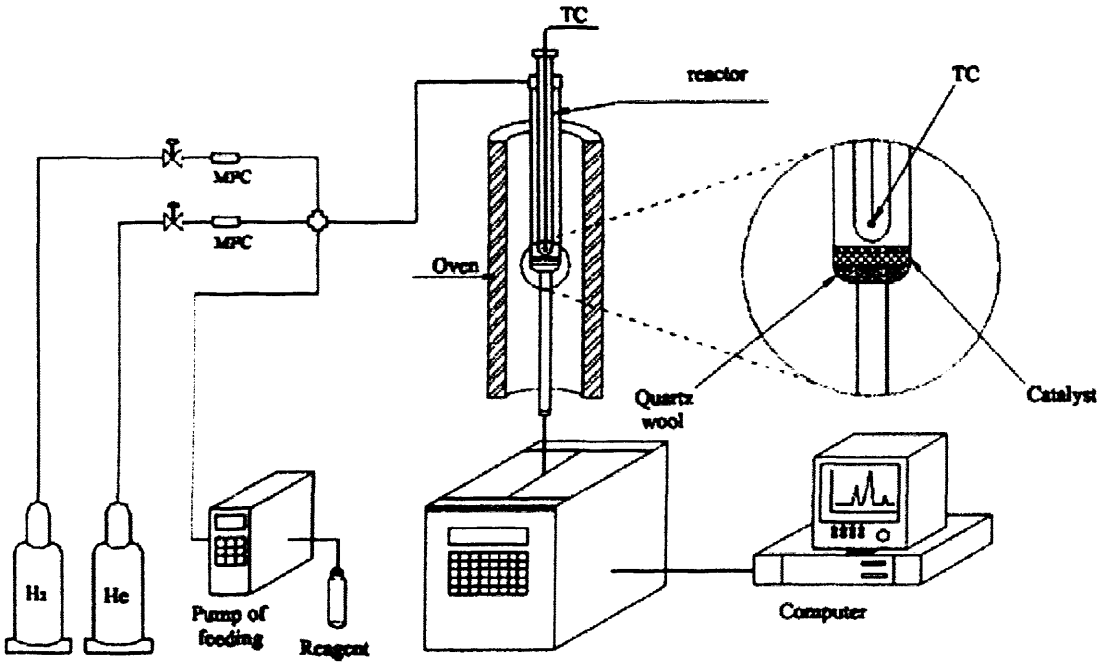

Figure 2.6. Scheme of Temperature programmed reduction (TPR) apparatus.

The sample is normally placed in a stream of inert gas firstly. After degassing for one or two hours, the mixtures of the hydrogen and an inert gas are introduced with a linear temperature ramp controlled by the temperature program, during which the consumption of hydrogen is detected. The profile of hydrogen uptake versus temperature can be obtained subsequently. TPR can also supply quantitative values for the surface process such as activation energies, pre-exponential factors and even turnover numbers can be calculated [10, 11].

Analysis was performed using a Thermo TPDRO 1100. The machine is designed to perform several experiments including pulse chemisorption, temperature programmed

reduction, desorption and oxidation. The sample (15mg) was suspended in a plug of silica wool in a straight wall sample tube. The sample tube is loaded into the furnace. The sample is degassed in Ar for 1h prior to analysis. The TPDRO machine is controlled by a PC, which is loaded with reaction conditions that operate during analysis. The sample is heated from ambient temperature to 600°C at a rate of 5°C/min. The reducing gas used was a mixture of 10% H_2 in balance Ar.

2.7 X-ray photoelectron spectroscopy (XPS)

X-ray photoelectron spectroscopy (XPS) also called electron spectroscopy for chemical analysis (ECSA) is a surface chemical analysis technique. It is a powerful quantitative tool to determine the elemental composition, chemical state, empirical formula and chemical or electronic state of elements on the surface of detected specimen [12]. An XPS normally consists of a source of fixed-energy radiation, an electron energy analyser and a high vacuum environment as shown in Figure 2.7.

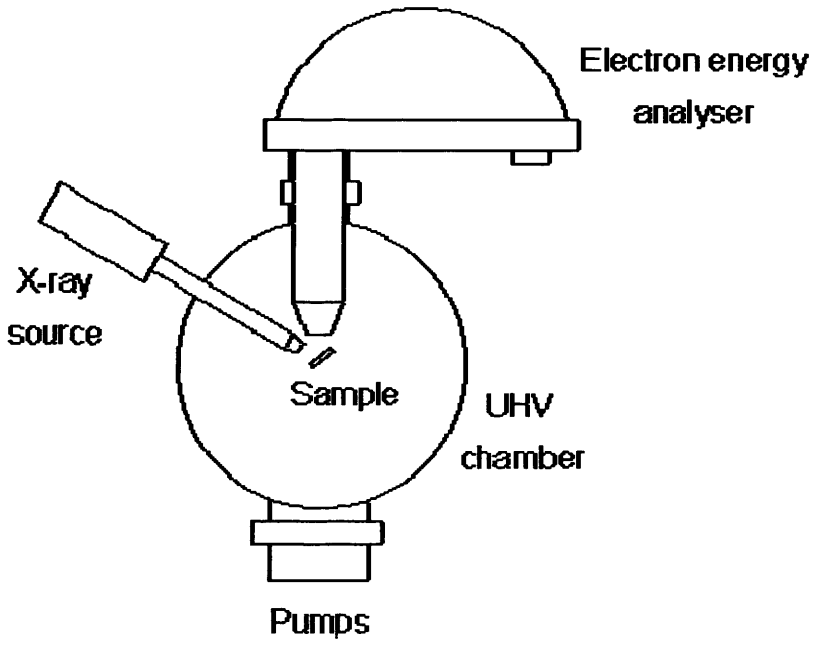

Figure 2.7. Scheme of X-ray photoelectron spectrometer

A sample is bombarded with monochromatic X-rays, and photoelectrons are ejected

from various atomic shells. The intensity of electrons emitted from the first few atomic monolayers is high, but that emitted from subsequent layers falls exponentially as a limit of about 10 nm is approached. The electrons can be resolved for their kinetic energy, which gives their binding energy. In order to count the number of electrons with the minimum of error, XPS has to be carried on under ultra high vacuum (UHV) conditions. Each element has a characteristic set of XPS peaks at its characteristic binding energy. These peaks correspond to the electron configuration of atoms such as 1s, 2s, 2p, 3s, etc. XPS is normally sensitive to most of elements with an atomic number (Z) between those of lithium (Z=3) and lawrencium (Z=103) but hydrogen and helium. The electron energy analyser is used to disperse the emitted electrons according to their kinetic energy, and measure the flux of emitted electrons of a particular energy. In the high vacuum, the emitted photoelectrons can be analysed without interference from gas phase collisions

In principle, XPS is based upon the photoelectric effect also termed the Hertz Effect [13] which describes the process of photons in and electrons emitted from matter after the absorption of energy from electromagnetic radiation such as X-rays. The energy of a photon is given by Einstein equation:

$$E = h\nu$$

Where h is Planck constant (6.62×10^{-34} J s), ν is the frequency (Hz) of the radiation. In XPS, the photon is absorbed by an atom in a molecule or solid, leading to ionization and the emission of a core (inner shell) electron. An atom is ionized by an X-ray photon to produce an emitted free electron from the core shell of the atom, as shown in Figure 2.8.

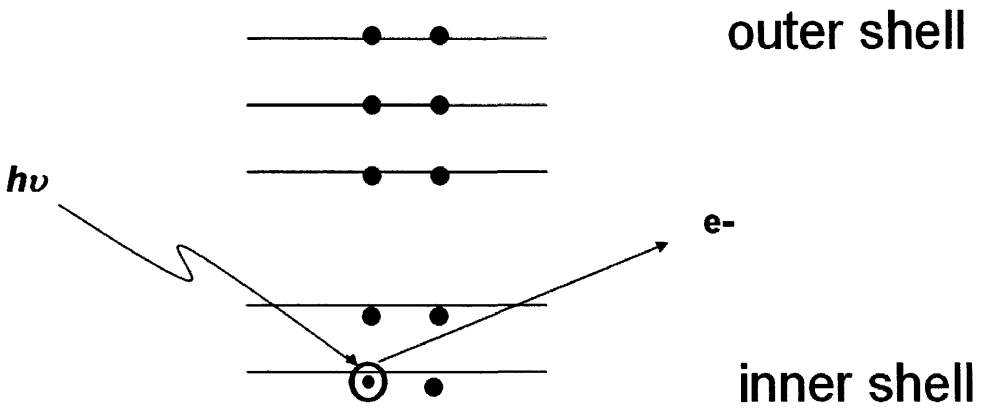

Figure 2.8. Emission of electrons excited by X-rays.

The kinetic energy distribution of the emitted photoelectrons, usually the number of emitted photoelectrons as a function of their kinetic energy, can be recorded using some appropriate electron energy analyser and a photoelectron spectrum can thus be obtained. The overall process of photoionization can be considered as follows:

$$A + h\nu \rightarrow A^{+} + e- \qquad (2.1)$$

Then conservation of energy requires that:

$$E(A) + h\nu = E(A^{+}) + E(e-) \qquad (2.2)$$

Since the electron's energy is present solely as kinetic energy (KE) this can be rearranged to give the following expression for the KE of the photoelectron:

$$KE = h\nu - [E(A^{+}) - E(A)] \qquad (2.3)$$

The final term in square brackets, representing the difference in energy between the ionized and neutral atoms, is generally called the binding energy (BE) of the electron - this leads to the following commonly quoted equation:

$$KE = h\nu - BE \qquad (2.4)$$

Practically, the binding energies (BE) of energy levels in solids are conventionally measured with respect to the Fermi-level of the solid, rather than the vacuum level. This

involves a small correction to the equation given above in order to account for the work function (Φ) of the solid. Thus the above equation has been expressed by Ernest Rutherford as following:

$$KE = h\nu - BE - \Phi \qquad (2.5)$$

The emitted electron signal excited by X-rays can be plotted as a spectrum of binding energies. The energy of core is so specific for the element in the atom that the spectrum could produce the fingerprint of the atom with measuring the kinetic energies and the binding energies. An example of XPS spectrum of palladium metal has been shown in Figure 2.9, where the most intense peak at 335 eV points to the emission from 3*d* levels of Pd atoms, while 3p and 3s levels give rise to the peaks at 534/561 eV and 673 eV respectively.

In this work, XPS analysis was performed with an ESCALAB 220 spectrometer using an achromatic AlKα source and an analyser pass energy of 100 eV.

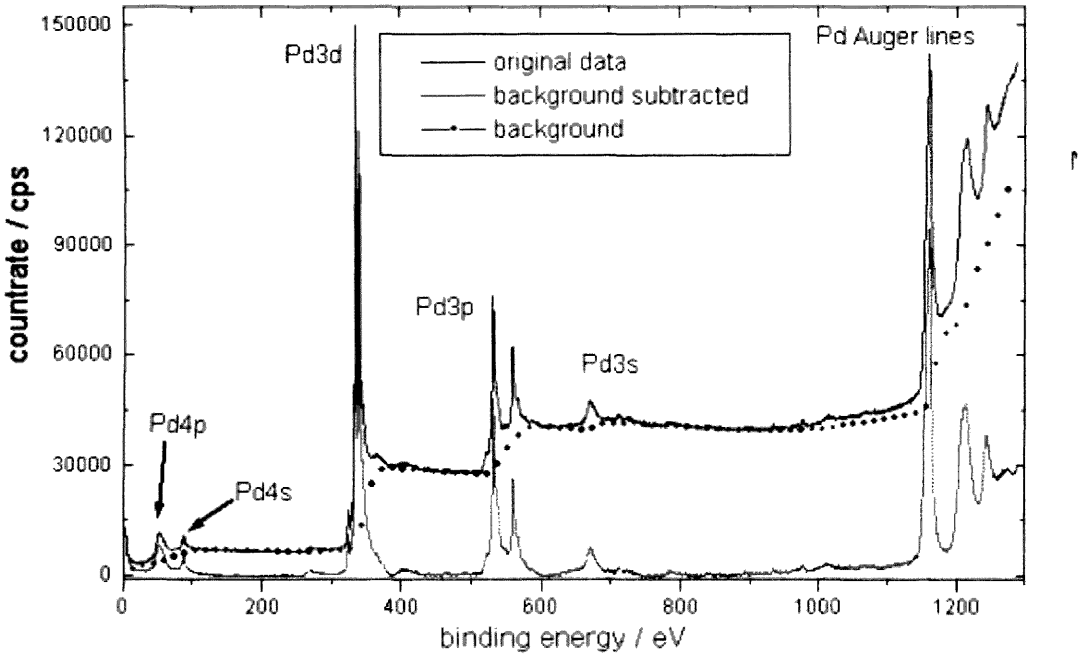

Figure 2.9. XPS spectrum of the Pd metal.

2.8 References

[1] Cullity, B. D.; Stock, S. R. *Elements of X-ray Diffraction* 3rd Ed. Addison-Wesley, **2001**.

[2] Jenkins, R.; Snyder, R. L. *Introduction to X-ray Powder Diffractiometry* John Wiley, **1996**.

[3] Harris and Bertolucci *Symmetry and Spectroscopy.* Dover Publications, **1989**.

[4] Gardiner, D. J. *Practical Raman Spectroscopy.* Springer-Verlag, **1989**.

[5] Hodnett B. K. *Heterogeneous Catalytic Oxidation: fundamental and technological aspects of the selective and total oxidation of organic compounds* John Wiley, **2000**.

[6] Brunauer, S., Emmett, P. H., Teller, E., *J. Am. Chem. Soc.* **1938**, *60*, 309.

[7] Staniforth, M.; Goldstein, J.; Newbury, D. E.; Lyman, C. E.; Echlin, P.; Lifshin, E.; Sawyer, L. C.; Michael, J. R.; Joy, D. C. *Scanning Electron Microscopy and X-ray Microanalysis* Springer **2002**.

[8] Robertson, S. D., McNicol, B. D., De Baas, J. H., Kloet, S. C., Jenkins, J. W., *J. Cat.* **1975**, *37*, 424.

[9] Jenkins, J. W., McNicol, B. D., Robertson, S. D., *Chem. Tech.* **1977**, 316.

[10] Kislyuk, M. U., Sklyarov, A. V., Dangyan, T. M., *Izv. Akad. Nauk. SSSR, Ser. Khim.* **1975**, 2161.

[11] Sklyarov, A. V., Rozanov, V. V., Kislyuk, M. U., *Kinet. Katal.* **1978**, *19*, 416.

[12] Watts, J. F., Wolstenhome, J., *An introduction to Surface Analysis by XPS and AES* John Wiley & Sons, **2003**.

[13] *The American Journal of Science* New Haven: J.D. & E.S. Dana **1880**.

Chapter 3.
Gas-phase selective oxidation of *n*-butane to maleic anhydride in a gas-gas periodic flow reactor

3.1 Introduction

Maleic anhydride, abbreviated MA, is a versatile chemical intermediate used to make unsaturated polyester resins, lubricant oil additives, alkyd resins, and a variety of other products. MA was traditionally manufactured by the oxidation of benzene or aromatic compounds. However, owing to the rising cost of benzene, MA industry has been converting benzene plants to new plants with *n*-butane used as a feedstock [1].

$$2\ CH_3CH_2CH_2CH_3 + 7\ O_2 \rightarrow 2\ C_2H_2(CO)_2O + 8\ H_2O \qquad (3.1)$$

Over the last five years, global MA consumption grew by 6-7% a year to 1.5 million metric tons per year in 2006, with the fastest growth occurring in Asia, where it was used as an intermediate for production of 1,4-butanediol.

The oxidation of butane to maleic anhydride is currently the only commercial oxidation process involving a light alkane. In early work, operation of these catalysts used continuous feed mode in which the butane was fed together with oxygen or air through a packed bed of catalyst. The concentration of butane is usually under the lower explosion limit [2]. In an alternative approach, Contractor and co-workers [3-7] have developed the riser/circulating fluidised bed (CFB) reactor for this oxidation reaction, and this process is based upon the observation that many oxides operate as oxidation catalysts by a Mars-van Krevelen mechanism, i.e. in the absence of a co-fed oxidant, the hydrocarbon reacts to produce the selective oxidation products by

reacting with lattice oxygen (O^{2-}). In the CFB process, butane reacted with the vanadium phosphate catalyst in the absence of air in a riser reactor. However, it does not lead to the elimination of the formation of CO_2 as a non-desired by-product for this reaction [8]. Du Pont CFB Technology published its recent work and indicated that the benefit of operation in the absence of oxygen is that the selectivity can be maintained at higher levels (*ca.* 10%) but the effect is only observed at conversions > 60%. Subsequently the use of periodic flow reactors is now attracting increased attention for both gas-gas and gas-liquid reaction systems [9].

Vanadium phosphate catalysts have been the most well studied heterogeneous class of compounds since their discovery as an effective catalyst in 1966[10]. Although they are commercially significant for production of maleic anhydride, some questions remain so unclear as to how they work. In early patents, a vanadium phosphate catalyst denoted "phase A" was prepared by many different methods. The structure of this material, now known as vanadyl hemihydrate, $VOHPO_4 \cdot 0.5H_2O$ is particularly important as it is the precursor of $(VO)_2P_2O_7$ crystallized phase in the final activated VPO catalyst at low temperature. Heat treatment of the precursor will result in the formation of vanadyl pyrophosphate, $(VO)_2P_2O_7$ which has been considered as the active phase by many researchers. The pre-treatment could be carried out not only in 1.5% butane in air but also in an inert atmosphere such as N_2, He.

Recently, most of preparation studies focus on both the reaction of V_2O_5 and H_3PO_4 with an alcohol and a related reaction of $VOPO_4 \cdot 2H_2O$ with an alcohol despite vanadyl hemihydrate, $VOHPO_4 \cdot 0.5H_2O$ was developed by many earlier synthesis. Horowitz *et al.* [11] reported the preparation of the precursor was greatly affected by the nature of the alcohol. In the study of transformation to vanadyl pyrophosphate, $(VO)_2P_2O_7$, They concluded that the morphology of the precursor was a controlling factor in the catalytic properties. Johnson *et al.* [12] showed the importance of the alcohol in controlling the morphology of the hemihydrate precursor and the pyrophosphate generated on activation.

Usually, $VOHPO_4 \cdot 0.5H_2O$ can be prepared by three routes as following equations.

VPA route: $V_2O_5 + HCl \xrightarrow{1.\Delta,2h;2.H_3PO_4} VOHPO_4 \cdot 0.5H_2O$ (3.2)

VPO route: $V_2O_5 + H_3PO_4 + \text{alcohol} \xrightarrow{\Delta,16h} VOHPO_4 \cdot 0.5H_2O$ (3.3)

VPD route: $V_2O_5 + H_3PO_4 \xrightarrow{H_2O,\Delta,16h} VOPO_4 \cdot 2H_2O \xrightarrow{alcohol,\Delta,16h} VOHPO_4 \cdot 0.5H_2O$ (3.4)

In VPA method, the precursor is mainly made up of the hemihydrate $VOHPO_4 \cdot 0.5H_2O$ while significant amounts of an impurity $VO(H_2PO_4)_2$ are also obtained using water as the solvent. Instead of water and anhydrous HCl, the organic solvent such as an alcohol could decrease the impurity formation to generate a more active final catalyst. The VPO method, as a variant of VPA process, is regarded to be the standard preparation method. The VPD method, first invented by Horowitz *et al.* [11] and further described by Johnson *et al.*, [12] is based on the observation of the reaction of V_2O_5 and H_3PO_4 with water as solvent, which forms the V^{5+} dihydrate phase $VOPO_4 \cdot 2H_2O$. After refluxing recovered and dried dihydrate with an alcohol, it leads to produce the formation of hemihydrate. The morphology of the precursor hemihydrate depends upon the structure of the alcohol. All three methods can be used for preparation of $VOHPO_4 \cdot 0.5H_2O$ although there are many differences among surface areas, morphologies and impurities. Under traditionally preparation condition, $VO(H_2PO_4)_2$ is readily formed as an impurity. The comparison of the catalytic reactivity between hemihydrate and $VO(H_2PO_4)_2$ has partly been a purpose of this work.

Among the VPO composition and a variety of crystalline phases, $(VO)_2P_2O_7$ appears to play a central role in the oxidation of *n*-butane to maleic anhydride on the (100) crystalline face [13,14]. Many groups suggested that V^{5+} phases are important in the active catalyst and are formed as a result of a red-ox mechanism [15-17]. The activation of *n*-butane by oxygen associated with V^{4+}, while oxygen associated with

V^{5+} should be incorporated on later [18]. They are associated with electron vacancies

$$p^+: V^{5+} \rightarrow V^{4+} + p^+ \qquad (3.5)$$

Such an electron vacancy could be filled by one neighbouring O^{2-} anion:

$$O^{2-} + p^+ \rightarrow O^- \qquad (3.6)$$

Which gives totally:

$$V^{5+} + O^{2-} \rightarrow V^{4+} + O^- \qquad (3.7)$$

The V^{4+}/O^- couple should be the centre for n-butane activation based on the following scheme: $C_4H_{10} + O^- \rightarrow C_4H_9\bullet + O^{2-} + H^+$ (3.8)

$C_4H_9\bullet$ radicals should be the starting reacting entities for further oxygen insertion [19]. It has been proposed that the *P/V* ratio during the preparation of the VPO catalysts is one of significant factors in determining the reactivity and selectivity [20]. However, the lattice oxygen (O^{2-}) plays the very key role in the reaction.

Additionally, butane oxidation is one of the themes of the ATHENA project and one area of study, which this work addresses, is the oxidation of C4 hydrocarbons. The reactivity of $VOHPO_4 \cdot 0.5H_2O$ (VPD), $VO(H_2PO_4)_2$ (Phase E) and some supported vanadium oxide catalysts has been compared for the oxidation of butane to maleic anhydride in a gas-gas periodic flow reactor with the aim of achieving higher selectivity than current systems. Usually, supported catalysts mainly refer to supported oxide catalysts, which represent the catalytic models for fundamental studies. Although it is not the focus of this chapter, wide applications can be found and explored through the further investigation of catalytic effect data combined with the molecular and electronic structural information of the active sites.

3.2 Experimental

3.2.1 Catalysts preparation and activation of precursors

VPD catalyst is the reduction of vanadium phosphate $VOPO_4 \cdot 2H_2O$ with alcohol as reducing agent and solvent, which could be prepared according to the following standard procedure [21]. The dehydrate $VOPO_4 \cdot 2H_2O$ (4 g, Aldrich) was refluxed with isobutanol (80 ml) for 24 h. The pale blue solid was recovered by vacuum filtration and washed with alcohol (50 ml) and acetone (50 ml). The recovered solid was then heated under reflux in water (9 ml H_2O/g solid) for 2 h to remove the impurity $VO(H_2PO_4)_2$. The suspension was then filtered hot, washed with warm water (100 ml) and dried in air (110 °C, 24 h).

$VO(H_2PO_4)_2$ (Phase E) can be obtained by reduction of $VOPO_4 \cdot 2H_2O$ with 3-octanol [22, 23]. Bartley [24] also suggested that it could be synthesized by the reaction of V_2O_5 and H_3PO_4, together with an aldehyde or ketone.

$VO(H_2PO_4)_2$ (Phase E), $VOHPO_4 \cdot 0.5H_2O$ (VPD) and IDIP51 (a confidential VPO-VPD mixture sample) preheated in a continuous flow reactor (1.5% butane in air) at 400°C were converted to active catalysts, respectively. The original sample and the final catalysts were characterized using X-ray diffraction (Enraf Nonius FR590 X-ray generator with a Cu-K_α source fitted with an Inel CPS120 hemispherical detector) and Raman spectroscopy (Renishaw Ramanscope spectrograph fitted with a green Ar^+ laser λ=514.532 nm).

3.2.2 Analysis with a gas-gas periodic flow reactor

The reactor fabricated from stainless steel (i.d. = 4.4 mm) was operated at 1 bar pressure, containing catalyst (250-300 μm particles, 0.25g) diluted with quartz

(250-300 μm particles, 0.25g). A six port sample valve fitted with a 250 μl sample loop is positioned as the upstream of the reactor so that the feed gases were fed to the reactor via this valve. The sample valve for this analysis system was located prior to the reactor while the one in the continuous flow reactor was between the reactor and GC. The downstream of the reactor was made up of the gas chromatograph columns so that the effluent gases form the catalyst bed were continuously fed to the analytical columns and a TCD detector. An "80/100 Porapak Q" stainless steel column and a "80/100 Molecular Sieve 13X" column were fitted in the oven of the gas chromatograph system. The reactor containing the catalyst was fed with helium as a carrier gas (15 ml/min). Prior to the beginning of a reaction, the catalyst was heated to the required temperature in a stream of flowing air to make it fully oxidized at the start of the cycle. Butane together with air were introduced to the reactor through a calibrated mass flow controller (total flow rate = 50 ml/min). During every experiment, a single 250 μl pulse of the reactants was going through the catalyst bed and the products were analysed. The gas chromatographic analysis will last between 30 and 50 minutes. The helium flow via the catalyst bed was held all the time.

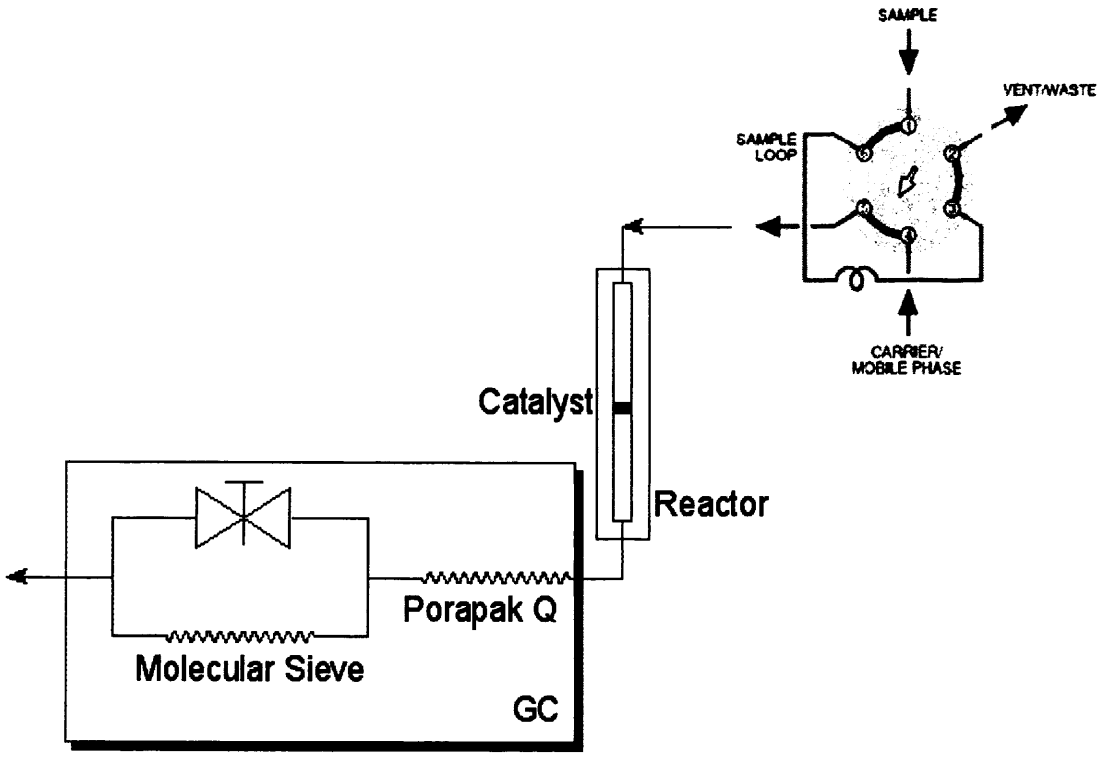

Figre 3.1. Scheme of gas-gas periodic flow reactor.

CO_2 could be separated at 30°C through "Molecular Sieve 13X" column, while maleic anhydride has to be isolated with "Porapak Q" column at 70°C or higher temperature. If both of the partitions appear in one pulse process, the temperature increasing step will disturb maleic anhydride isolation too much to obtain the quantitative data about maleic anhydride accurately. Then two pulse programs have to be run to isolate CO_x and maleic anhydride, respectively. In the first pulse program as shown in Figure 3.2, maleic anhydride (8.6 min), air (13-15 min) and CO (16.9 min) will appear at 70°C one by one after CO_2 (3.3 min) isolated at 30°C. During the second pulse program (Figure 3.3), all products will go through "Porapak Q" only and just maleic anhydride (5.0 min) can be well isolated since "Porapak Q" could not separate CO_x from air. In both of processes, the final step is to increase oven temperature up to 140°C for analysis of butane (25.2 min in Figure 3.2 and 18.4 min in Figure 3.3).

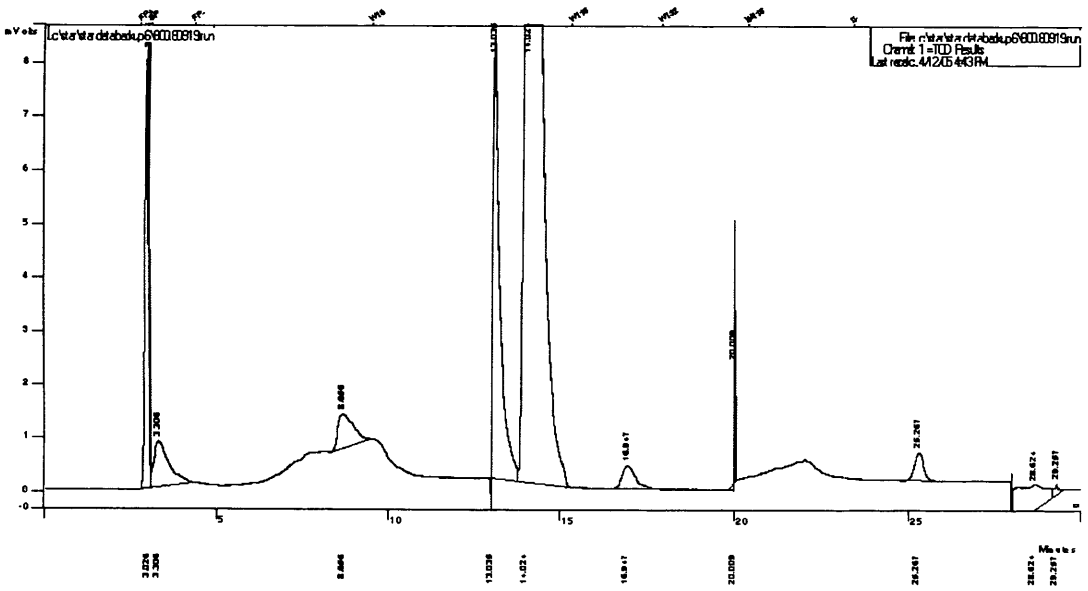

Figre 3.2. Program for isolation of CO_x, maleic anhydride, air and butane.

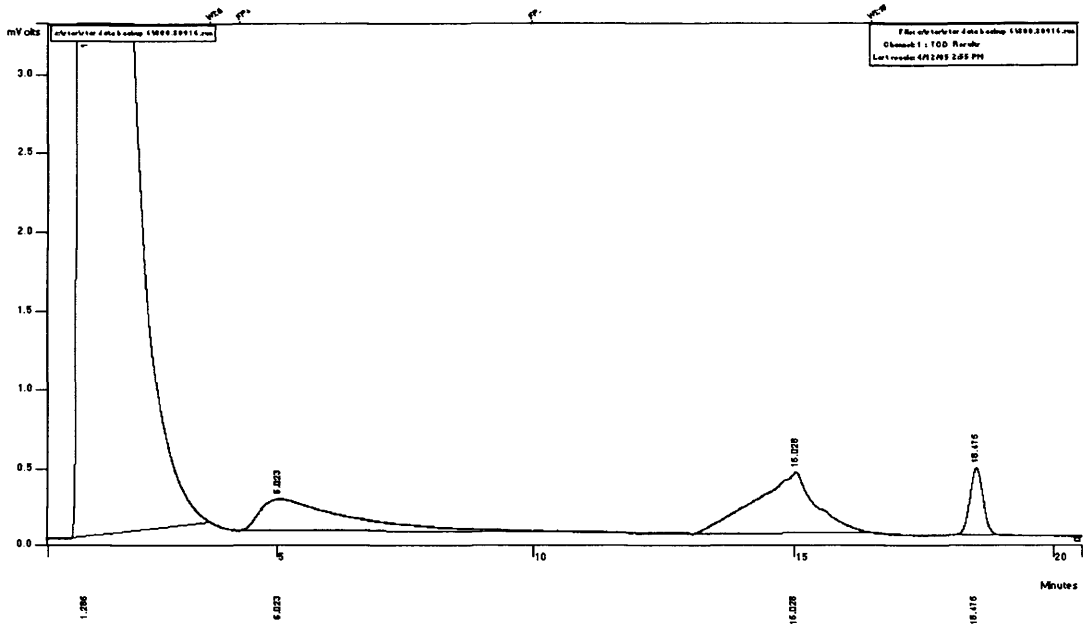

Figre 3.3. Program for isolation of maleic anhydride and butane.

Two sets of experiments were performed using the non-promoted vanadium phosphate catalysts. One set of experiments were carried out using a fixed butane concentration (1.5%) and the temperature increased sequentially from 330 to 400°C, while another ones ran at 350°C with butane concentration between 0.9% and 2.9%.

3.3 Results and discussion

3.3.1 Characterization of VPD and phase E

3.3.1.1 XRD analysis of VPD and phase E

X-ray diffraction patterns of $VOHPO_4 \cdot 0.5H_2O$ (VPD) are shown in Figure 3.4-3.5. The [220] reflection is the only feature of the diffraction pattern for VPD while there are a number of other reflections assigned to $VO(H_2PO_4)_2$ in the phase E.

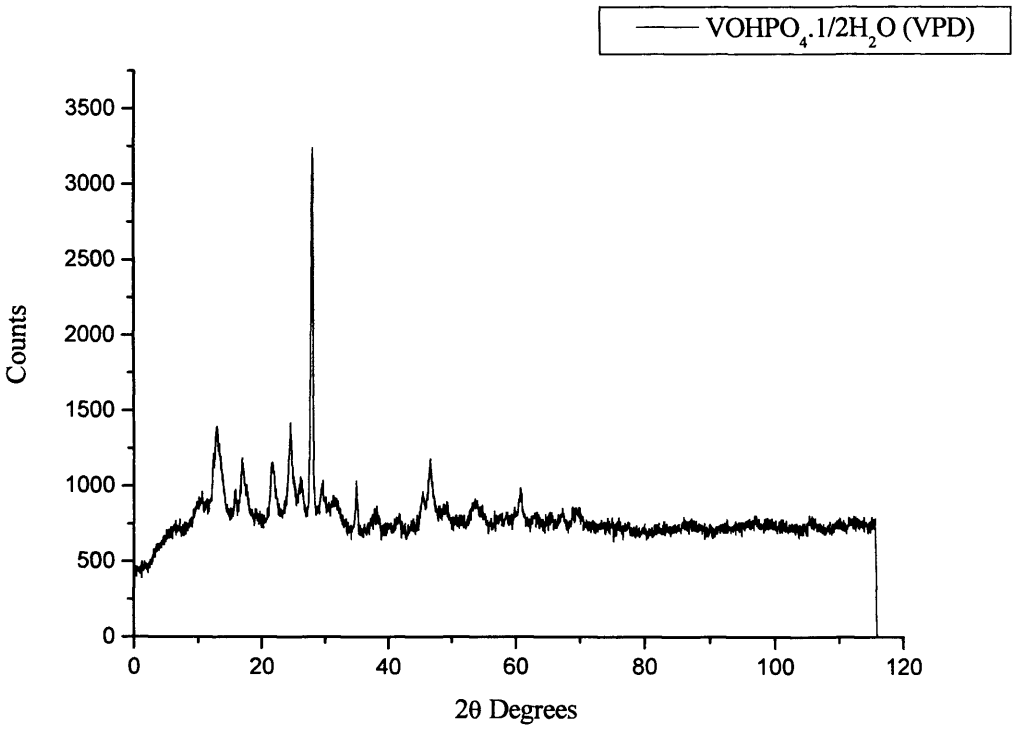

Figure 3.4. The XRD pattern of $VOHPO_4 \cdot 0.5H_2O$ (VPD).

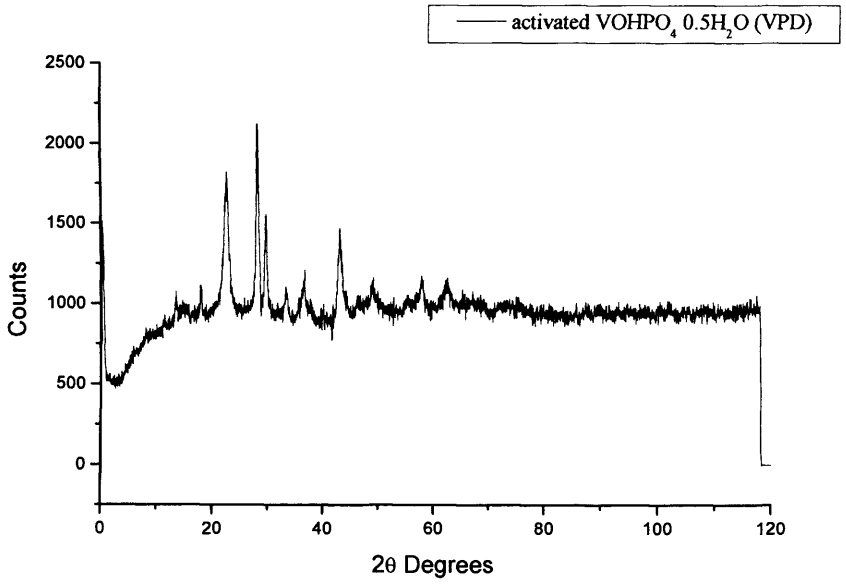

Figure 3.5. The XRD pattern of VPD activated with 1.5% butane/air at 400°C for 72 h.

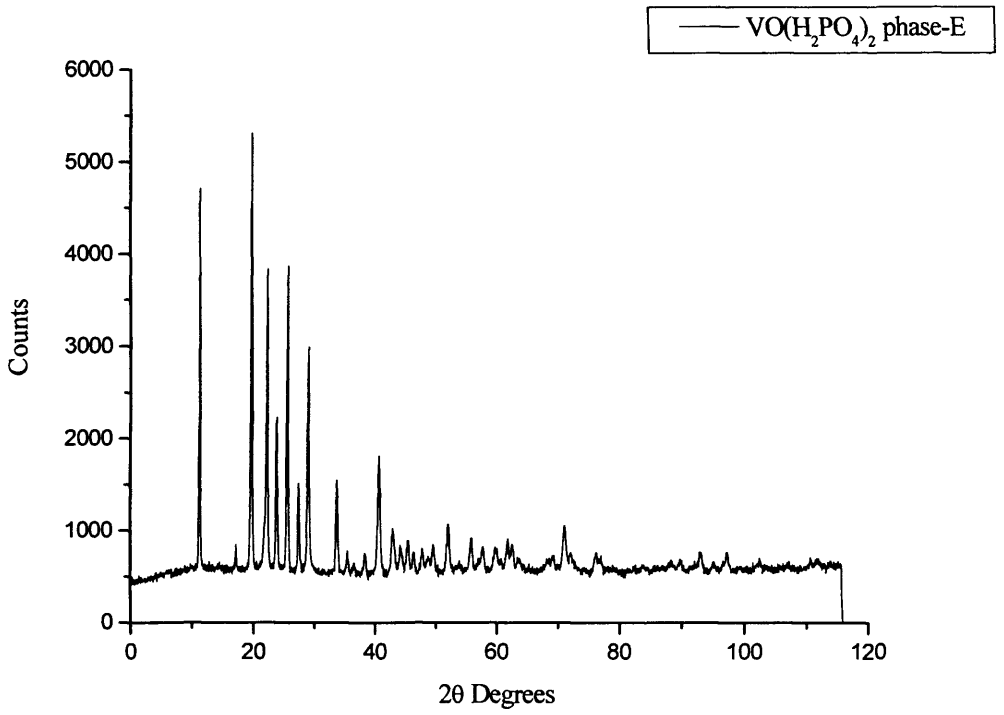

Figure 3.6. The XRD pattern of $VO(H_2PO_4)_2$ (phase-E).

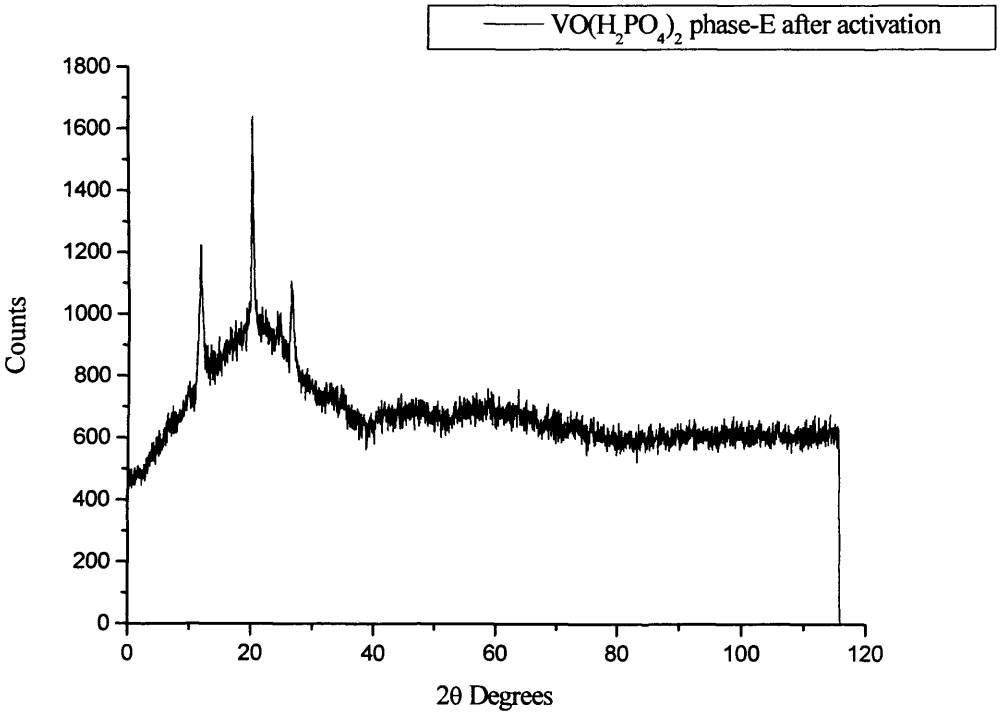

Figure 3.7. The XRD pattern of $VO(H_2PO_4)_2$ (phase-E) after activation with 1.5% butane/air at 400°C for 72 h.

3.3.1.2 Raman analysis of VPD and phase E

Raman profiles of VPD and phase E have been shown in Figure 3.6-3.9. The band of VPD at 993 cm^{-1} is owing to P-O stretching mode while phase E shows the region of 930 cm^{-1} due to the P-O stretch of $VO(H_2PO_4)_2$. Some researchers reported that there are the bonding frequency of V=O at 1113 cm^{-1} and V-O-P bands at a high frequency, 1156 cm^{-1}, in the spectra of VPD. But these peaks did not appear in the spectra because of background fluorescence.

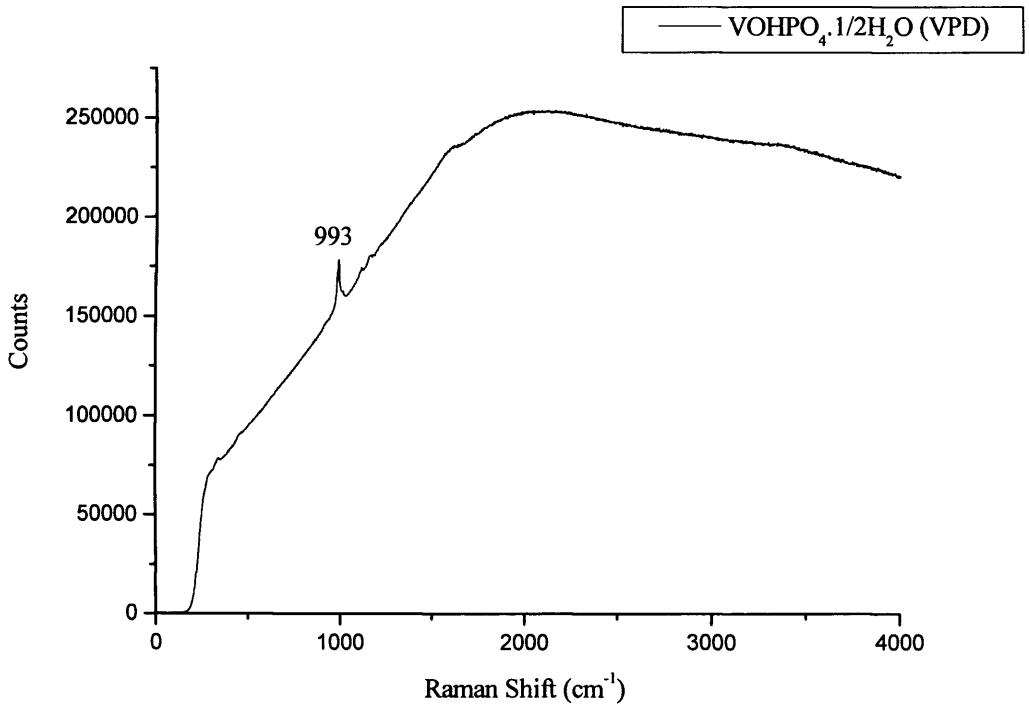

Figure 3.6. The Raman of $VOHPO_4 \cdot 0.5H_2O$ (VPD).

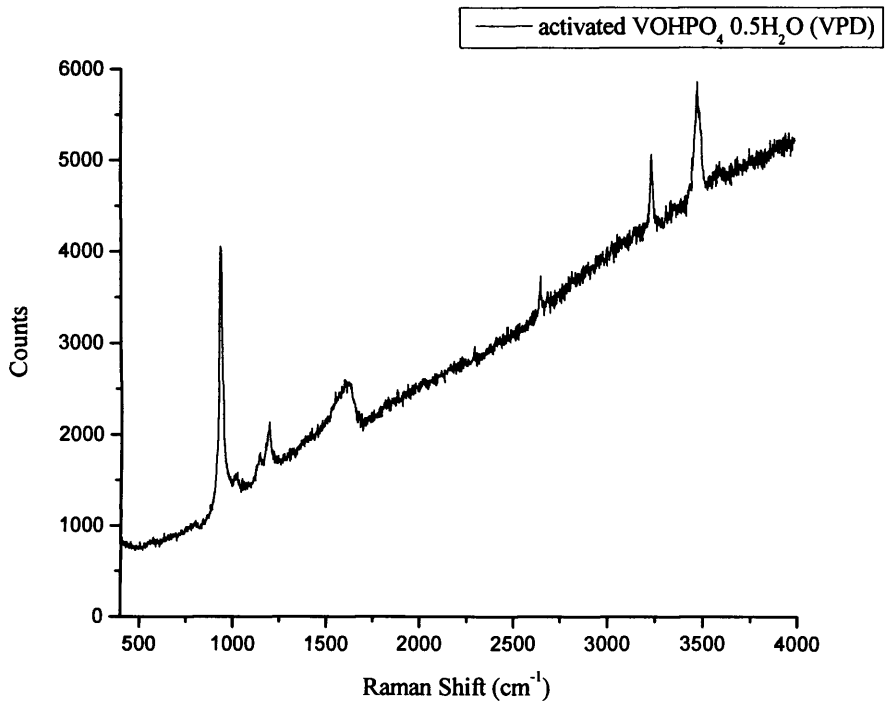

Figure 3.7. Raman of VPD activated with 1.5% butane/air at 400°C for 72 h.

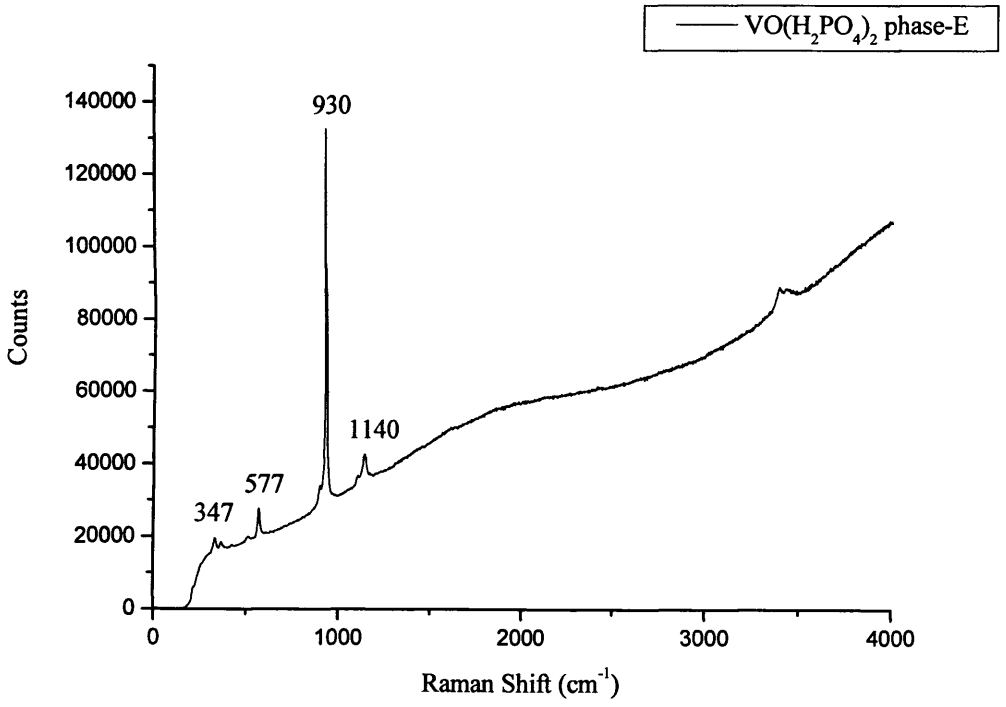

Figure 3.8. Raman of $VO(H_2PO_4)_2$ (phase-E).

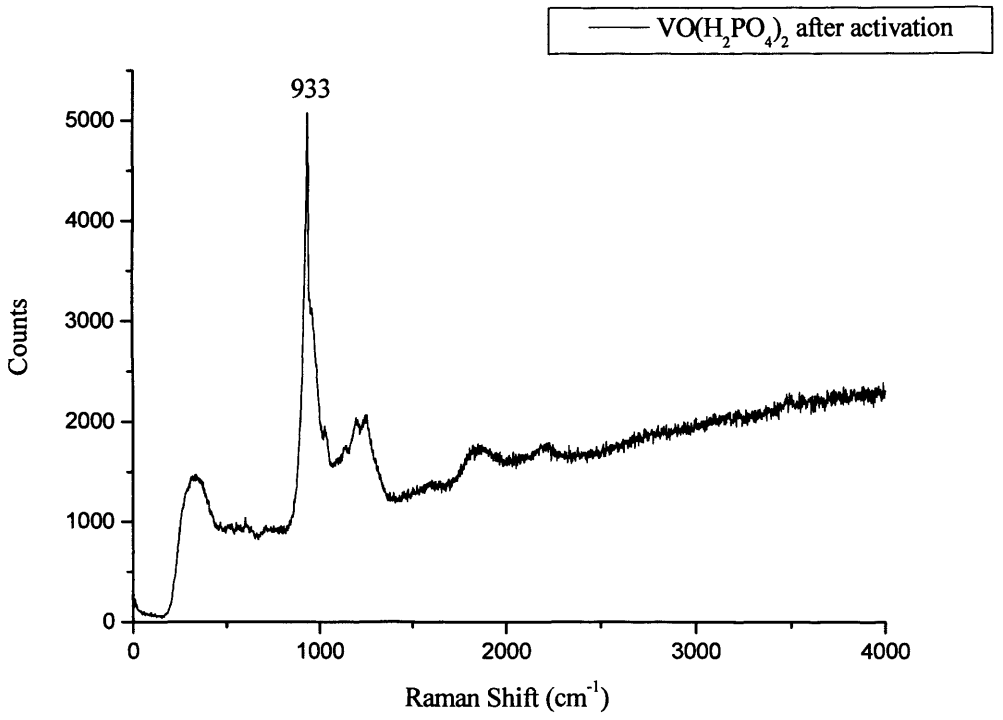

Figure 3.9. Raman of $VO(H_2PO_4)_2$ (phase-E) after activation with 1.5% butane/air at 400°C for 72 h.

3.3.2 Catalytic activity results of VPD and phase E

For the phase E catalyst tested using 1.5% butane/air (Table 3.1), the observed conversion was quite low and high maleic anhydride selectivity was obtained. In the anaerobic conditions, the conversion was even lower between 0.4-1.7% while carbon monoxide as the only product. Similar results were observed when it was tested at 350°C with butane concentration in the range of 0.9-2.9% (Table 3.2). It should be noted that the remarkably increased maleic anhydride selectivity and conversion observed in the aerobic conditions contrast to those accompanied with the anaerobic periodic flow. This suggests that a low surface concentration of a selective oxidising species is available on the surface of $VO(H_2PO_4)_2$ material, but when excess flow air is pressed, this species is diminished in concentration.

Table 3.1. Effect of reaction temperature on the operation in a gas-gas periodic flow reactor over phase E using 1.5% butane/air or butane/argon.

Temp /°C	Butane/air					Butane/Ar followed by O_2				
	Conv %	Sel %			Yield %	Conv %	Sel %			Yield %
		CO_2	CO	MA			CO_2	CO	MA	
330	5.4	21.0	21.5	57.5	3.1	0.4	0	100	0	0
350	5.3	18.0	19.9	62.1	3.3	0.7	0	100	0	0
380	9.6	16.3	18.5	65.2	6.3	0.8	0	100	0	0
400	13.6	14.0	20.2	65.8	8.9	1.7	0	100	0	0

Table 3.2. Effect of reaction concentration on the operation in a gas-gas periodic flow reactor over Phase E at 350°C.

Butane %	Butane/air					Butane/Ar followed by O_2				
	Conv %	Sel %			Yield %	Conv %	Sel %			Yield %
		CO_2	CO	MA			CO_2	CO	MA	
0.9	3.3	12.4	21.5	66.1	2.2	0.6	0	100	0	0
1.5	3.0	15.3	19.4	65.3	2.0	0.7	0	100	0	0
2.1	1.8	14.9	29.0	56.1	1.0	0.6	0	100	0	0
2.9	1.7	16.9	31.8	51.3	0.9	0.6	0	100	0	0

For the VPD catalyst, the lower conversion and selectivity were observed in the absence of co-fed oxygen than those in the presence of oxygen (Table 3.3). It is interesting that furan appeared as a product in anaerobic conditions. Similar results were obtained when the catalyst was tested at 350°C with butane concentration in the range of 0.9-2.9% (Table 3.4). It should be noted that the remarkably decreased maleic anhydride selectivity and conversion observed in the anaerobic conditions contrast to those accompanied with the aerobic periodic flow, but the formation of carbon oxides especially carbon monoxide was enhanced (Table 3.3-3.4).

Table 3.3. Effect of reaction temperature on the operation in a gas-gas periodic flow reactor over VPD using 1.5% butane/air or butane/argon.

Temp /°C	Butane/air					Butane/Ar followed by O_2						
	Conv	Sel %			Yield	Conv	Sel %				Yield %	
	%	CO_2	CO	MA	%	%	CO_2	CO	MA	Furan	MA	Furan
330	64.7	29.0	19.8	51.2	33.1	37.6	19.0	70.2	2.2	8.6	0.8	3.2
350	83.3	36.7	27.8	35.5	29.6	76.9	21.3	60.0	11.9	6.8	9.2	5.2
380	99.5	37.2	34.6	28.2	28.1	99.1	28.0	56.7	13.5	1.8	13.4	1.8
400	100	34.5	41.5	24.0	24.0	100	31.2	57.0	11.4	0.4	11.4	0.4

Table 3.4. Effect of reaction concentration on the operation in a gas-gas periodic flow reactor over VPD at 350 °C.

Butane %	Butane/air					Butane/Ar followed by O_2						
	Conv	Sel %			Yield	Conv	Sel %				Yield %	
	%	CO_2	CO	MA	%	%	CO_2	CO	MA	Furan	MA	Furan
0.9	98.4	16.2	37.2	46.6	45.9	83.9	15.3	57.6	15.4	11.7	12.9	9.8
1.5	83.3	36.7	27.8	35.5	29.6	76.9	21.3	60.0	11.9	6.8	9.2	5.2
2.1	84.6	18.1	35.6	46.3	39.2	80.3	20.3	58.1	12.7	8.9	10.2	7.1
2.9	61.3	13.7	26.7	59.6	36.5	33.0	22.8	50.3	15.4	11.5	5.1	3.8

To compare the catalytic performances between Phase E and VPD in aerobic conditions, the profiles have been shown in Figure 3.10-3.11. Phase E has shown better selectivity to MA than VPD but the conversion in *n*-butane oxidation. The reaction for effect of temperature has been carried out firstly, while the test for *n*-butane concentration follows later on. The reaction for 1.5% *n*-butane/air concentrations will not be performed at 350°C again to save the whole reaction time as the catalyst has been kept in the reaction condition for a relatively long time. Therefore, the data in the table of latter reaction look slightly incompatible with those of 1.5% concentration. According to their yields, VPD is currently better than Phase E

in the butane oxidation to maleic anhydride not only in the aerobic condition but also in the anaerobic environment. From the view of industry, it is worthy of studying how to improve the conversion over Phase E as the gas feed can be recycled.

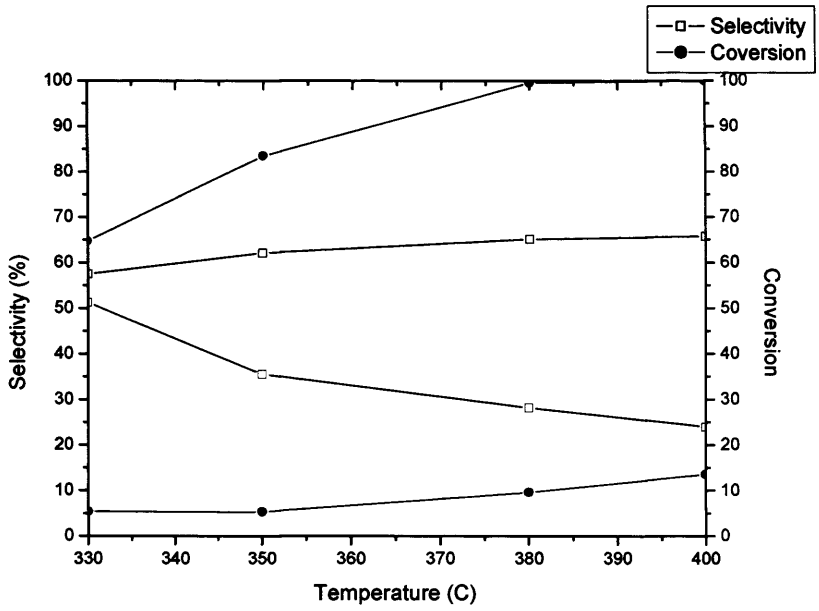

Figure 3.10. Effect of reaction temperature on the operation in a gas-gas periodic flow reactor over Phase E and VPD (red point) using 1.5% butane/air.

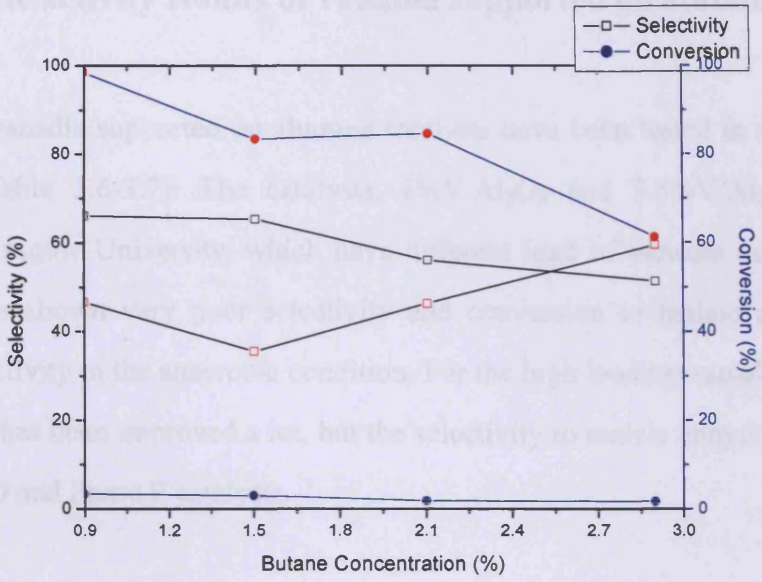

Figure 3.11. Effect of reaction concentration on the operation in a gas-gas periodic flow reactor over Phase E and VPD (red point) using 1.5% butane/air.

Additionally, a confidential catalyst sample marked IDIP51 was tested in both aerobic and anaerobic conditions as well. The results shown in Table 3.5 are similar as phase E.

Table 3.5. Effect of reaction temperature on the operation in a gas-gas periodic flow reactor over IDIP51 using 1.5% butane/air or butane/argon.

Temp /°C	Butane/Air					Butane/Ar followed by O_2				
	Conv %	Sel %			Yield %	Conv %	Sel%			Yield %
		CO_2	CO	MA			CO_2	CO	MA	
330	2.8	11.4	14.6	74.0	2.1	—	—	—	—	—
350	4.9	13.7	15.4	70.9	3.5	—	—	—	—	—
380	9.5	14.3	19.5	66.2	6.3	1.9	0	100	0	0
400	15.2	10.1	25.4	64.5	9.8	5.1	0	100	0	0

3.3.3 Catalytic activity results of vanadia supported on alumina

Two different vanadia supported on alumina catalysts have been tested in a series of temperature (Table 3.6-3.7). The catalysts, $1\%V/Al_2O_3$ and $3.5\%V/Al_2O_3$, were prepared by Glasgow University, which have different load of vanadia on alumina. The former has shown very poor selectivity and conversion to maleic anhydride, especially no activity in the anaerobic condition. For the high loading vanadia catalyst, the conversion has been improved a lot, but the selectivity to maleic anhydride is still lower than VPD and Phase E catalysts.

Table 3.6. Effect of reaction temperature on the operation in a gas-gas periodic flow reactor over $1\%V/Al_2O_3$ using 1.5% butane/air or butane/argon.

Temp /°C	Butane/Air					Butane/Ar followed by O_2				
	Conv %	Sel %			Yield %	Conv %	Sel%			Yield %
		CO_2	CO	MA			CO_2	CO	MA	
330	0.2	63.5	36.5	0	0	0	0	0	0	0
350	0.3	65.2	34.8	0	0	0	0	0	0	0
380	0.4	63.3	36.7	0	0	0	0	0	0	0
400	0.6	62.8	37.2	0	0	0	0	0	0	0

Table 3.7. Effect of reaction temperature on the operation in a gas-gas periodic flow reactor over $3.5\%V/Al_2O_3$ using 1.5% butane/air or butane/argon.

Temp /°C	Butane/air						Butane/Ar followed by O_2				
	Conv %	Sel %				Yield %	Conv %	Sel %			Yield %
		CO_2	CO	MA	Furan			CO_2	CO	MA	
330	48.1	21.8	46.6	25.7	5.9	12.4	56.3	19.6	76.4	4.0	2.3
350	81.7	16.9	37.5	32.2	13.4	26.3	79.8	21.3	74.9	3.8	3.0
380	98.8	21.3	41.9	28.3	8.5	28.0	98.4	24.0	72.3	3.7	3.6
400	100	22.5	44.1	27.0	6.4	27.0	100	25.6	70.5	3.9	3.9

3.3.4 Conclusions

Usually, commercial VPO catalysts are mixtures which primarily consist of $VOHPO_4 \cdot 0.5H_2O$ and $VO(H_2PO_4)_2$. The former is the major component of VPD, while Phase E is mainly made up of the latter one. In fact, the XRD pattern of VPD has shown that the dominant feature is the rosette structure as there is a remarkable peak corresponding to the [220] reflection while phase E being the counterpart of the platelet morphology. According to above-mentioned results, following conclusions have been drawn.

Under anaerobic condition, the catalytic performances of $VO(H_2PO_4)_2$ and VPD decrease. Over VPD, furan could be observed in the anaerobic environment while the formation of carbon monoxide was enhanced. $VO(H_2PO_4)_2$ shows enhanced selectivity in aerobic periodic flow and there is no selectivity to maleic anhydride in the absence of oxygen. The high loading vanadia supported on alumina is more reactive than the lower one. No selectivity to maleic anhydride for the latter can be observed in both aerobic and anaerobic flow.

Based on previous work [25], some typical catalysts such as VPD and 3.5% V/Al_2O_3 have been compared with standard VPO catalyst in a continuous flow reactor, as shown in Table 3.8. VPD has shown better catalytic performances with both selectivity to maleic anhydride and conversion than that of standard VPO catalyst. Figure 3.12 also summarizes the performances of above-mentioned catalysts for *n*-butane oxidation in terms of a selectivity-conversion plot. In morphological view point, it has proved that the catalysts with rosette structure have the considerably higher activity than the platelet morphology. On the other hand, the platelet structures are more selective than rosette ones. Horowitz *et al.* suggested that this is due to the rosette structure obscuring the active plane [26].

Clearly, the traditional continuous flow reactor cannot give data of transient reaction, while the periodic flow reactor operated in a gas-gas flow could do. In the latter transient operation, the reactants could only react incompletely during the short time of contact so that more by-products of partial oxidation are produced. As many commercial operations of *n*-butane oxidation are performed above 80% conversion at a limiting selectivity of about 65% [27], the periodic flow reactor has offered an alternative route for heterogeneous catalysis. The selectivity to target products is usually lower than that in continuous flow reactor. In another word, it could be expected that a catalyst that gives high selectivity to products in the periodic flow operation have better catalytic performances in a continuous flow reactor.

These are just the initial work of periodic gas-gas flow reactor. The morphologies of vanadia species have not been applied in the operation. Therefore, it is necessary that the comparison of the catalytic effect for different morphologies be studied further in the future work.

Table 3.8. Effect of reaction temperature on the operation in a continuous flow reactor over VPO (in previous work), VPD and 3.5% V/Al_2O_3.

	Temp /°C	Conv %	Sel % (MA)	Yield %
VPO	380	19.8	63.8	12.6
	400	29.9	61.4	18.4
VPD	380	45.2	67.2	30.4
	400	60.4	63.5	38.4
3.5% V/Al_2O_3	380	75.0	16.2	12.0
	400	86.4	17.1	14.7

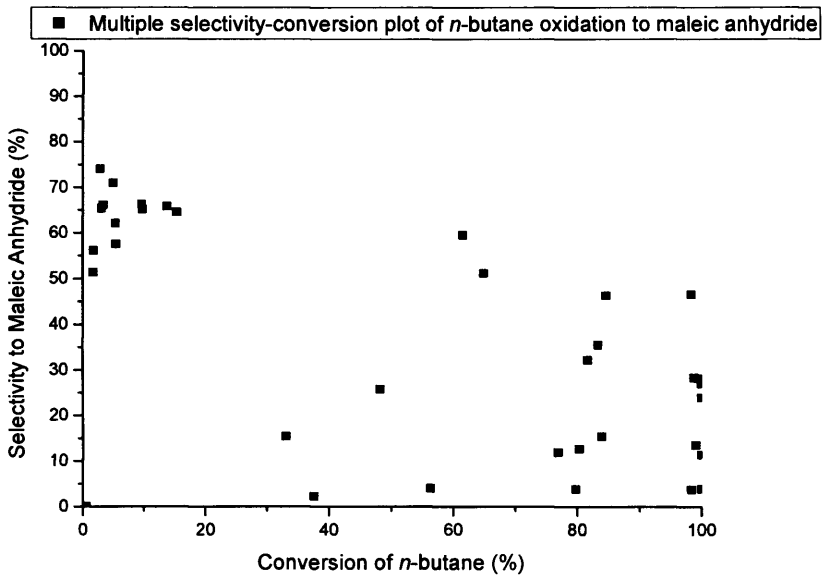

Figure 3.12. Multiple selectivity-conversion plot for *n*-butane selective oxidation to maleic anhydride over catalysts tested in this work. in a variety of reaction conditions.

3.4. References

[1] Dmuchovsky, B., Franz, J. E., "Maleic Anhydride", *Kirk-Othmer Encyclopedia of ChemicalTechnology, Volume 12*, John Wiley and Sons, Inc., New York, NY, 1967, pp. 819-837.

[2] Hutchings G. J., *Appl. Catal.* **1991**, *72*, 1.

[3] Contractor R. M., US Patent 4668802 (1987), assigned to E. I. Du Pont de Nemours and Co.

[4] Contractor R. M., Bergna H. E., Horowitz H. S., Blackstone C. M., Malone B., Torardi C. C., Griffiths B., Chowdhry U., Sleight A. W., *Catal. Today* **1987**, *1*, 49.

[5] Contractor R. M., Sleight A. W., *Catal. Today* **1988**, *3*, 175.

[6] Contractor R. M., Garnett D. I., Horowitz H. S., Bergna H. E., Patience G. S., Schwartz J. T., Sisler G. M., *Stud. Surf. Sci. Catal.* **1994**, *82*, 233.

[7] Contractor R. M., *Chem. Eng. Sci.* **1999**, *54*, 5627.

[8] Emig G., Uihlein K., Hacker C.-J., New Developments in Selective Oxidation II, Elsevier (Eds, V. Cortes Corberan, S. Bellon) 1994, 243.

[9] Yongsunthon I., Alpay E., *Chem. Eng. Sci.* **1999**, *54*, 2647.

[10] Bergman, R. L., Frisch, N. W., *U.S. Pat.*, **1966**, 3 293 268.

[11] Horowitz, H. S., Blackstone, C. M., Sleight, A. W., Teufer, G., *Appl. Catal.* **1988**, *38*, 211.

[12] Johnson, J. W., Johnston, D. C., Jacobson, A. J., Brody, J. F., *J. Am. Chem. Soc.* **1984**, *106*, 8123.

[13] Centi G., Trifiro F., Ebner J. R., Franchetti V. M., *Chem. Rev.* **1988**, *88*, 55.

[14] Volta J.-C., Bere K., Zhang Y. J., Olier R., in: Ted Oyama S., Hightower J. W. (Eds.), Catalytic selective oxidation, ACS Symposium Series 523, ACS Washington DC, 1993, p.217.

[15] Volta J.-D., *Catal. Today* **1996**, *32*, 29.

[16] Okuhara T., Misono M., *Catal. Today* **1993**, *16*, 61.

[17] Schuurmann Y., Gleaves J. T., *Ind. Eng. Chem. Res.* **1993**, *33*, 2935.

[18] Bordes E., *Catal. Today* **1996**, *16*, 61.

[19] Herrmann J.-M., Vernoux P., Bere K. E., Abon M., *J. Catal.* **1997**, *167*, 106.

[20] Ruiz P., Bastians P., Caussin L., Reuse R., Daza L. Acosta D., Delmon B., *Catal. Today* **1993**, *16*, 99.

[21] Sananes, M. T., Ellison, I. J., Sajip, S., Burrows, A., Kiely, C. J., Volta, J. C., Hutchings, G. J., *J. Chem. Soc. Faraday Trans.* **1996**, *92(1)*, 173.

[22] Bartley, J. K., Wells, R. P. K., Hutchings, G. J., *J. Cat.* **2000**, *195*, 423.

[23] Ellison, I. J., Hutchings, G. J., Sananes, M. T., Volta, J. C., *J. Chem. Soc. Chem. Commun.* **1994**, 1093.

[24] Bartley, J. K., Rhodes, C., Kiely, C. J., Carley, A. F., Hutchings, G. J., *Phys. Chem. Chem. Phys.* **2000**, *2*, 4999.

[25] Song, N. X., Xuan, Z. Q., Bartley, J. K., Taylor, S. H., Chadwick, D., Hutchings, G. J., *Catal. Lett.* **2006**, *106(3-4)*, 127.

[26] Jackson, S. D., Hargreaves, J. S. J., Metal Oxide Catalysis, Wiley-VCH, 2008, Volume 2, p511.

[27] Batiot, C., Hodnett, B. K., *Appl. Catal. A General* **1996**, *137*, 179.

Chapter 4.

Gas-phase selective epoxidation of propylene to propylene oxide over catalysts supported on zinc oxide

4.1 Introduction

Propylene oxide (PO) is one of the most important chemical feedstocks for producing polyurethane, propylene glycols, resins, etc. Polyether polyols consume 60-70% of PO, which are one of the main components in polyurethane production. Propylene glycols make up the second largest share of PO usage, while propylene-based glycol ethers consume about 5%. 6 million metric tons of PO are approximately produced worldwide with an average annual growth rate of 5% [1]. Industrial production of propylene oxide is mainly from co-oxidation of propylene with other chemicals.

In 2005, about half of the world production was yielded through chlorohydrin technology which could be described as following process.

Propylene + Chlorine + Lime (chlorine absorber) → PO + $CaCl_2$

Additionally, one third of PO production was from PO/SM technology, and the other came from PO/TBA technology.

Propylene + ethylbenzene → PO + styrene **(PO/SM)**

Propylene + isobutene → PO + t-butyl alcohol **(PO/TBA)**

The above two technologies, also called the Halcon method [2, 3], create large amounts of additional side products. These processes are reported to be complex and need heavy capital investment.

The oxidation of propylene to propylene oxide without any co-product in a more environmental friendly way has been an important objective for chemists. In April 2003, Sumitomo Chemical commercialised the first PO-only plant in Japan, which produces propylene oxide from oxidation of cumene over titanium-based catalysts without significant production of other products [4]. This is a variant of the PO/SM process that uses cumene instead of ethylbenzene and recycles the coproducts via dehydration and hydrogenation back to cumene.

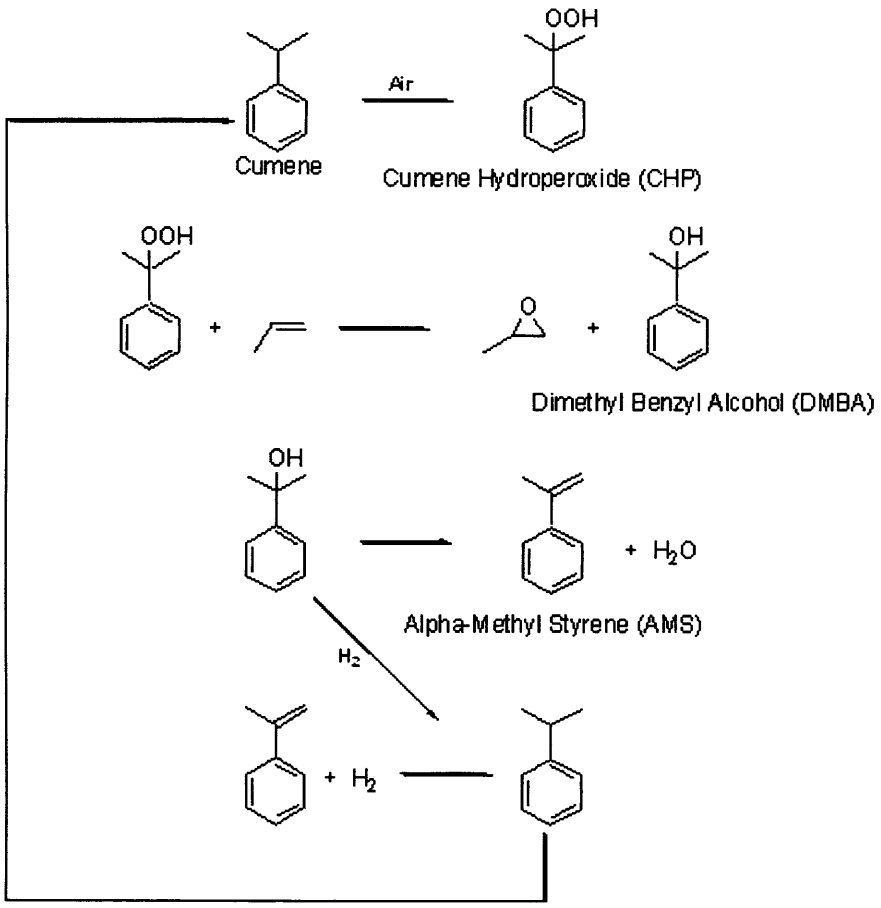

Figure 4.1. The process applied by Sumitomo Chemical.

The difficulty in the direct epoxidation of propylene is primarily owing to the facile abstraction of the hydrogen in labile allylic atoms, which results in combustion rather than selective epoxidation [5, 6]. In current research, TS-1 (titanium silicalite-1) has been reported a catalyst in alternative direct epoxidation processes, in which hydrogen peroxide can be efficiently used for the selective epoxidation of propylene to PO (*ca.* 95% selectivity) [7]. However, the drawback of the process is that propylene oxide and hydrogen peroxide have comparable market values.

$$C_3H_6 + H_2O_2 \rightarrow C_3H_6O + H_2O$$

In the new HPPO-Process recently developed by BASF and Dow Chemical, the defect of the high cost of hydrogen peroxide for propylene epoxidation has been resolved using the *in situ* production of hydrogen peroxide, while no byproducts other than water are generated. The first technical plant is currently being built in Antwerp and due to begin production in 2008 [8]. On the other hand, a direct propylene epoxidation process over molten salt has been published by Olin, which gives a PO selectivity of 65% and propylene conversion of 15% at a pressure of 20 bar and a temperature of 473K [9].

Propylene expoxidation using nitrous oxide (N_2O) as an oxidant has also been reported [10, 11]. Panov represented the selective oxidation over Fe-ZSM-5 zeolite can be performed using N_2O [12]. Wang's group reported a process with PO selectivity of 80% at propylene conversion of 5% over a potassium-promoted iron oxide on SBA-15 catalyst [13]. Recently, the effect of alkali metal salts on SBA-15 supported iron catalysts for propylene epoxidation using N_2O has been studied in detail [14]. However, studies about N_2O for propylene epoxidation are relatively rare and the major defect is that N_2O is not commercially available in large quantities.

In 1998, Haruta [15] published that supported gold catalyst could give extremely high selectivity to PO (almost 100%) despite at low conversion. Furthermore, the conversion of 9.8% and selectivity to PO, *ca.* 90%, over a gold catalyst supported on 3D mesoporous silylated titanosilicates using a mixture of hydrogen and oxygen, have been published by his group [16]. It is worthy of being noted that hydrogen is necessary as a sacrificial feed gas in this catalysis process, while its efficiency is insufficient, typically <30%. The problems about catalyst deactivation and hydrogen efficiency need be further resolved in order of commercial requirements [17,18].

Recently, more and more studies have been carried out on propylene epoxidation using only molecular oxygen over supported metal or mixed metal catalysts. Lambert [19] has shown Cu/SiO_2 catalysts prepared by either a micro-emulation technique or an impregnation method, has a potential for the direct gas-phase epoxidation of propylene by O_2 at atmospheric pressure, which gives the highest selectivity to PO *ca.*

53% at propylene conversion, *ca.* 0.25%. The catalysts performance is comparable with that published by Haruta's group in their first paper on TiO_2 supported gold catalyst. Li *et al.* [20] also represented the direct epoxidation of propene by molecular oxygen over a NaCl-modified $VCe_{1-x}Cu_x$ oxide catalyst. The selectivity to PO of 43% was obtained at 0.19% propylene conversions. These two studies propose that metallic Cu(0) may be the major active phase over Cu-based materials for direct propylene epoxidation.

Wang also reported that a halogen-free K^+-modified CuOx/SBA-15 catalyst which was much better than other Cu-based catalysts reported for direct propylene epoxidation. Selectivity to PO could be kept between *ca.* 15-50%, while the propylene conversion increased from *ca.* 1 to 12% [21]. Wang suggested that it was not the metallic Cu(0), but the copper of some oxidized state that accounted for the propylene epoxidation by molecular oxygen. If so, the nature and active sites on supported Cu catalysts are complicated and further investigation are necessary [19-21].

Copper or copper-based catalysts were referred in the above-mentioned studies quite frequently. It is indicated Cu could be potentially an inexpensive catalyst for propylene epoxidation. The aim of research is to look for novel supported catalysts for epoxidation of propylene to PO only using molecular oxygen but hydrogen. This chapter focuses on the direct gas-phase epoxidation of propylene to PO using only molecular oxygen over copper-based catalysts in which ZnO are mainly used as support.

4.2 Experimental

4.2.1 Catalyst preparation

4.2.1.1 Preparation of Ni, Ag, Cu or Au supported on ZnO catalysts

A 2wt% Ni supported on ZnO catalyst was prepared by a wet impregnation method. The procedure is as follows: 98% $Ni(NO_3)_2 \cdot 6H_2O$ (0.202g) was dissolved in deionised water (10ml) and 99.9% ZnO (1.873g) was impregnated by this solution and then vigorously stirred for 2h. The catalyst was then dried at 80°C for 16h.

A 2wt% Ag supported on ZnO catalyst was prepared by a wet impregnation method. The procedure is as follows: silver nitrate ($AgNO_3$, 0.063g) was dissolved in deionised water (10ml) and 99.9% ZnO (1.937g) was impregnated by this solution and then vigorously stirred for 2h. The catalyst was then dried at 80°C for 16h.

A 2wt% Cu supported on ZnO catalyst was prepared by a wet impregnation method, similar to the preparation of Ag catalyst: 98% $CuNO_3 \cdot 2.5H_2O$ (0.150g) was dissolved in deionised water (10ml) and 99.9% ZnO (1.879g) was impregnated by this solution and then vigorously stirred for 2h. The catalyst was then dried at 80°C for 16h.

A 2wt% Au supported on ZnO catalyst was prepared by a wet impregnation method, similar to the preparation of Ag catalyst: $HAuCl_4 \cdot 3H_2O$ (0.145g) was dissolved in deionised water (10ml) and 99.9% ZnO (2g) was impregnated by this solution and then vigorously stirred for 2h. The catalyst was then dried at 80°C for 16h.

All catalysts were treated at 450°C in air or 5%H_2/Ar for 2h before reaction.

4.2.1.2 Preparation of Cu-Ni, Cu-Ag or Cu-Au bimetallic supported on ZnO catalysts

A 2wt-2wt% Cu-Ni supported on ZnO catalyst was prepared by a wet impregnation method. The procedure is as follows: 98% $Ni(NO_3)_2 \cdot 6H_2O$ (0.202g) and 98% $CuNO_3 \cdot 2.5H_2O$ (0.150g) were dissolved in deionised water (10ml) and 99.9% ZnO (1.752g) was impregnated by this solution, and then vigorously stirred for 3h. The catalyst was then dried at 80°C for 16h. Catalysts were treated at 450°C in air, N_2 or 5%H_2/Ar for 2h.

A 5wt-2wt% Cu-Ni supported on ZnO catalyst was prepared by a wet impregnation method. The procedure is as follows: 98% $Ni(NO_3)_2 \cdot 6H_2O$ (0.202g) and 98% $CuNO_3 \cdot 2.5H_2O$ (0.375g) were dissolved in deionised water (10ml) and 99.9% ZnO (1.568g) was impregnated by this solution, and then vigorously stirred for 3h. The catalyst was then dried at 80°C for 16h. Catalysts were treated at 450°C in air, N_2 or 5%H_2/Ar for

2h.

A 2wt-2wt% Cu-Ag supported on ZnO catalyst was prepared by a wet impregnation method. The procedure is as follows: $AgNO_3$ (0.063g) and 98% $CuNO_3 \cdot 2.5H_2O$ (0.150g) were dissolved in deionised water (10ml) and 99.9% ZnO (1.787g) was impregnated by this solution, and then vigorously stirred for 3h. The catalyst was then dried at 80°C for 16h. Catalysts were treated at 450°C in air or 5%H_2/Ar for 2h.

A 2wt-2wt% Cu-Au supported on ZnO catalyst was prepared by a wet impregnation method. The procedure is as follows: $HAuCl_4 \cdot 3H_2O$ (0.145g) and 98% $CuNO_3 \cdot 2.5H_2O$ (0.150g) were dissolved in deionised water (10ml) and 99.9% ZnO (1.787g) was impregnated by this solution, and then vigorously stirred for 3h. The catalyst was then dried at 80°C for 16h. Catalysts were treated at 450°C in air or 5%H_2/Ar for 2h.

4.2.1.3 Preparation of Cu-Ag-Ni trimetallic supported on ZnO catalysts

A 2wt-2wt-2wt% Cu-Ag-Ni supported on ZnO catalyst was prepared by a wet impregnation method. The procedure is as follows: $AgNO_3$ (0.063g), 98% $CuNO_3 \cdot 2.5H_2O$ (0.150g) and 98% $Ni(NO_3)_2 \cdot 6H_2O$ (0.202g) were dissolved in deionised water (10ml) and 99.9% ZnO (1.689g) was impregnated by this solution, and then vigorously stirred for 3h. The catalyst was then dried at 80°C for 16h. Catalysts were treated at 450°C in air or 5%H_2/Ar for 2h.

All catalysts were not washed further with ionized water. The weight percentage of loading denotes calculation values in the catalyst preparation. Some real values of loading detected by EDX have been claimed in the results and discussion.

4.2.2 Reaction conditions

The propylene expoxidations were performed in a fixed-bed tube reactor as shown in Figure 4.2 and 4.3. The reaction temperature was increased from 180°C to 250°C where 0.1g catalyst was applied. Then the temperature was going to be set fluctuated

between a low point (such as 200°C) and a comparatively high temperature (such as 220°C). This process was to test used catalyst performance and to collect time-on-line data. The volume ratio of propylene: oxygen: helium was 22: 4: 74 and the GHSV (gas hourly space velocity) was 47760h^{-1} based on the total flow rate. The analysis of reaction products were carried out with a Varian Star 3800 fitted with a TCD and FID detector. Standard calibration cylinders containing known concentrations of PO and CO_2 were used to quantify the amount of PO and CO_2 generated during the reaction.

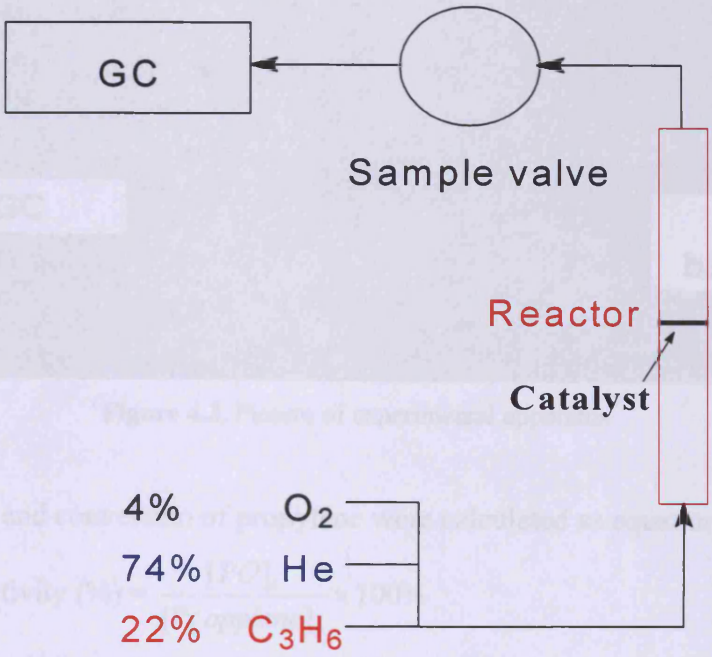

Figure 4.2. Scheme of experimental apparatus.

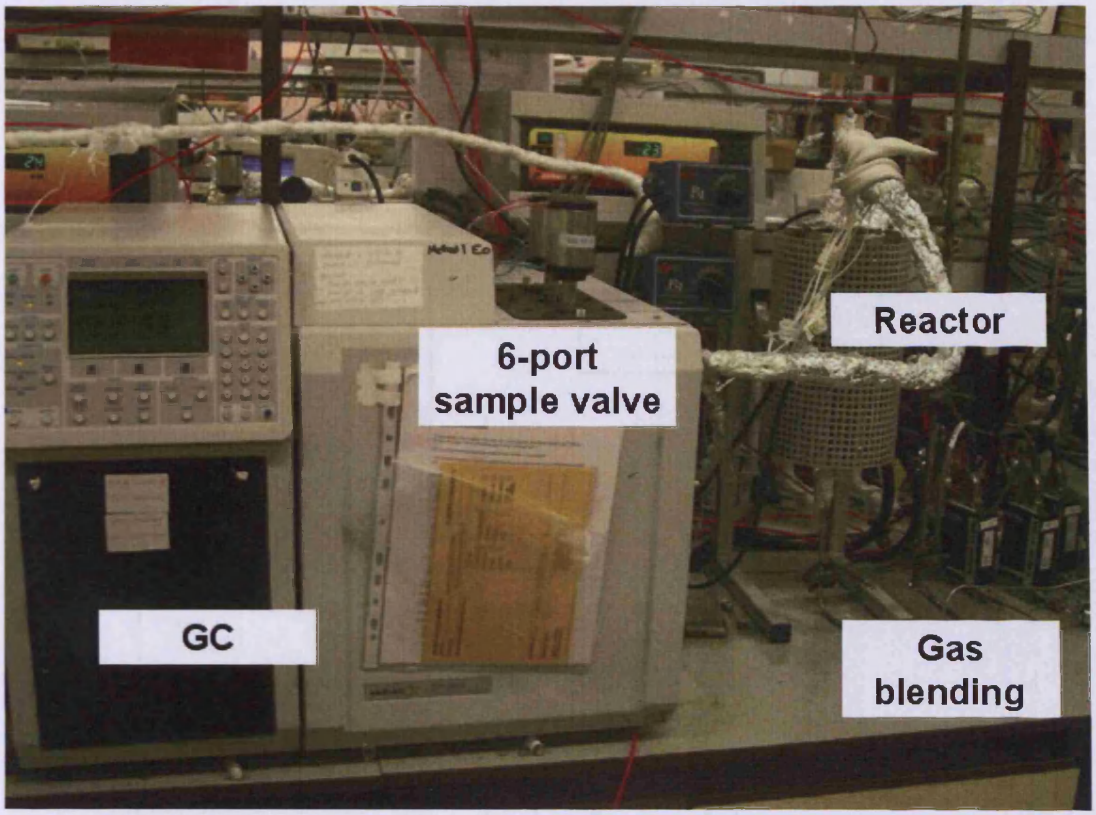

Figure 4.3. Picture of experimental apparatus

The selectivity and conversion of propylene were calculated as equations (4.1-4.3):

$$\text{PO selectivity (\%)} = \frac{[PO]_t}{[\text{Pr}opylene]_c} \times 100\% \quad (4.1)$$

$$\text{CO}_2\text{ selectivity (\%)} = \frac{[CO_2]_t}{3[\text{Pr}opylene]_c} \times 100\% \quad (4.2)$$

$$\text{Propylene conversion (\%)} = \frac{[PO]_t + [CO_2]_t / 3}{[\text{Pr}opylene]_i} \times 100\% \quad (4.3)$$

Where $[PO]_t$ and $[CO_2]_t$ are the concentrations, vol%, of PO and CO_2 at time t, respectively; $[Propylene]_c$ is the concentration of converted propylene, while $[Propylene]_i$ is the initial concentration, vol%, of propylene.

4.3 Results and discussion

4.3.1 Characterization of ZnO supports and catalysts

4.3.1.1 XRD analysis of ZnO

The XRD patterns of regular and nano-powder ZnO have been shown in Figure 4.4.

The nano-powder ZnO has a similar XRD as regular ZnO since there are not many differences between both of the particle sizes. The strongest scatter (002) peak can be observed, which has been reported by many researchers [22-25].

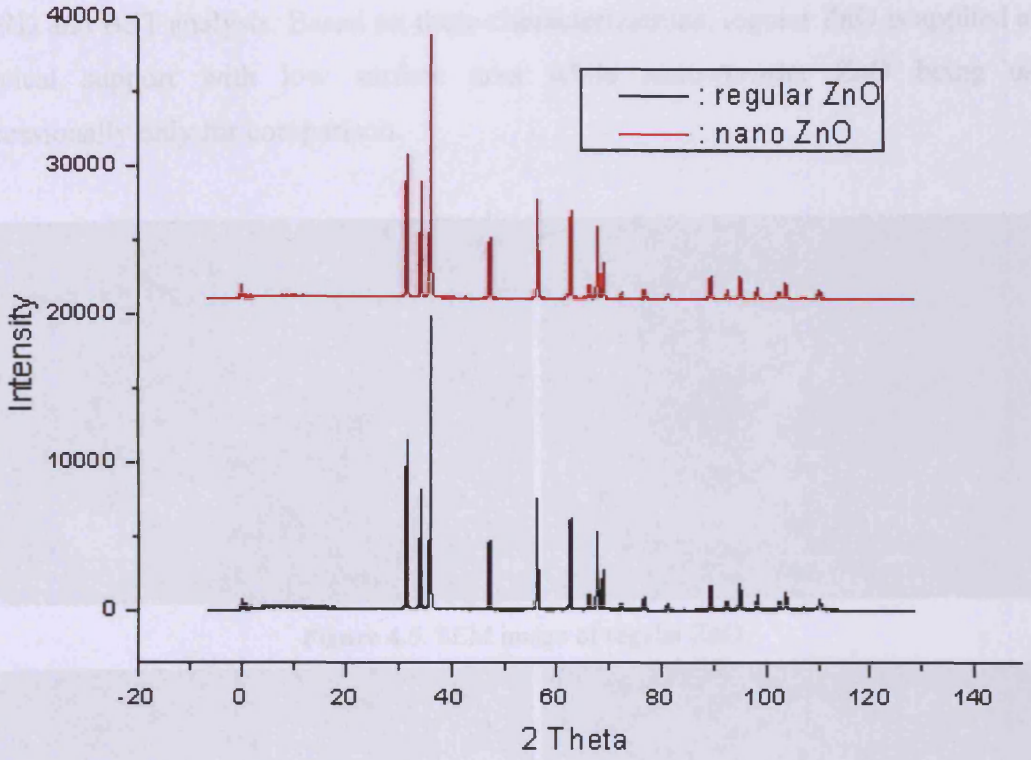

Fig.4.4. XRD pattern of regular and nano-powder ZnO.

4.3.1.2 BET analysis of ZnO supports

Table 4.1 compares the surface area between regular and nano-powder ZnO. They both have the low surface area. The surface area of the final catalysts supported on ZnO does not change a lot after pre-treatments.

Table 4.1 Surface area of ZnO supports by BET analysis.

Support materials	Surface area (m^2/g)
Regular ZnO	8
ZnO nanopowder	12

4.3.1.3 SEM images of ZnO supports

The SEM images in Figure 4.5 and 4.6 have shown few differences between regular and nano-powder ZnO. Both of the surface morphologies are quite similar, which indicates that there is not any distinct differences between them as the particle size of regular ZnO is just a little bit bigger than that of nano-powder. It is in accordance with XRD and BET analysis. Based on these characterizations, regular ZnO is applied as a typical support with low surface area while nano-powder ZnO being used occasionally only for comparison.

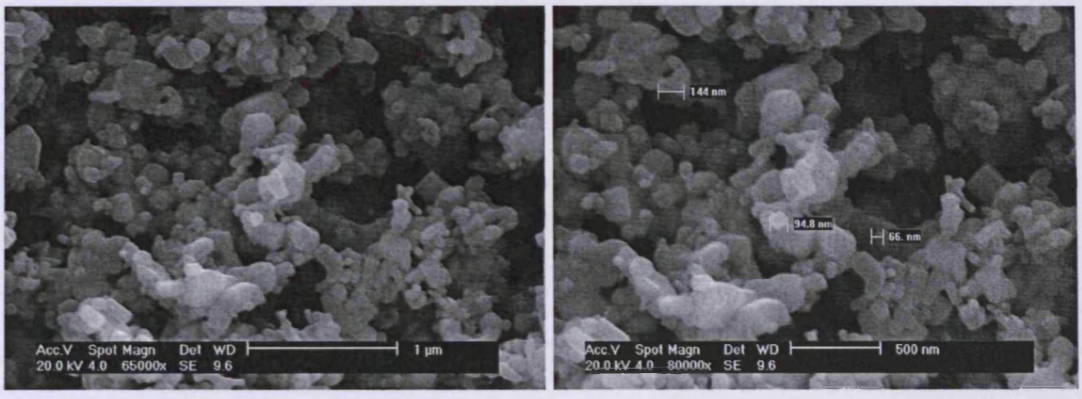

Figure 4.5. SEM image of regular ZnO.

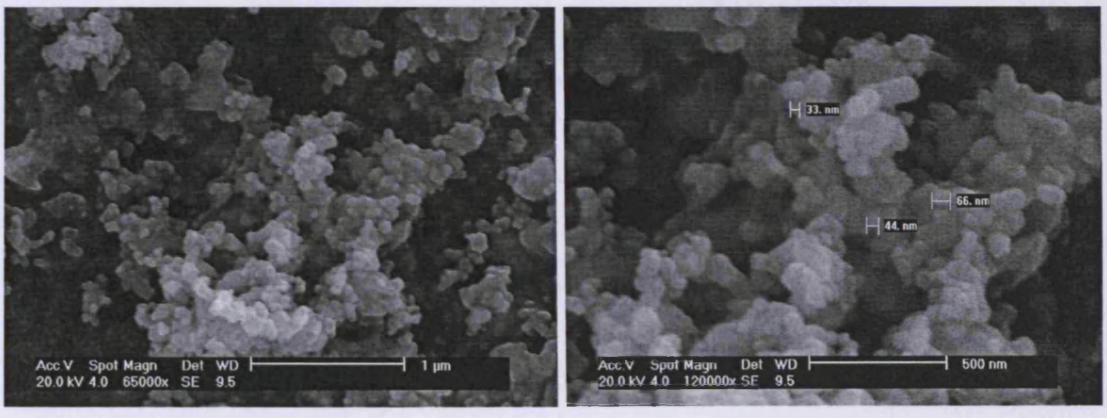

Figure 4.6. SEM image of nano-powder ZnO.

4.3.2 Calibration for PO and CO_2 by FID and TCD detector

The calibration and analysis for PO were performed with an FID detector, while that for CO_2 was carried out with a TCD detector. The concentrations, vol%, of PO and CO_2 at time t, $[PO]_t$ and $[CO_2]_t$ can be deducted by equations (4.4-4.5), where ${}^{PO}A_t$ and ${}^{CO2}A_t$ are the counts of peak area at time t, while ${}^{PO}A_c$ and ${}^{CO2}A_c$ are the counts of peak area at standard concentrations $[PO]_c$ and $[CO_2]_c$, separately.

$$[PO]_t = [PO]_c \frac{{}^{PO}A_t}{{}^{PO}A_c} \quad (4.4)$$

$$[CO_2]_t = [CO_2]_c \frac{{}^{CO2}A_t}{{}^{CO2}A_c} \quad (4.5)$$

Two calibration curves for PO and CO_2 were obtained in Fig 4.7 and 4.8, respectively.

Table 4.2 PO calibration (Peak counts of PO = 13.83366[PO])

[PO] in gas mixtures (ppm)	Peak counts
0	0
59.28	807.6
98.8	1304.8
197.6	2697
296.4	4147.8

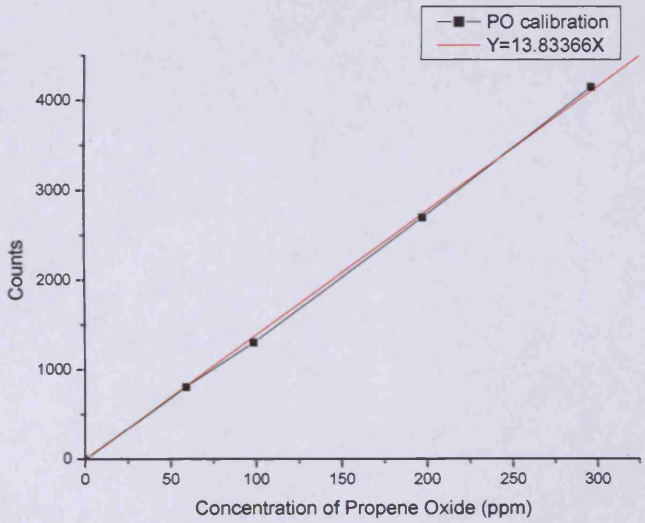

Figure 4.7. Calibration of [PO] by FID detector.

Table 4.3 CO_2 calibration (Peak counts of CO_2 = 1.5627[CO_2])

[CO_2] in gas mixtures (ppm)	Peak counts
0	0
102.95	149.9
205.9	319.5
308.85	439.8
452.98	740.6

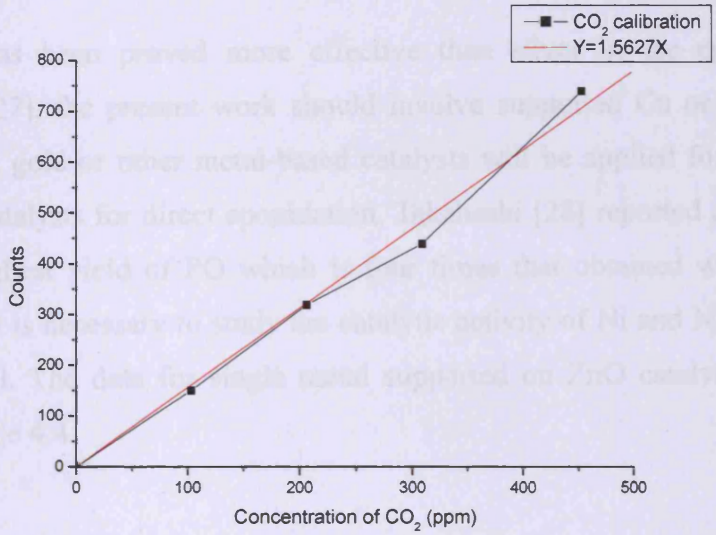

Figure 4.8. Calibration of [CO_2] by TCD detector.

4.3.3 Propylene epoxidation over Ag, Au, Cu or Ni supported on ZnO catalysts

In direct oxidation of ethylene to ethylene oxide (EO), Ag-based catalysts have been applied industrially for many years. In principal, ethylene epoxidation, as one of the least exothermic of industrial oxidations, is atom efficient while there is a strong thermodynamic driving force towards the total oxidation, as shown in equations (4.6-4.7).

Selective oxidation: $C_2H_4 + 1/2O_2 \rightarrow C_2H_4O$ (EO) $\quad \Delta G = -404$ kJ/mol (4.6)

Total oxidation: $C_2H_4 + 3O_2 \rightarrow 2CO_2 + 2H_2O$ $\quad \Delta G = -1315$ kJ/mol (4.7)

However, compared to the selective oxidation of ethylene, propylene epoxidation is much difficult to take place according to thermodynamic point of view [26] in equations (4.8-4.9).

Selective oxidation: $C_3H_6 + 1/2O_2 \rightarrow C_3H_6O$ (PO) $\quad \Delta G = -88.5$ kJ/mol (4.8)

Total oxidation: $C_3H_6 + 9/2O_2 \rightarrow 3CO_2 + 3H_2O$ $\quad \Delta G = -1957$ kJ/mol (4.9)

This is owing to the abstraction of allylic hydrogen atoms, which prefers combustion to epoxidation to PO.

Since copper has been proved more effective than silver in the epoxidation of propylene [19, 27], the present work should involve supported Cu or copper-based catalysts. Silver, gold or other metal-based catalysts will be applied for comparison. For Ag-based catalysts for direct epoxidation, Takahashi [28] reported addition of Ni afforded the highest yield of PO which is four times that obtained with Ag single catalyst. Thus, it is necessary to study the catalytic activity of Ni and Ni-mixed metal catalysts as well. The data for single metal supported on ZnO catalysts have been shown from Table 4.4.

Table 4.4. Results of propylene epoxidation over 2%Cu/ZnO, 2%Ag/ZnO and 2%Au/ZnO pre-treated in 5% H_2/Ar 450°C for 2h, respectively.

Catalyst	Temp (°C)	Selectivity to PO (%)	Conversion (%)
2%Cu/ZnO (pre-treated in 5% H_2/Ar 450°C for 2h)	200	60.6	0.007
	210	53.7	0.010
	220	46.9	0.016
	230	46.0	0.026
	240	45.6	0.047
	230	47.2	0.027
	220	50.1	0.015
	210	55.4	0.010
	220	50.2	0.017
	230	46.5	0.029
	220	57.0	0.017
2%Ag/ZnO (pre-treated in 5% H_2/Ar 450°C for 2h)	230	21.4	0.003
	240	19.2	0.005
	250	28.9	0.008
	240	25.3	0.006
	230	25.9	0.005
	240	21.4	0.008
	230	35.0	0.006
2%Au/ZnO (pre-treated in 5% H_2/Ar 450°C for 2h)	260	-	0.003
	270	-	0.004
	280	55.0	0.007
	290	50.4	0.010
	300	47.8	0.013
	290	48.3	0.010
	280	49.9	0.008
	270	51.4	0.008
	280	48.0	0.010
	270	46.8	0.006

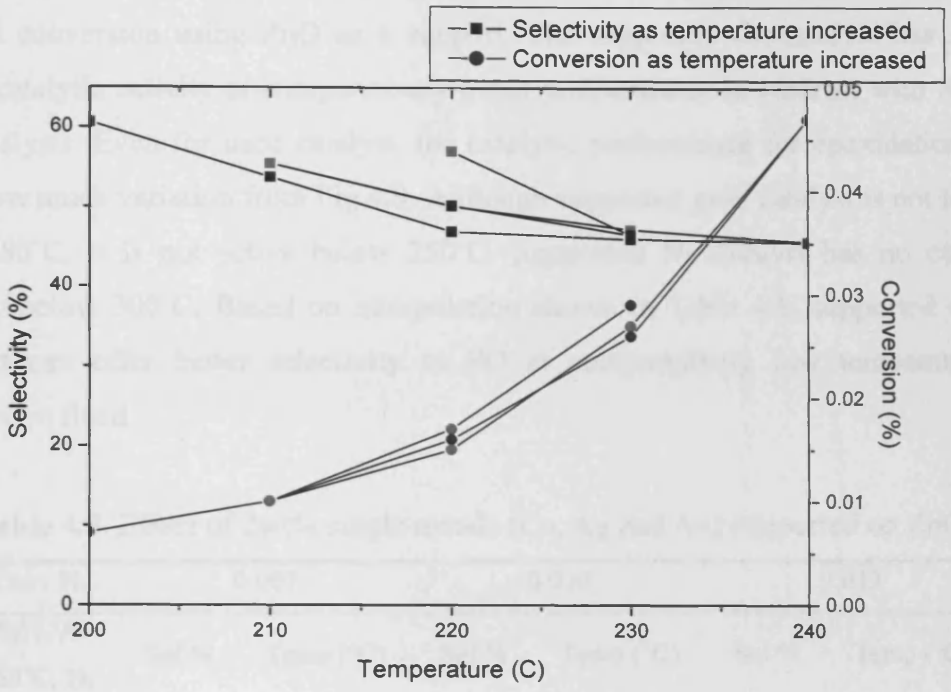

Figure 4.9. Catalytic performance for selective epoxidation of propylene using 2%Cu/ZnO catalyst between 200-240°C. (Red points represented the catalytic activity as temperature decreased.)

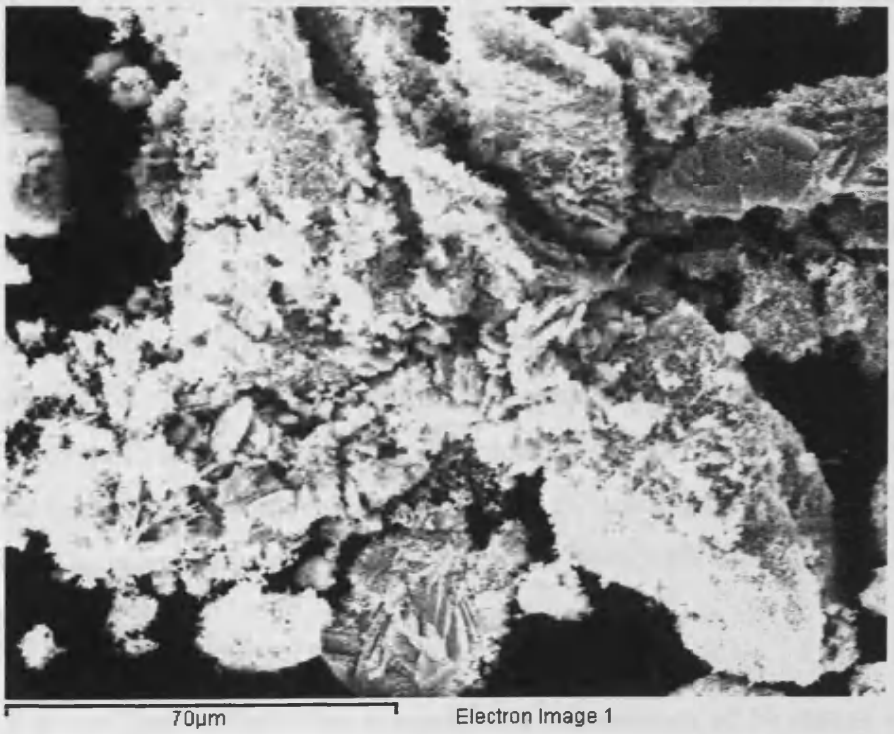

Figure 4.10. SEM image of 2%Cu/ZnO.

Based on the data among Table 4.4, it is shown that supported Cu catalyst has the highest conversion using ZnO as a support. The supported Cu catalyst has shown better catalytic activity at comparatively lower temperatures in contrast with Ag and Au catalysts. Even for used catalyst, the catalytic performance for epoxidation does not show much variation from Fig 4.9. Although supported gold catalyst is not too bad over 280°C, it is not active below 250°C. Supported Ni catalyst has no catalytic activity below 300°C. Based on interpolation shown in Table 4.5, supported copper catalyst can offer better selectivity to PO at comparatively low temperature as conversion fixed.

Table 4.5. Effect of 2wt% single metals (Cu, Ag and Au) supported on ZnO.

Conv %	0.007		0.010		0.013	
5%H_2/Ar 450°C, 2h	Sel %	Temp (°C)	Sel %	Temp (°C)	Sel %	Temp (°C)
Cu	60.6	200	53.7	210	50.3	215
Ag	25.7	247	-	-	-	-
Au	55.0	280	50.4	290	47.8	300

4.3.4 Propylene epoxidation over Cu-Ni, Cu-Ag, Cu-Au or Cu-Ag-Ni supported on ZnO catalysts

4.3.4.1 Propylene epoxidation over Cu-Ni supported on ZnO catalysts

In the study of direct epoxidation over silver-based catalysts containing 3d transition-metal species, Takahashi and co-workers [28] found that the highest PO selectivity, four times that obtained with the Ag single catalyst, is owing to the addition of Ni. They concluded Ni played an important role in controlling the particle size of Ag by acting as a spacer to isolate Ag particle. This lead to supported Cu-Ni catalysts being investigated in the direct propylene epoxidation to PO using only molecular oxygen in this chapter. The calculated ratios of 2wt-2wt% and 5wt-2wt% Cu-Ni/ZnO are applied in reactions, respectively.

According to the data in Table 4.6, it seems that the addition of Ni makes supported Cu-based catalysts less active. Higher ratio of Cu:Ni could improve both selectivity and conversion a little in propylene epoxidation. However, the contribution to the

yield is not distinct because of the low conversion.

Table 4.6. Results of propylene epoxidation over pre-treated Cu-Ni/ZnO.

Catalyst	Temp (°C)	Selectivity to PO (%)	Conversion (%)
2%Cu-2%Ni/ZnO (pre-treated in 5% H_2/Ar 450°C for 2h)	200	30.7	0.009
	210	30.8	0.012
	220	27.8	0.016
	230	26.4	0.030
	240	16.0	0.049
	250	13.9	0.085
	240	15.9	0.042
	230	25.0	0.023
	220	29.6	0.011
	210	31.9	0.007
	200	33.0	0.005
	210	39.3	0.006
	220	28.7	0.011
	230	26.1	0.020
	220	32.9	0.011
	210	29.2	0.007
5%Cu-2%Ni/ZnO (pre-treated in 5% H_2/Ar 450°C for 2h)	200	61.9	0.009
	210	42.8	0.016
	220	42.4	0.021
	230	38.5	0.034
	240	34.2	0.059
	250	29.3	0.098
	240	34.6	0.063
	230	39.5	0.030
	220	45.2	0.015
	210	54.2	0.010
	220	57.0	0.014
	230	42.3	0.030
	220	43.6	0.019
	210	51.1	0.010
	200	47.9	0.007

Continued Table 4.6. Results of propylene epoxidation over pre-treated Cu-Ni/ZnO.

Catalyst	Temp (°C)	Selectivity to PO (%)	Conversion (%)
2%Cu-2%Ni/ZnO (pre-treated in air 450°C for 2h)	200	34.6	0.007
	210	44.2	0.009
	220	33.2	0.014
	230	26.4	0.021
	240	24.5	0.036
	250	19.5	0.064
	240	22.4	0.034
	230	29.8	0.020
	220	31.6	0.010
	210	42.0	0.009
	200	37.6	0.005
	210	31.7	0.006
	220	43.7	0.008
	230	34.9	0.015
	220	37.8	0.009
	210	41.3	0.006
5%Cu-2%Ni/ZnO (pre-treated in air 450°C for 2h)	210	46.6	0.006
	220	33.9	0.010
	230	27.1	0.017
	240	30.7	0.022
	250	26.5	0.036
	240	33.6	0.021
	230	43.9	0.010
	220	63.1	0.006
	230	43.7	0.009
	220	47.2	0.006

Continued Table 4.6. Results of propylene epoxidation over pre-treated Cu-Ni/ZnO.

Catalyst	Temp (°C)	Selectivity to PO (%)	Conversion (%)
2%Cu-2%Ni/ZnO (pre-treated in N_2 450°C for 2h)	210	39.0	0.011
	220	32.8	0.016
	230	31.3	0.027
	240	22.9	0.056
	250	15.6	0.100
	240	23.3	0.049
	230	28.3	0.027
	220	30.9	0.015
	210	32.5	0.010
	220	34.2	0.013
	230	28.9	0.025
	220	33.1	0.015
5%Cu-2%Ni/ZnO (pre-treated in N_2 450°C for 2h)	200	45.6	0.007
	210	41.5	0.010
	220	43.0	0.019
	230	31.1	0.026
	240	28.8	0.042
	250	21.7	0.071
	240	27.7	0.049
	230	31.9	0.028
	220	41.1	0.013
	230	34.6	0.024
	220	42.4	0.011

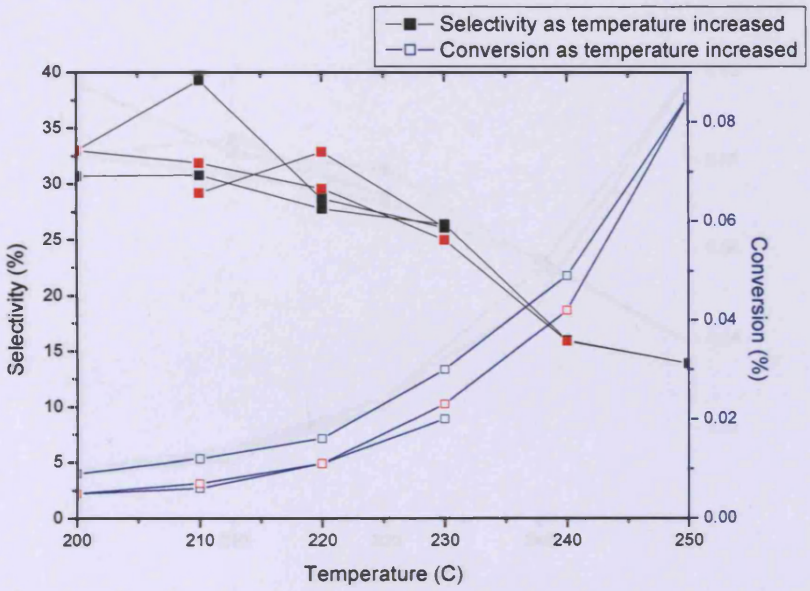

Figure 4.11. Catalytic performance for selective epoxidation of propylene using 2%Cu-2%Ni/ZnO catalyst pre-treated in 5% H_2/Ar 450˚C for 2h. (Red points represented the catalytic activity as temperature decreased.)

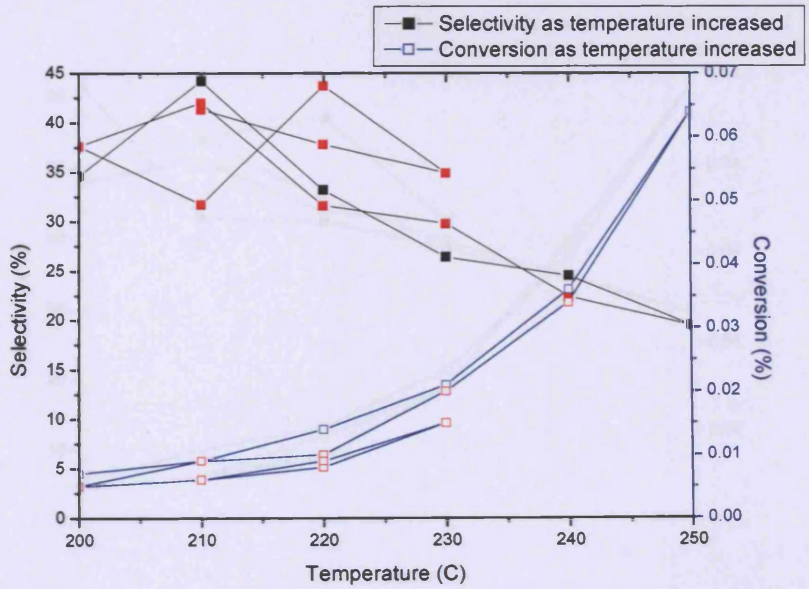

Figure 4.12. Catalytic performance for selective epoxidation of propylene using 2%Cu-2%Ni/ZnO catalyst pre-treated in air 450˚C for 2h. (Red points represented the catalytic activity as temperature decreased.)

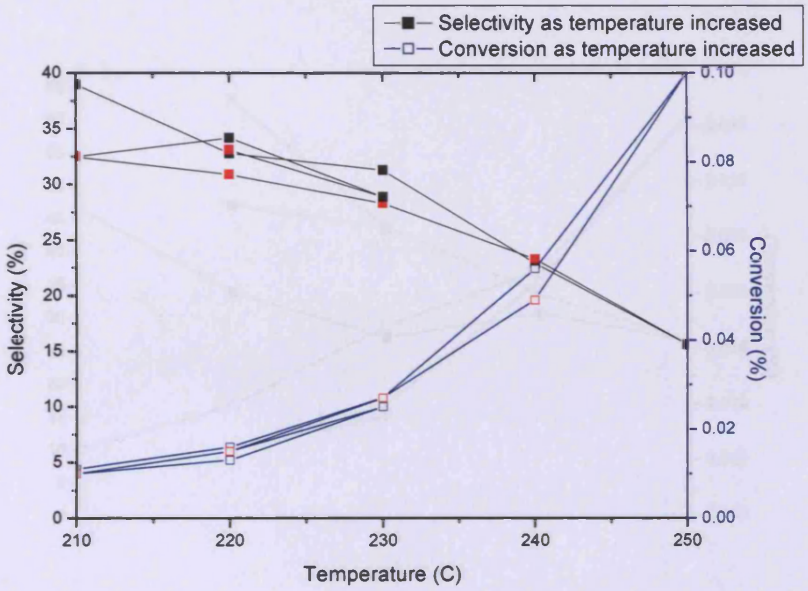

Figure 4.13. Catalytic performance for selective epoxidation of propylene using 2%Cu-2%Ni/ZnO catalyst pre-treated in N_2 450°C for 2h. (Red points represented the catalytic activity as temperature decreased.)

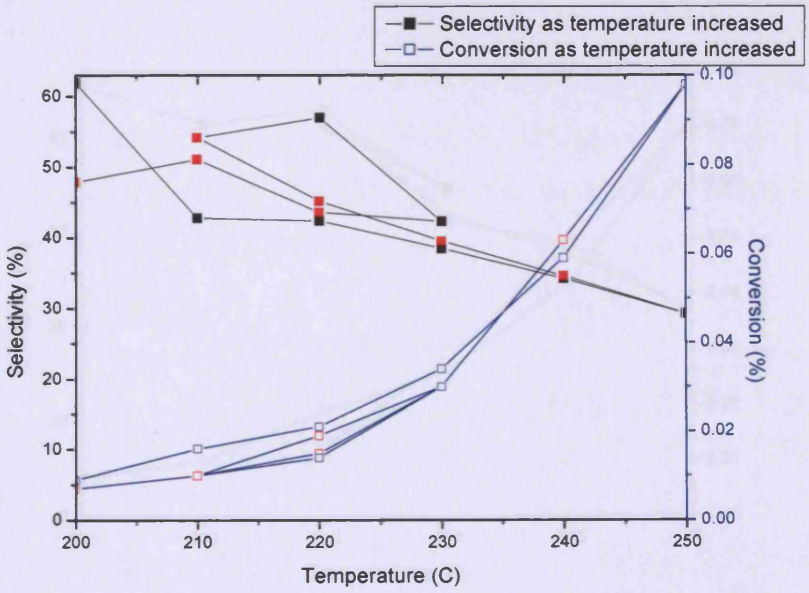

Figure 4.14. Catalytic performance for selective epoxidation of propylene using 5%Cu-2%Ni/ZnO catalyst pre-treated in 5% H_2/Ar 450°C for 2h. (Red points represented the catalytic activity as temperature decreased.)

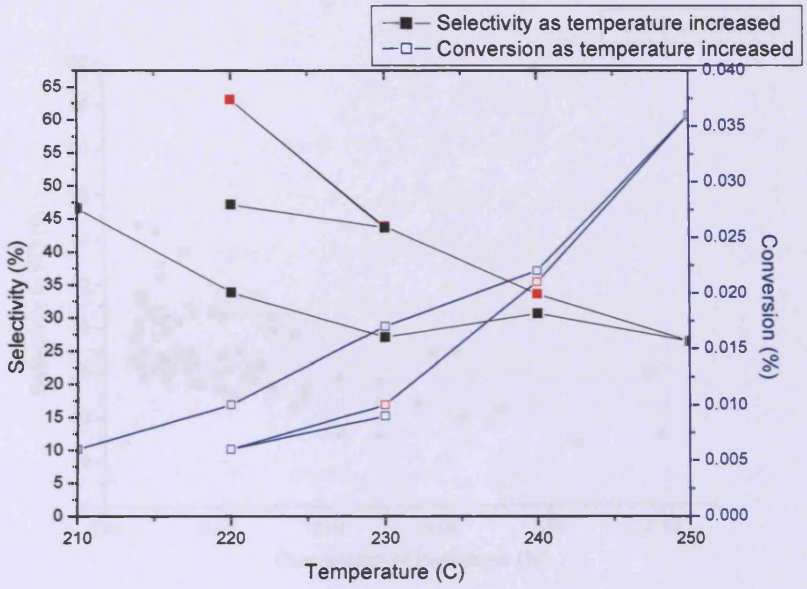

Figure 4.15. Catalytic performance for selective epoxidation of propylene using 5%Cu-2%Ni/ZnO catalyst pre-treated in Air 450°C for 2h. (Red points represented the catalytic activity as temperature decreased.)

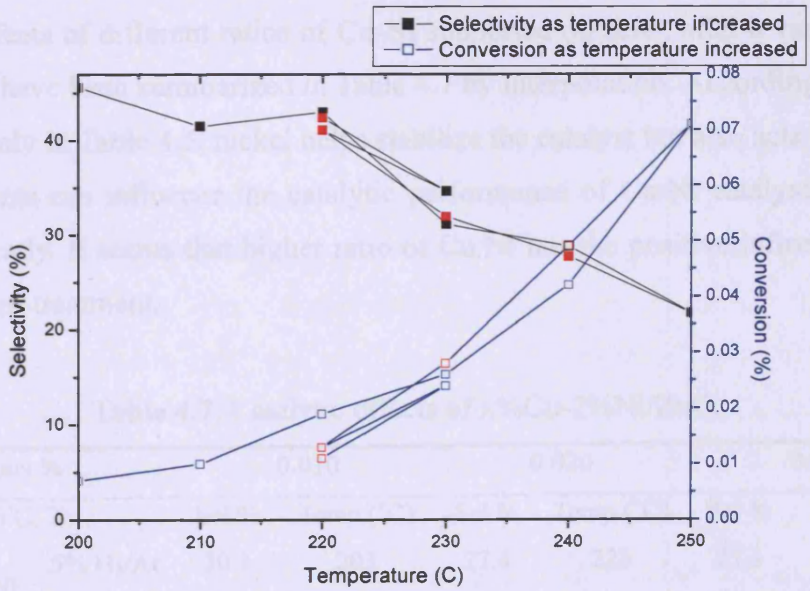

Figure 4.16. Catalytic performance for selective epoxidation of propylene using 5%Cu-2%Ni/ZnO catalyst pre-treated in N_2 450°C for 2h. (Red points represented the catalytic activity as temperature decreased.)

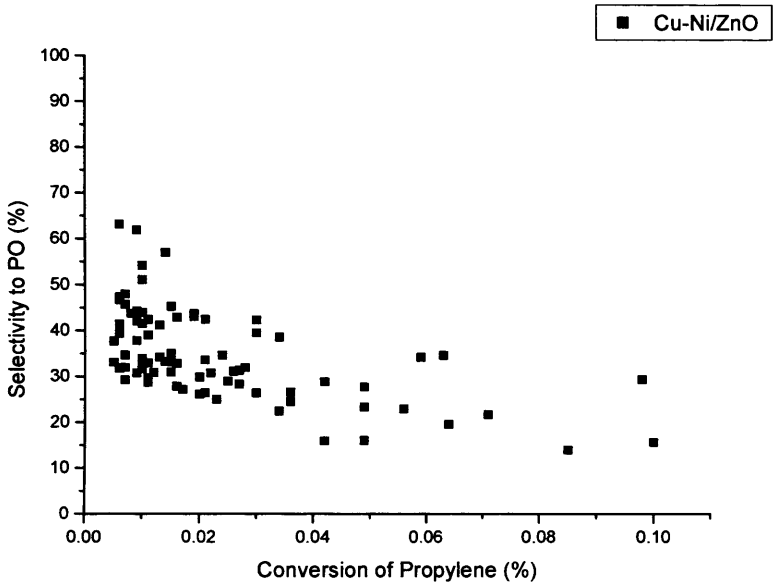

Figure 4.17. Multiple selectivity-conversion plot for propylene epoxidation to propylene oxide (PO) over Cu-Ni supported on ZnO catalysts.

Figure 4.17 depicts Cu-Ni/ZnO system for propylene epoxidation in terms of a selectivity vs. conversion plot and shows the upper limit of optimum selectivity. The catalytic effects of different ratios of Cu-Ni supported on ZnO, after a variety of pre-treatments, have been summarized in Table 4.7 by interpolation. According to the data of copper only in Table 4.5, nickel helps stabilize the catalyst but also acts as a poison. Pre-treatments can influence the catalytic performance of Cu-Ni catalysts supported on ZnO greatly. It seems that higher ratio of Cu:Ni has the positive influence only in reduction pre-treatment.

Table 4.7. Catalytic effects of x%Cu-2%Ni/ZnO.

Conv %		0.010		0.020		0.036	
450°C, 2h		Sel %	Temp (°C)	Sel %	Temp (°C)	Sel %	Temp (°C)
2%Cu-2%Ni / ZnO	5% H_2/Ar	30.3	203	27.4	223	23.1	233
	Air	42.0	212	27.4	229	24.5	240
	N_2	40.2	208	32.3	224	28.7	233
5%Cu-2%Ni / ZnO	5% H_2/Ar	59.2	201	42.5	218	38.2	231
	Air	33.9	220	29.3	236	26.5	250
	N_2	41.5	210	41.3	221	29.7	236

In the same time, the catalysts pre-treated by two typical pre-treatment conditions (in air and reduction 5% H_2/Ar) were analyzed through SEM-EDX as well. The composition on the catalyst surface could be scanned by EDX in detail. For 2%Cu-2%Ni/ZnO, the air pre-treatment makes 3.3% copper on the surface while no nickel exposed on the surface. On the other hand, the pre-treatment in 5% H_2/Ar offers 2.2% Cu and 2.5% Ni together on the surface of the catalyst. Apparently, the exposed nickel on the surface affects the selectivity of the catalyst greatly. The nickel does not contribute positively to selectivity to PO in the mixed metal catalyst.

4.3.4.2 Propylene epoxidation over Cu-Ag supported on ZnO catalysts

Ag-based catalysts have been greatly studied a lot in the epoxidation to both EO and PO. Then it is logical to take into account of Cu-Ag, when investigating the copper-based mixed metal catalysts in the epoxidation to PO. Recently, a density functional theory research on the design of Cu-Ag bimetallic catalysts for ethylene epoxidation was performed by Barteau [29], which suggested that Cu-Ag catalysts should be much more selective for ethylene epoxidation than Ag alone.

Table 4.8 and Figures 4.18-23 have listed the results of Cu-Ag supported on regular ZnO. The catalysts pre-treated in the 5% H_2/Ar have shown very good selectivity (70-80%) at about 200 °C, in spite of low conversion. Evidently, pre-treatments in both air and nitrogen could not offer catalysts better catalytic performances than that in reduction pre-treatment. This also implies that some reduced phases could be the active sites in the epoxidation to PO, although almost no difference is observed from SEM images as shown in Figure 4.26. The time-on-line (TOL) profile for 2wt-2wt% Cu-Ag/ZnO at 230 °C is shown in Figure 4.19. Clearly, the Cu-Ag mixed metal has shown a little deactivation since the TOL test was performed after the catalyst reacted for about 12 hours. The high ratio of Cu:Ag does not improve selectivity further. Table 4.9 and Figure 4.24 have also shown the catalytic performance of Cu-Ag supported on nano-ZnO after the reduction pre-treatment. Since the particle size of nano powder ZnO is quite similar to the regular one, there are not any distinct benefits for the nano powder ZnO. A profile of selectivity vs. conversion of Cu-Ag/ZnO

system for propylene epoxidation is shown in Figure 4.25, which is shown to be the better catalytic system than Cu-Ni/ZnO.

The best catalyst in this section, 2wt-2wt% Cu-Ag/ZnO pre-treated in 5% H_2/Ar was analyzed by SEM-EDX as well. According to the EDX scan and calculation, the reduction condition provides 2.4% copper on the surface area of the catalyst. In fact, there is not any silver exposed on the surface but zinc oxide support and copper. It seems that silver plays no role in the propylene epoxidation reaction. However, the catalyst surface is well-distributed in the SEM images as shown in Figure 4.26. From this point of view, silver does not play the directly catalytic role in the reaction, which impacts upon the catalytic performance of the mixed metal catalyst indirectly through pre-treatment.

Table 4.8. Results for propylene epoxidation over pre-treated Cu-Ag/ZnO.

Catalyst	Temp (°C)	Selectivity to PO (%)	Conversion (%)
2%Cu-2%Ag/ZnO (pre-treated in 5% H_2/Ar 450°C for 2h)	180	100	0.003
	190	100	0.004
	200	100	0.005
	210	81.2	0.011
	220	78.5	0.012
	230	62.4	0.015
	240	61.2	0.019
	230	66.2	0.012
	220	74.1	0.009
	230	55.3	0.010
	220	55.2	0.006
2%Cu-2%Ag/ZnO (pre-treated in air 450°C for 2h)	200	40.8	0.008
	210	38.1	0.01
	220	32.1	0.014
	230	31.8	0.017
	240	28.9	0.023
	250	26.0	0.029
	240	32.4	0.017
	230	38.2	0.01
	220	37.4	0.008
	230	35.5	0.01
	220	37.1	0.009
2%Cu-2%Ag/ZnO (pre-treated in N_2 450°C for 2h)	200	38.0	0.007
	210	45.8	0.009
	220	44.1	0.012
	230	31.1	0.017
	240	33.4	0.027
	250	33.6	0.028
	240	35.2	0.017
	230	40.7	0.01
	220	53.5	0.006
	230	36.8	0.009

Continued Table 4.8. Results for propylene epoxidation over pre-treated Cu-Ag/ZnO.

Catalyst	Temp (°C)	Selectivity to PO (%)	Conversion (%)
	190	75.4	0.007
	200	70.0	0.012
	210	62.0	0.017
	220	60.2	0.027
	230	52.7	0.038
	240	51.8	0.057
	250	42.4	0.080
	240	48.5	0.046
5%Cu-2%Ag/ZnO	230	47.2	0.027
(pre-treated in 5% H_2/Ar 450°C for 2h)	220	52.1	0.015
	210	50.2	0.010
	200	49.9	0.006
	210	46.3	0.009
	220	42.6	0.012
	230	28.6	0.02
	220	36.7	0.01
	210	40.5	0.009
	200	31.6	0.009
	210	32.0	0.010
	220	31.5	0.014
	230	35.8	0.018
	240	30.9	0.027
	250	27.1	0.036
5%Cu-2%Ag/ZnO	240	28.6	0.021
(pre-treated in air 450°C for 2h)	230	24.3	0.014
	220	35.6	0.010
	210	44.5	0.006
	220	39.6	0.009
	230	30.1	0.013
	220	33.4	0.009
	210	37.1	0.007

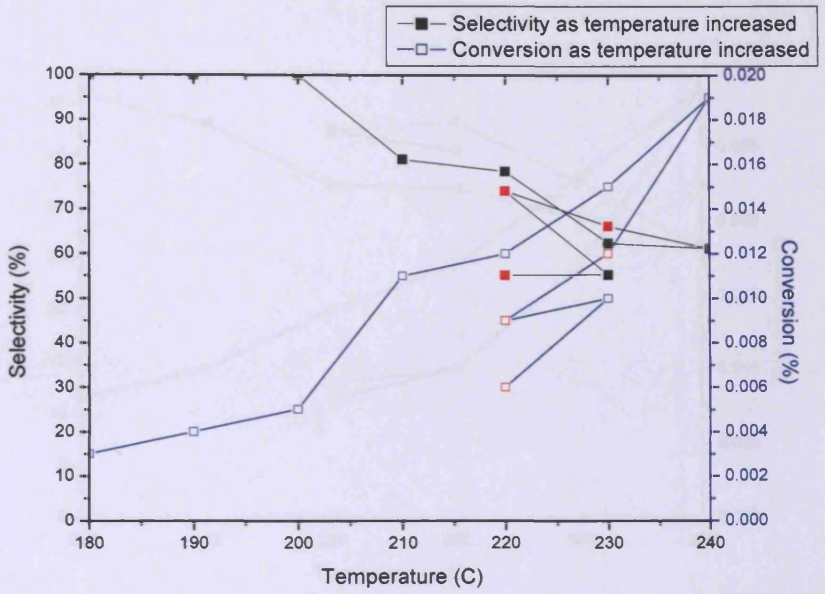

Figure 4.18. Catalytic performance for selective epoxidation of propylene using 2%Cu-2%Ag/ZnO catalyst pre-treated in 5% H_2/Ar 450˚C for 2h. (Red points represented the catalytic activity as temperature decreased.)

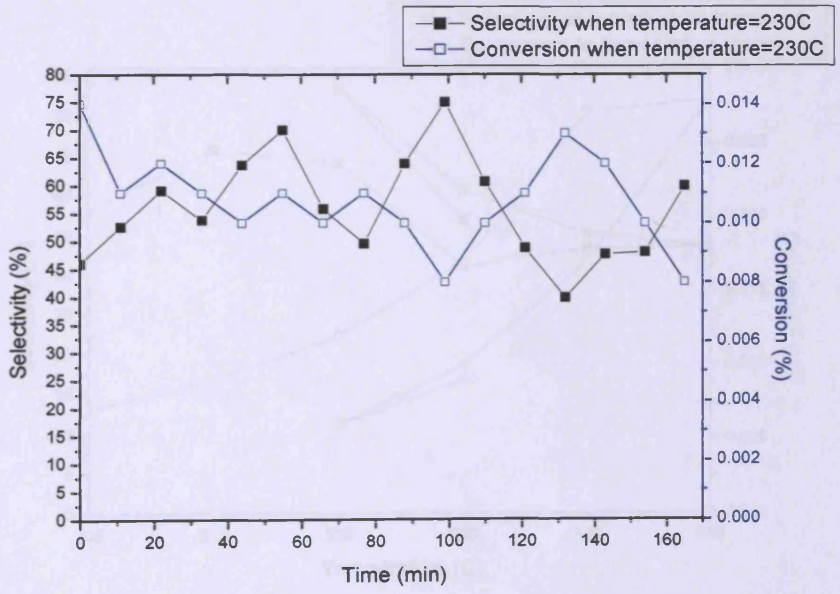

Figure 4.19. The time-on-line profile for 2%Cu-2%Ag/ZnO catalyst pre-treated in 5% H_2/Ar 450˚C for 2h at 230˚C.

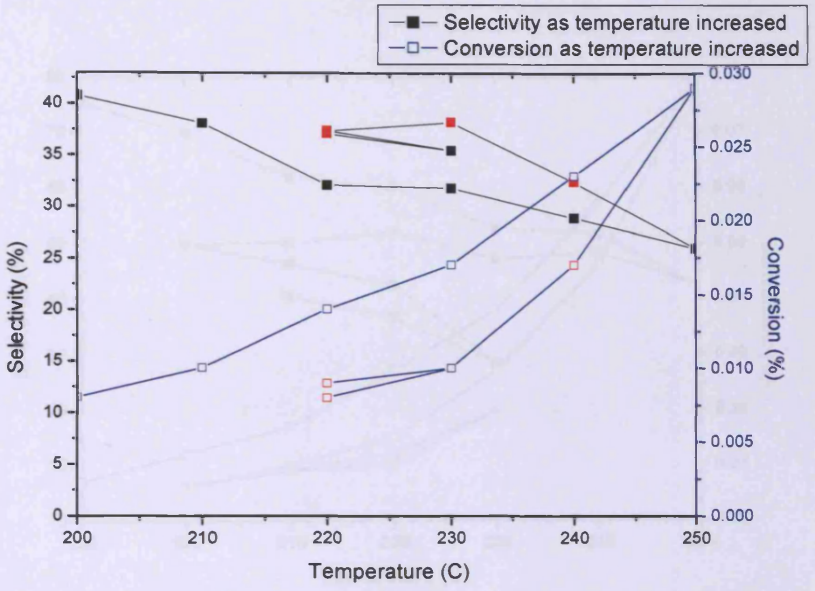

Figure 4.20. Catalytic performance for selective epoxidation of propylene using 2%Cu-2%Ag/ZnO catalyst pre-treated in air 450°C for 2h. (Red points represented the catalytic activity as temperature decreased.)

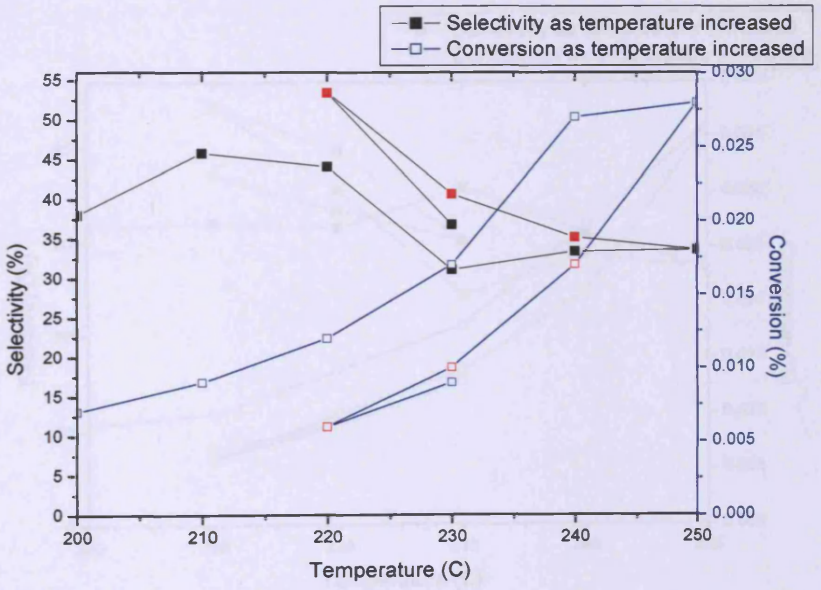

Figure 4.21. Catalytic performance for selective epoxidation of propylene using 2%Cu-2%Ag/ZnO catalyst pre-treated in N_2 450°C for 2h. (Red points represented the catalytic activity as temperature decreased.)

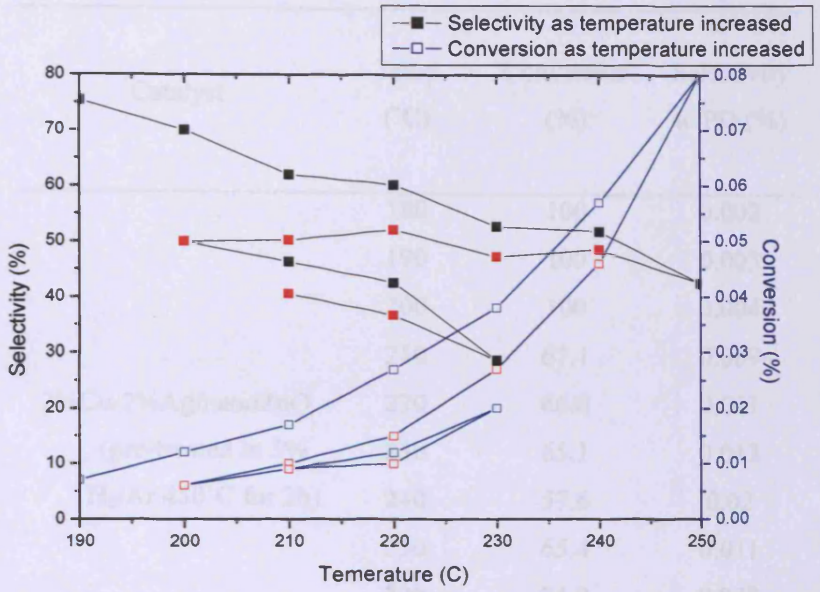

Figure 4.22. Catalytic performance for selective epoxidation of propylene using 5%Cu-2%Ag/ZnO catalyst pre-treated in 5% H_2/Ar 450°C for 2h. (Red points represented the catalytic activity as temperature decreased.)

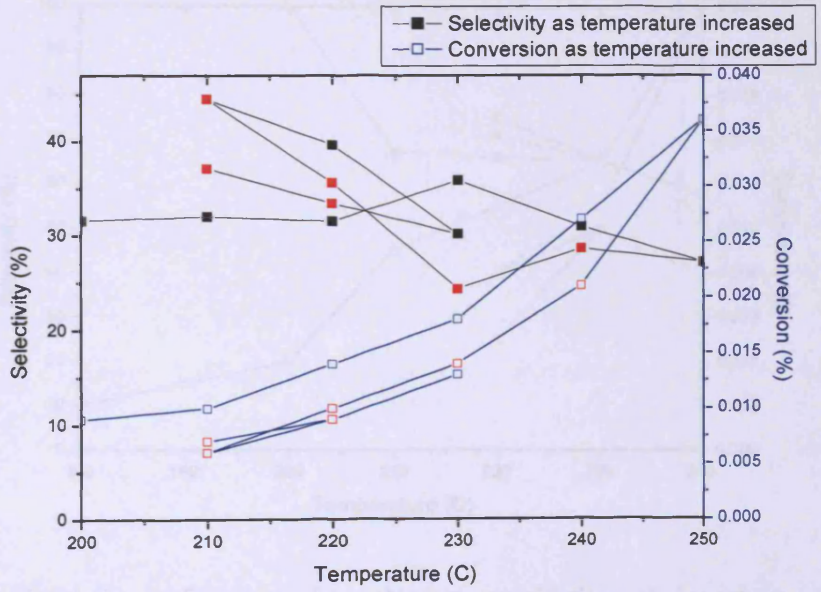

Figure 4.23. Catalytic performance for selective epoxidation of propylene using 5%Cu-2%Ag/ZnO catalyst pre-treated in air 450°C for 2h. (Red points represented the catalytic activity as temperature decreased.)

Table 4.9. Results for propylene epoxidation over Cu-Ag/nano-ZnO pre-treated in 5% H_2/Ar.

Catalyst	Temp (°C)	Conversion (%)	Selectivity to PO (%)
2%Cu-2%Ag/nanoZnO (pre-treated in 5% H_2/Ar 450°C for 2h)	180	100	0.002
	190	100	0.003
	200	100	0.004
	210	67.1	0.009
	220	66.0	0.011
	230	65.1	0.013
	240	57.6	0.02
	230	65.4	0.011
	220	74.9	0.008
	230	65.2	0.010
	220	70.8	0.005

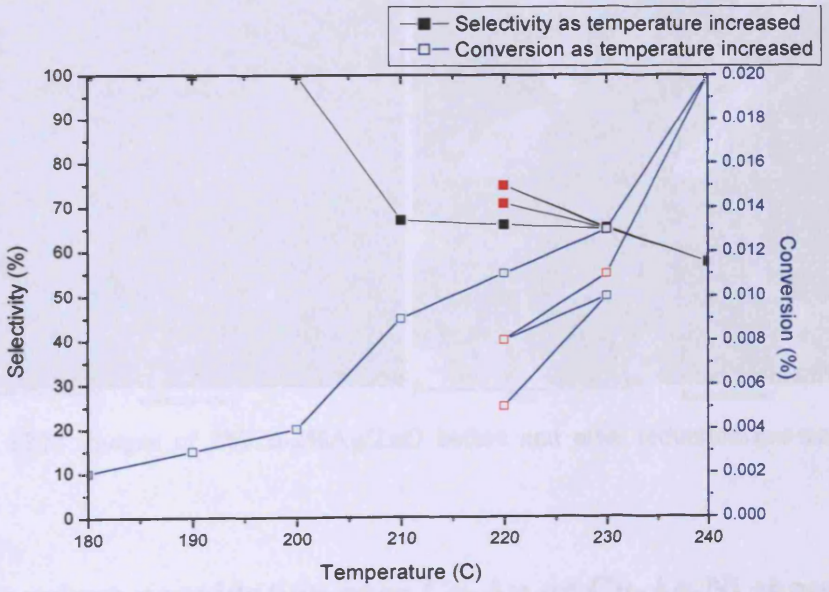

Figure 4.24. Catalytic performance for selective epoxidation of propylene using 2%Cu-2%Ag/nano-ZnO catalyst pre-treated in 5% H_2/Ar 450°C for 2h. (Red points represented the catalytic activity as temperature decreased.)

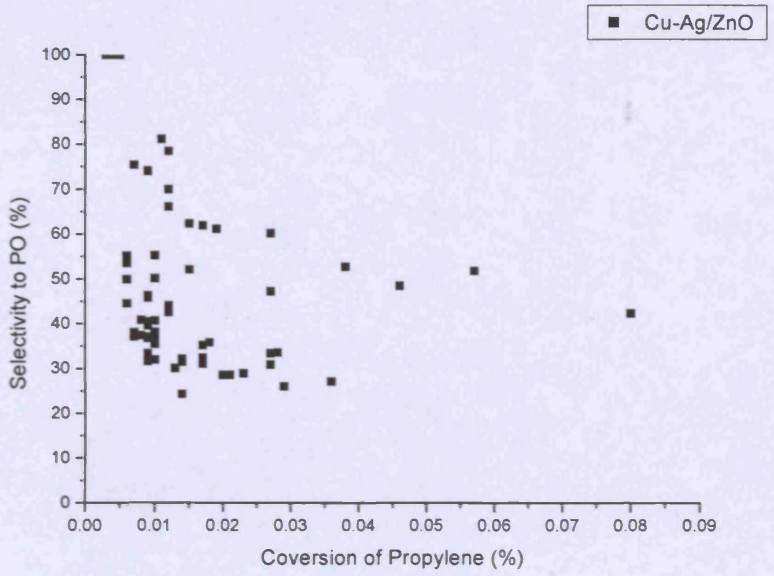

Figure 4.25. Multiple selectivity-conversion plot for propylene epoxidation to propylene oxide (PO) over Cu-Ag supported on ZnO catalysts.

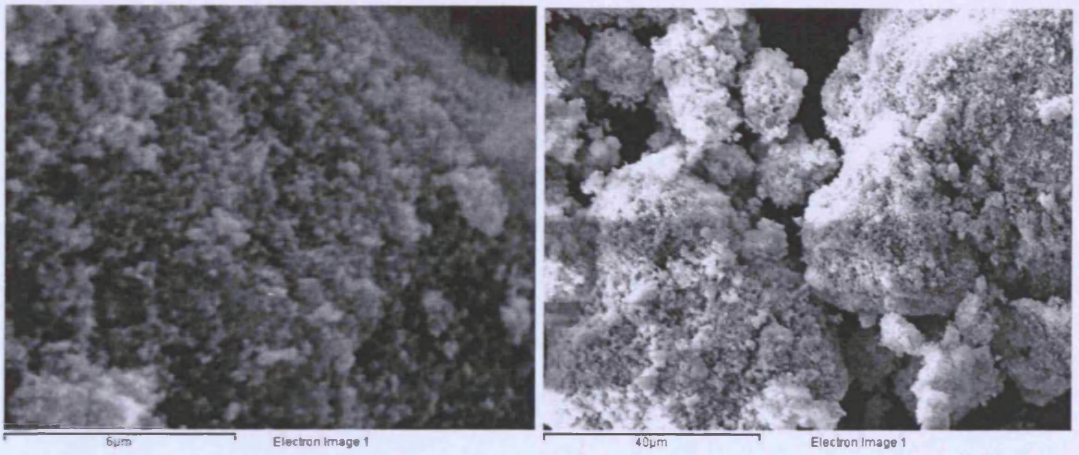

Figure 4.26. SEM images of 2%Cu-2%Ag/ZnO before and after reduction pre-treatment (5% H_2/Ar, 2h).

4.3.4.3 Propylene epoxidation over Cu-Au or Cu-Ag-Ni supported on ZnO catalysts

To compare with Cu-Ag supported on ZnO catalyst pre-treated in the reduction condition, Cu-Au and Cu-Ag-Ni have been studied as well. From Table 4.10 and Figure 4.27, it seems that gold does not contribute positively, which is similar as shown in Table 4.4. For Cu-Ag supported on ZnO catalyst, the addition of Ni did not

improve both selectivity to PO and conversion distinctly (Table 4.11 and Figure 4.28).

Table 4.10. Results for propylene epoxidation over pre-treated Cu-Au/ZnO.

Catalyst	Temp (°C)	Selectivity to PO (%)	Conversion (%)
	190	100	0.002
	200	100	0.003
	210	100	0.004
	220	61.9	0.008
2%Cu-2%Au/ZnO	230	56.7	0.011
(pre-treated in 5% H_2/Ar 450°C for 2h)	240	53.0	0.014
	230	56.6	0.011
	220	60.7	0.007
	230	55.5	0.008
	220	55.3	0.005

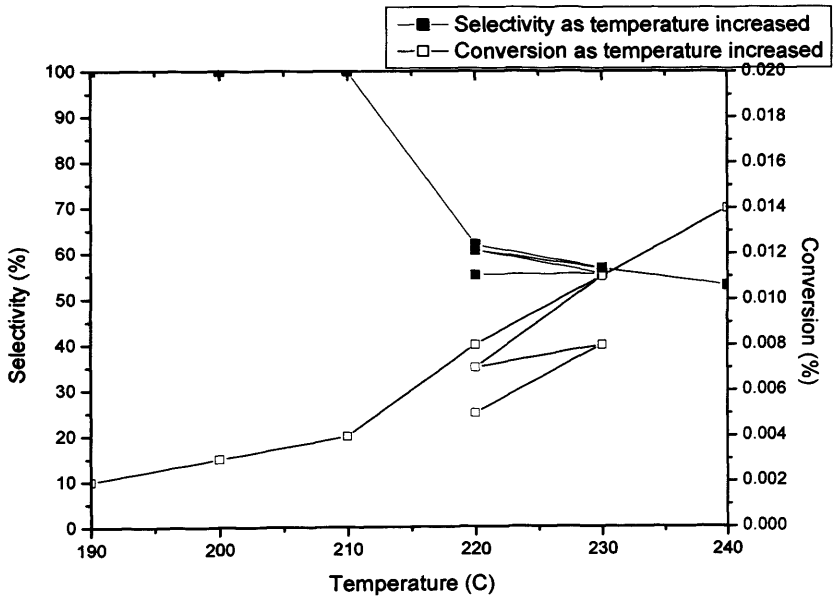

Figure 4.27. Catalytic performance for selective epoxidation of propylene using 2%Cu-2%Au/ZnO catalyst pre-treated in 5% H_2/Ar 450°C for 2h. (Red points represented the catalytic activity as temperature decreased.)

Table 4.11. Results for propylene epoxidation over pre-treated Cu-Ag-Ni/ZnO.

Catalyst	Temp (°C)	Selectivity to PO (%)	Conversion (%)
2%Cu-2%Ag-2%Ni/ZnO (pre-treated in 5% H_2/Ar 450°C for 2h)	180	100	0.002
	190	100	0.002
	200	63.3	0.006
	210	50.2	0.007
	220	49.8	0.01
	230	43.8	0.015
	240	34.9	0.02
	250	33.1	0.034
	240	40.4	0.022
	230	38.2	0.011
	220	46.0	0.007
	210	53.4	0.003
	220	50.7	0.008
	230	40.7	0.011
	220	50.2	0.006

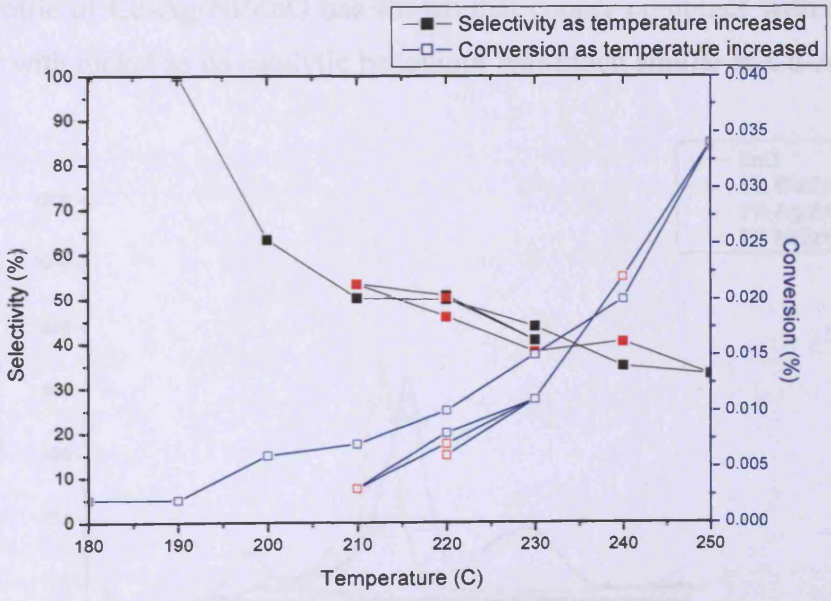

Figure 4.28. Catalytic performance for selective epoxidation of propylene using 2%Cu-2%Ag-2%Ni/ZnO catalyst pre-treated in 5% H_2/Ar 450°C for 2h. (Red points represented the catalytic activity as temperature decreased.)

4.4 Conclusion

In summary, heterogeneous selective epoxidation of propylene to PO has been studied over Cu, Ag, and Au catalysts, bimetallic (Cu-Ni, Cu-Ag, Cu-Au) and even some trimetallic (Cu-Ag-Ni) mixed metal catalysts supported on ZnO using only molecular oxygen.

The TPR profiles of several single metals or mixed metals supported on ZnO catalysts indicate most of catalysts have been fully reduced at 450°C in the reduction pre-treatment (Figure 4.29-4.30). In the TPR profile of 2wt% Cu/ZnO, the peak together with the shoulder at about 280°C has apparently characterized copper content as the shoulder appeared in the mixed metal with lower Cu/ZnO ratio [30]. The peak between 200°C and 250°C could be attributed to the reduction of Cu^{2+} to Cu^{0}. On the other hand, the peaks between 250°C and 340°C are owing to the reduction of Cu^{+} to Cu^{0}. Contrast to copper and nickel, the Ag catalyst is even much easier to be reduced at lower temperature (below 300°C). For bi-metallic catalysts, the addition of silver broadens and shifts the copper peak to low temperature area. On the contrary, nickel's addition leads to the reversed shift of copper. Compared to the bi-metallic catalysts, the TPR profile of Cu-Ag-Ni/ZnO has shown that copper combines with silver more tightly than with nickel as its catalytic behaviour was much similar as Cu-Ag/ZnO.

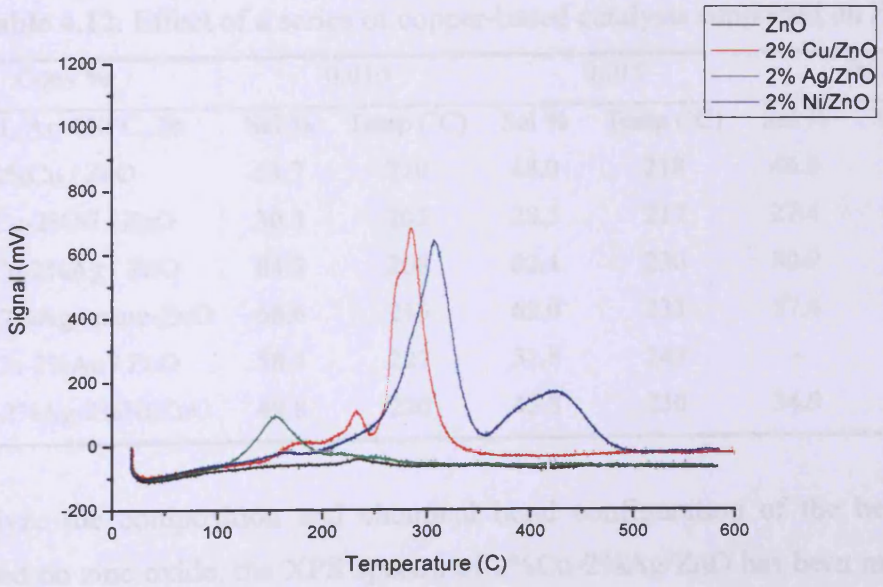

Figure 4.29. TPR profiles of ZnO and single metals (Cu, Ag, Ni) supported on ZnO.

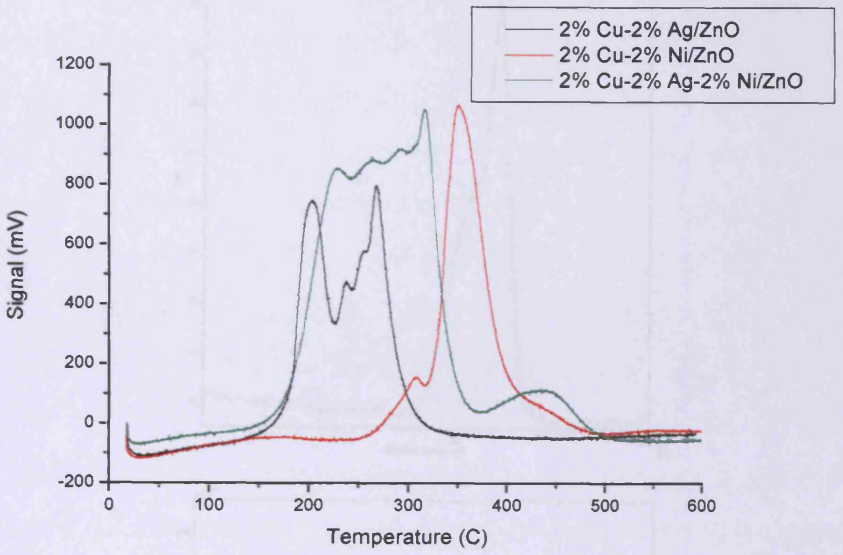

Figure 4.30. TPR profiles of Cu-Ni, Cu-Ag and Cu-Ag-Ni mixed metals supported on ZnO.

Based on the interpolation/extrapolation method, Table 4.12 summarizes the catalytic performances of a series of copper-based catalysts with fixed conversion. Obviously, nickel's addition acts as the poison and makes copper-based catalysts less selective to PO. At comparatively lower reaction temperatures (e.g. <230˚C), Cu-Ag is undoubtedly the best catalytic system based on regular ZnO support.

Table 4.12. Effect of a series of copper-based catalysts supported on ZnO.

Conv %	0.010		0.015		0.020	
5% H_2/Ar, 450˚C, 2h	Sel %	Temp (˚C)	Sel %	Temp (˚C)	Sel %	Temp (˚C)
2%Cu / ZnO	53.7	210	48.0	218	46.5	224
2%Cu-2%Ni / ZnO	30.3	203	28.5	217	27.4	223
2%Cu-2%Ag / ZnO	84.3	208	62.4	230	60.9	242
2%Cu-2%Ag / nano-ZnO	66.6	215	63.0	233	57.6	240
2%Cu-2%Au / ZnO	58.4	227	51.8	243	-	-
2%Cu-2%Ag-2%Ni/ZnO	49.8	220	43.8	230	34.9	240

To analyze the composition and chemical bond configuration of the best catalyst supported on zinc oxide, the XPS spectra of 2%Cu-2%Ag/ZnO has been measured as shown in Figures 4.31-4.33.

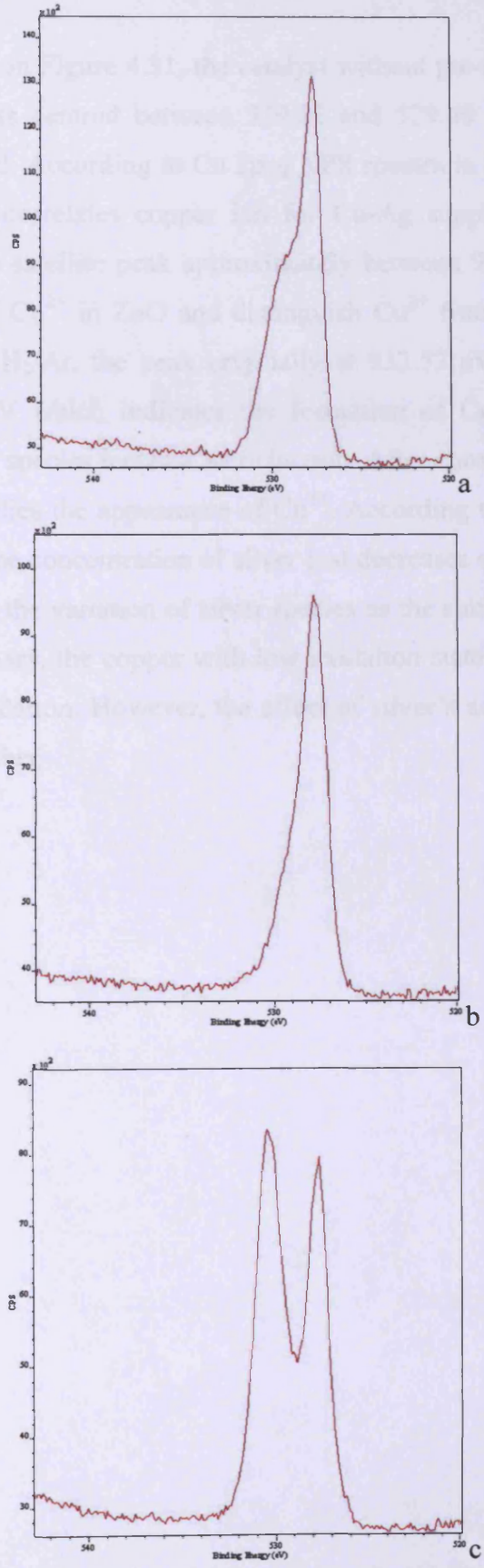

Figure 4.31. The O 1s XPS spectra of (a) Cu-Ag supported on ZnO (b) Cu-Ag/ZnO pre-treated in 5% H_2/Ar (c) after epoxidation.

From O 1s XPS spectra in Figure 4.31, the catalyst without pre-treatment reveals that there are shoulder peaks centred between 529.22 and 529.49 eV, which implies a variety of oxides existed. According to Cu $2p_{3/2}$ XPS spectra in Figure 4.32, the peak centered at 932.52 eV correlates copper ion for Cu-Ag supported on zinc oxide. Additionally, the Cu 2p satellite peak approximately between 940 and 943 eV could denote the existence of Cu^{2+} in ZnO and distinguish Cu^{2+} from Cu^{0} and Cu^{1+} [31]. After reduction in 5% H_2/Ar, the peak originally at 932.52 eV has been shifted to about 929.59-930.18 eV which indicates the formation of Cu^{0}. Subsequently, the concentration of copper species increase as reduction. After epoxidation, that the peak shifts to 930.44 eV implies the appearance of Cu^{1+}. According to Ag 3d XPS spectra shown in Figure 4.33, the concentration of silver just decreases a little after reduction. It is difficult to identify the variation of silver species as the shifts of peaks are nearly imperceptible. In summary, the copper with low oxidation state plays very important role in propylene epoxidation. However, the effect of silver's addition is still unclear and need be studied further.

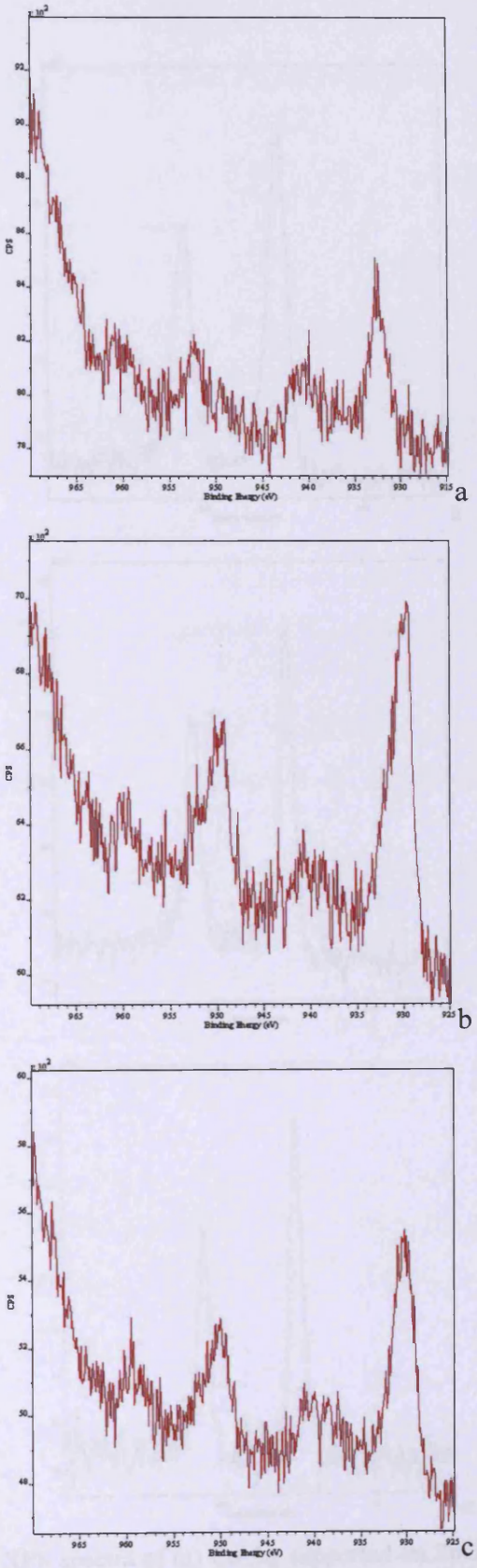

Figure 4.32. The Cu $2p_{3/2}$ XPS spectra of (a) Cu-Ag supported on ZnO (b) Cu-Ag/ZnO pre-treated in 5% H_2/Ar (c) after epoxidation.

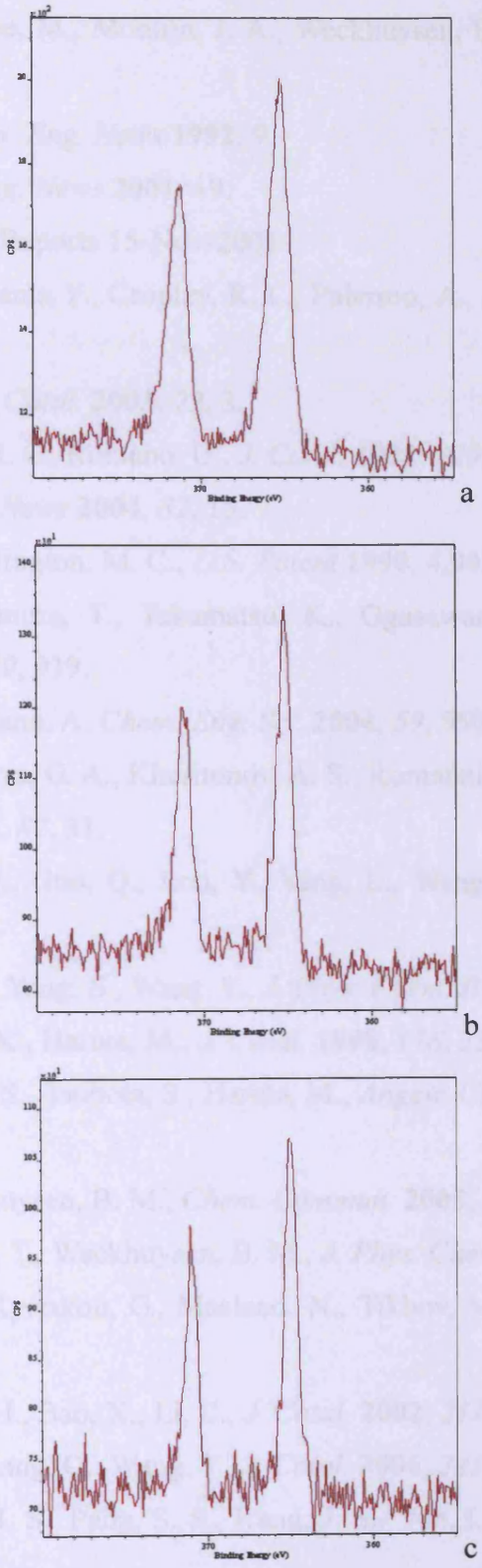

Figure 4.33. The Ag 3d XPS spectra of (a) Cu-Ag supported on ZnO (b) Cu-Ag/ZnO pre-treated in 5% H_2/Ar (c) after epoxidation.

4.5 References

[1] Nijhuis, T. A., Makkee, M., Moulijn, J. A., Weckhuysen, B. M. *Ind. Eng. Chem. Res.* **2006**, *45*, 3347.

[2] Ainsworth, S. J., *Chem. Eng. News* **1992**, 9.

[3] McCoy, M., *Chem. Eng. News* **2001**, 19.

[4] Nexant Chemsystems Reports 15-Nov-2001.

[5] Lambert, R. M., Williams, F., Cropley, R. L., Palermo, A., *J. Mol. Catal. A* **2005**, *228*, 27.

[6] Barteau, M. A., *Topic. Catal.* **2003**, *22*, 3.

[7] Clerici, M. G., Bellussi, G., Romano, U., *J. Catal.* **1991**, *129*, 159.

[8] Tullo, A., *Chem. Eng. News* **2004**, *82*, 15.

[9] Pennington, B. T., Fullington, M. C., *U.S. Patent* **1990**, 4,943,643.

[10] Iwasawa, Y., Nakamura, T., Takamatsu, K., Ogasawara, S., *J. Chem. Soc. Faraday Trans., 1* **1980**, *79*, 939.

[11] Ananieva, E., Reitzmann, A. *Chem. Eng. Sci.* **2004**, *59*, 5509.

[12] Panov, G. T., Sheveleva, G. A., Kharitonov, A. S., Romannikov, V. N., Vostrikova, L. A., *Appl. Catal. A* **1992**, *82*, 31.

[13] Wang, X., Zhang, Q., Guo, Q., Lou, Y., Yang, L., Wang, Y., *Chem. Commun.* **2004**, 1396.

[14] Wang, X., Zhang, Q., Yang, S., Wang, Y., *J. Phys. Chem. B* **2005**, *109*, 23500.

[15] Hayashi, T., Tanaka, K., Haruta, M., *J. Catal.* **1998**, *178*, 256.

[16] Sinha, A. K., Seelan, S., Tsubota, S., Haruta, M., *Angew. Chem. Int. Ed.* **2004**, *43*, 1546.

[17] Nijhuis, T. A., Weckhuysen, B. M., *Chem. Commun.* **2005**, *48*, 6002.

[18] Nijhuis, T. A., Visser, T., Weckhuysen, B. M., *J. Phys. Chem. B* **2005**, *109*, 19309.

[19] Vaughan, O. P. H., Kyriakou, G., Macleod, N., Tikhov, M., Lambert, R. M., *J. Catal.* **2005**, *236*, 401.

[20] Lu, J., Luo, M., Lei, H., Bao, X., Li, C., *J. Catal.* **2002**, *211*, 552.

[21] Chu, H., Yang, L., Zhang, Q., Wang, Y., *J. Catal.* **2006**, *241*, 225.

[22] Shim, E. S., Kang, H. S., Pang, S. S., Kang, J. S., Yun, I., Lee, S. Y., *Mat. Sci. Eng.* **2003**, *B102*, 366.

[23] Krunks, M., Dedova, T., Açik, I. O., *Thin Solid Films* **2006**, *515*, 1157.

[24] Wang, X. B., Song, C., Geng, K. W., Zeng, F., Pan, F., *J. Phys. D: Appl. Phys.*

2006, *39*, 4992.

[25] Bauermann, L. P., Bill, J., Aldinger, F., *J. Phys. Chem. B* **2006**, *110*, 5182.

[26] Lu, G., Zuo, X., *Catal. Lett.* **1999**, *58*, 67.

[27] Cropley, R. L., Williams, F. J., Vaughan, O. P. H., Urquhart, A. J., Tikhov, M. S., Lambert, R. M., *Surf. Sci.* **2005**, *578*, L85.

[28] Takahashi, A., Hamakawa, N., Nakamura, I., Fujitani, T., *Appl. Catal. A: Gerneral* **2005**, *294*, 34.

[29] Linic, S., Jankowiak, J., Barteau, M., A. *J. Catal.* **2004**, *224*, 489.

[30] Fierro, G., Jacono, M. L., Inversi, M., Porta, P., Cioci, F., Lavecchia, R., *Appl. Catal. A* **1996**, *137*, 327.

[31] Lee, J. B., Lee, H. J., Seo, S. H., Park, J. S., *Thin Solid Film* **2004**, *398*, 641.

Chapter 5.
Gas-phase selective epoxidation of propylene to propylene oxide over catalysts supported on nano-silica

5.1 Introduction

Among supported catalytic materials, the support effect is an important factor for catalytic performances. Although the support effect may not be a major contributor to the catalytic activity in some cases, some degree of the catalytic activity is affected by different oxide supports. For example, Au supported on a reducible oxide (e.g. TiO_2) has been shown to be more active than that supported on an irreducible oxide (e.g. SiO_2) [1-3]. It has been suggested that a strong metal support interaction effect is one of the reasons about the specific phenomenon occurring in catalytic materials [4]. Although this effect is usually studied in relation to the supports of reducible oxides such as titania, vanadia or niobia [5, 6], it is also reported to occur on some oxide supports (e.g. SiO_2 or La_2O_3) [7, 8] which are generally considered to be hardly reducible.

In heterogeneous catalysis, catalysts are typically composed of active components such as metal nano-particles or mixed metals dispersed on solid supports, which often display catalytic activity of their own and also affect the behaviour of the other solid phases [5, 9]. Bimetallics and mixed metal have attracted much attention in the catalysis community because of their potential to tune electronic and geometric properties in metals [10, 11]. In selective oxidation and selective oxidative dehydrogenation reactions, it is suggested that surface atomic oxygen plays a particularly significant role [12, 13]. Oxygen modified surfaces are obviously different from metal oxide thin films grown on metal surfaces [14-17], in terms of

both structure and reactivity. For example, it is known that metallic silver and copper surfaces modified by atomic oxygen are selective for the epoxidation of certain olefins, but their metal oxides are not [18]. Beside these, other oxygenated compounds can be obtained oxidizing unsaturated C=C double bonds by adsorbed oxygen atoms as in the case of propylene to acetone [19]. The epoxidation reactions on transition metals have attracted particular attention in the hope of developing a general catalytic process for olefins other than ethylene. It is generally recognized that adsorbed oxygen atoms on silver surfaces and π-bonded alkane without allylic hydrogens are necessary for epoxidation. On the other hand, selective epoxidation reactions take place with higher efficiency on copper surfaces even with olefins containing allylic hydrogens (e.g. trans-methylstyrene or α-methylstyrene) [18, 20]. For ethylene epoxidation, the advantage of copper over silver surfaces was reported by a theoretical study [21]. In many catalytic processes, hydroxide surface plays a significant role as well. For example, it was found that the surface hydroxyl species together with adsorbed oxygen on Ag can inhibit the combustion of propylene and decrease the desorption temperatures of both propylene and propylene oxide [22, 23].

Driven by the requirement of addressing the role of the support in catalysis, there has been an impetus for the development of novel supported catalysts, especially nano-supported metal particles [24]. A large number of methods, such as microelectronic techniques and the vapour deposition of metals, have been developed for catalysts preparation [25-29]. For instance, size-controllable nano-particles have been prepared by colloidal methods and either deposited on oxides or encapsulated in mesoporous silica [30]. Nano-technology can offer to expand the selection of methods available for preparation of catalysts with better-defined properties such as pore size and catalytic site structure [31]. Compared with traditional single crystal surface chemistry, the effects of catalyst particle size and metal oxide interface on reactivity have been addressed in the studies of these supported catalysts.

In Chapter 4, selective epoxidation of propylene to propylene oxide has been

reviewed and copper-based catalysts over supported zinc oxide were investigated. As nano-powder supports have been widely used in many fields, nano-silica as a very typical support will be studied later in this work for comparison.

5.2 Experimental

5.2.1 Catalyst preparation

5.2.1.1 Preparation of Ni, Au, Ag or Cu supported on nano-SiO_2 catalysts

Although both regular and nano powder of SiO_2 come from Aldrich, they look like quite different according to XRD results as shown later in Figure 5.1. For convenience, nano powder of SiO_2 will be shortened as nano-SiO_2 in this work while regular powder of SiO2 abbreviated regular SiO_2.

A 2wt% Ni supported on nano-SiO_2 catalyst was prepared by a wet impregnation method. The procedure is as follows: 98% $Ni(NO_3)_2 \cdot 6H_2O$ (0.202g) was dissolved in deionised water (10ml) and 99.9% nano-SiO_2 (1.873g) was impregnated by this solution and then vigorously stirred for 2h. Finally, the catalyst was dried at 80°C for 16h.

A 2wt% Au supported on nano-SiO_2 catalyst was prepared by a wet impregnation method, similar to the preparation of Ag catalyst: $HAuCl_4 \cdot 3H_2O$ (0.145g) was dissolved in deionised water (10ml) and 99.9% nano-SiO_2 (2g) was impregnated by this solution and then vigorously stirred for 2h. The catalyst was then dried at 80°C for 16h.

A 2wt% Ag supported on nano-SiO_2 catalyst was prepared by a wet impregnation method. The procedure is as follows: silver nitrate ($AgNO_3$, 0.063g) was dissolved in

deionised water (10ml) and 99.9% nano-SiO_2 (1.937g) was impregnated by this solution and then vigorously stirred for 2h. The catalyst was then dried at 80°C for 16h.

A 2wt% Cu supported on nano-SiO_2 catalyst was prepared by a wet impregnation method, similar to the preparation of Ag catalyst: 98% $CuNO_3 \cdot 2.5H_2O$ (0.150g) was dissolved in deionised water (10ml) and 99.9% nano-SiO_2 (1.879g) was impregnated by this solution and then vigorously stirred for 2h. The catalyst was then dried at 80°C for 16h.

5.2.1.2 Preparation of Cu-Ni, Cu-Ag or Cu-Au bimetallic supported on nano-SiO_2 catalysts

A 2wt-2wt% Cu-Ni supported on nano-SiO_2 catalyst was prepared by a wet impregnation method. The procedure was as follows: 98% $Ni(NO_3)_2 \cdot 6H_2O$ (0.202g) and 98% $CuNO_3 \cdot 2.5H_2O$ (0.150g) were dissolved in deionised water (10ml) and 99.9% nano-SiO_2 (1.752g) was impregnated by this solution, and then vigorously stirred for 3h. The catalyst was then dried at 80°C for 16h. Catalysts were treated at 450°C in air, N_2 or 5%H_2/Ar for 2h.

A 2wt-2wt% Cu-Ag supported on nano-SiO_2 catalyst was prepared by a wet impregnation method. The procedure was as follows: $AgNO_3$ (0.063g) and 98% $CuNO_3 \cdot 2.5H_2O$ (0.150g) were dissolved in deionised water (10ml) and 99.9% nano-SiO_2 (1.787g) was impregnated by this solution, and then vigorously stirred for 3h. The catalyst was then dried at 80°C for 16h. Catalysts were treated at 450°C in air or 5%H_2/Ar for 2h.

A 2wt-2wt% Cu-Au supported on nano-SiO_2 catalyst was prepared by a wet impregnation method. The procedure was as follows: $HAuCl_4 \cdot 3H_2O$ (0.145g) and

98% $CuNO_3 \cdot 2.5H_2O$ (0.150g) were dissolved in deionised water (10ml) and 99.9% nano-SiO_2 (1.787g) was impregnated by this solution, and then vigorously stirred for 3h. The catalyst was then at 80°C for 16h. Catalysts were treated at 450°C in air or 5%H_2/Ar for 2h.

All catalysts were not washed further with ionized water. The weight percentage of loading denotes calculation values in the catalyst preparation. Some real values of loading detected by EDX have been claimed in the results and discussion.

5.3 Results and discussion

5.3.1 Characterization of nano-SiO_2 supports and catalysts

5.3.1.1 XRD analysis of nano-SiO_2

Although both regular and nano-powder of zinc oxide have almost the same XRD pattern in Chapter 4, there are obviously many differences between counterparts of silica in XRD pattern as shown in Figure 5.1. The strong signals reflect bigger particle size, while the smooth and broad reflections represent relatively small particle size. Nano-powder of silica is amorphous while regular SiO_2 is crystalline.

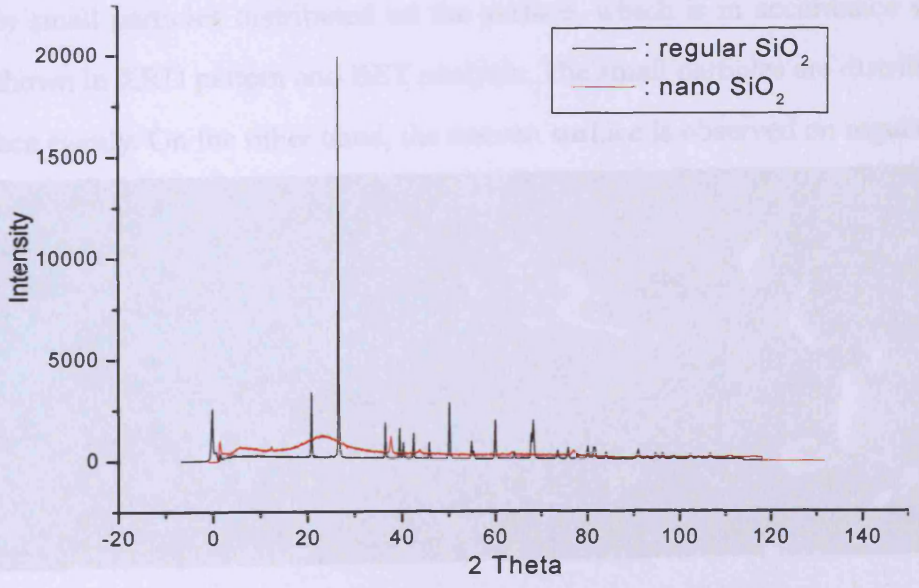

Figure.5.1. The XRD pattern of regular and nanopowder SiO_2.

5.3.1.2 BET analysis of SiO_2 supports

The surface area of regular and nano-powder SiO_2 are shown in Table 5.1. Clearly, the nano-powder SiO_2 has the smaller particle size than the regular one. Then nano-SiO_2 as a high surface area support will be studied in this chapter while the regular counterpart is only used occasionally for comparison. Although nano-SiO_2 itself has very high surface area, the BET of the final catalysts has lowered between 100 and 150 m^2/g.

Table 5.1 Surface area of SiO_2 supports by BET analysis.

Support materials	Surface area (m^2/g)
Regular SiO_2	5
SiO_2 nano-powder	456

5.3.1.3 SEM images of SiO_2 supports

The detailed information on surface morphology of regular and nano-powder silica has been shown in Figure 5.2-5.3. Undoubtedly, SiO_2 nano-powder represents relatively small particles distributed on the surface, which is in accordance with the results shown in XRD pattern and BET analysis. The small particles are distributed on the surface evenly. On the other hand, the uneven surface is observed on regular SiO_2.

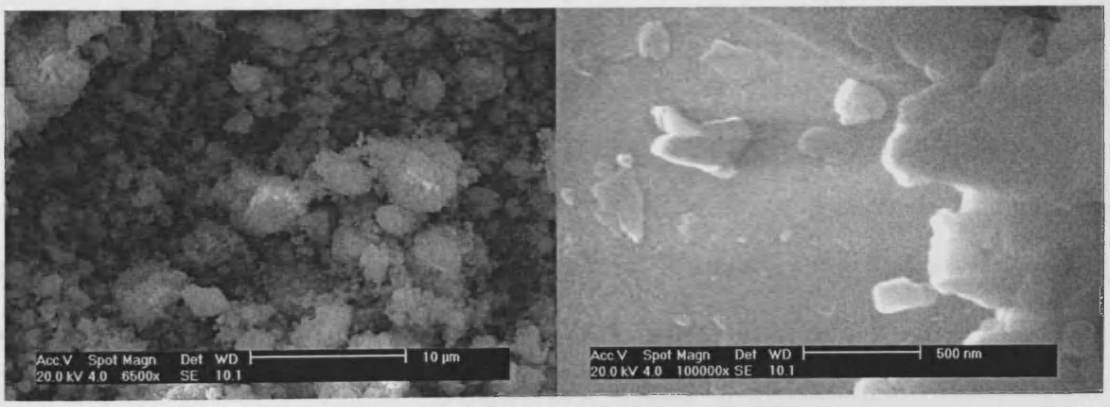

Figure.5.2. SEM images of regular SiO_2.

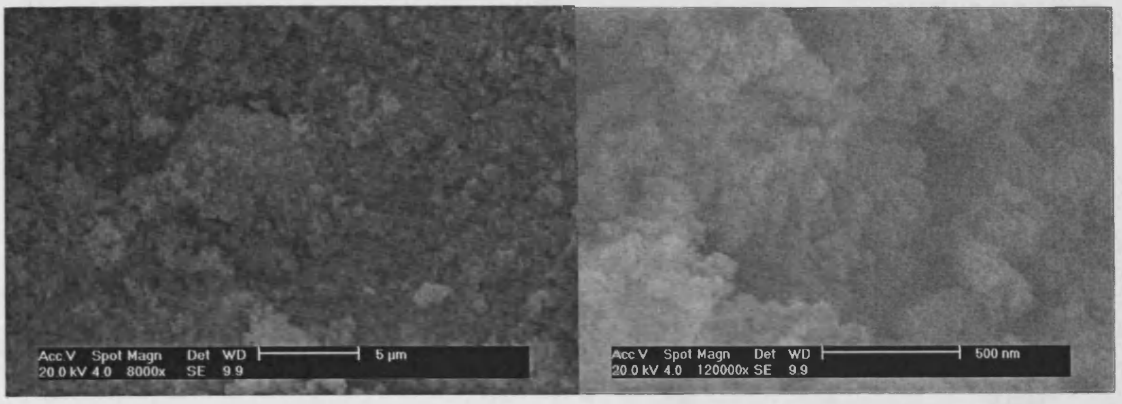

Figure.5.3. SEM images of SiO_2 nano-powder.

5.3.2 Propylene epoxidation over Ag, Cu, Au or Ni supported on nano-SiO_2 catalysts

In Chapter 4, the direct propylene epoxidation using only molecular oxygen has been performed in a fixed-bed reactor. In this chapter, the same reaction was carried out while just replacing the support with nano-SiO_2 and keeping the same reaction conditions. As Ni or Au supported on nano-SiO_2 catalyst displayed no activity, Tables 5.2 and 5.3 only compare the catalytic performances of Ag and Cu supported on nano-SiO_2, respectively. For silver only supported on nano-SiO_2, no PO could be observed below 260°C so that the epoxidation reaction was performed from 270°C. The whole profiles of Cu and Ag supported on nano-silica catalysts at different temperatures are shown in Figures 5.4-5.7.

Supported on nano-SiO_2, copper catalyst is undoubtedly more selective than silver, which is pre-treated not only in 5% H_2/Ar but also in nitrogen. In both pre-treatments, copper has shown stable catalytic performances whilst silver, pre-treated in reduction conditions is hardly comparable with copper. Therefore, copper-based catalysts supported on nano-SiO_2 are worthy of investigating more.

Table 5.2. Results of propylene epoxidation over pre-treated 2%Cu/nano-SiO_2 and 2%Ag/nano-SiO_2 (pre-treated in 5% H_2/Ar 450°C for 2h).

Catalyst	Temp (°C)	Selectivity to PO (%)	Conversion (%)
2%Cu/nano-SiO_2 (pre-treated in 5% H_2/Ar 450°C for 2h)	180	63.2	0.014
	190	61.5	0.020
	200	56.2	0.024
	210	56.0	0.043
	220	58.2	0.058
	230	57.6	0.078
	240	58.8	0.116
	250	57.0	0.165
	240	58.4	0.090
	230	59.9	0.053
	220	57.1	0.029
	210	56.3	0.016
	200	61.6	0.008
	210	62.4	0.016
2%Ag/ nano-SiO_2 (pre-treated in 5% H_2/Ar 450°C for 2h) Below 260°C, no selectivity to PO observed.	270	15.3	0.013
	280	17.7	0.022
	290	19.8	0.032
	300	21.9	0.054
	290	23.7	0.039
	280	25.8	0.029
	270	19.8	0.022
	280	23.9	0.029
	290	19.6	0.043
	280	19.4	0.029

Table 5.3. Results of propylene epoxidation over pre-treated 2%Cu/nano-SiO_2 and 2%Ag/nano-SiO_2 (pre-treated in N_2 450°C for 2h).

Catalyst	Temp (°C)	Selectivity to PO (%)	Conversion (%)
2%Cu/nano-SiO_2 (pre-treated in N_2 450°C for 2h)	190	64.4	0.016
	200	57.4	0.024
	210	56.5	0.032
	220	52.0	0.050
	230	52.0	0.070
	240	50.3	0.101
	230	51.3	0.059
	220	49.3	0.036
	210	54.7	0.016
	200	47.5	0.010
	190	100	0.002
	200	48.2	0.011
2%Ag/ nano-SiO_2 (pre-treated in N_2 450°C for 2h)	280	58.1	0.017
	290	45.7	0.026
	300	42.5	0.035
	290	42.1	0.028
	280	42.1	0.023
	290	43.0	0.031

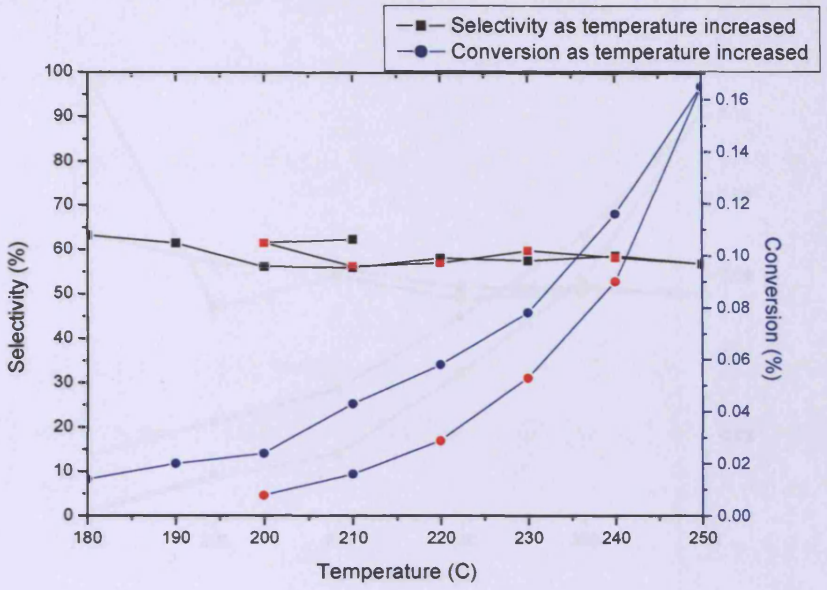

Figure 5.4. Catalytic performance for selective epoxidation of propylene between 180-250°C over 2%Cu/nano-SiO_2 catalyst pre-treated in 5% H_2/Ar for 2h. (Red points represented the catalytic activity as temperature decreased.)

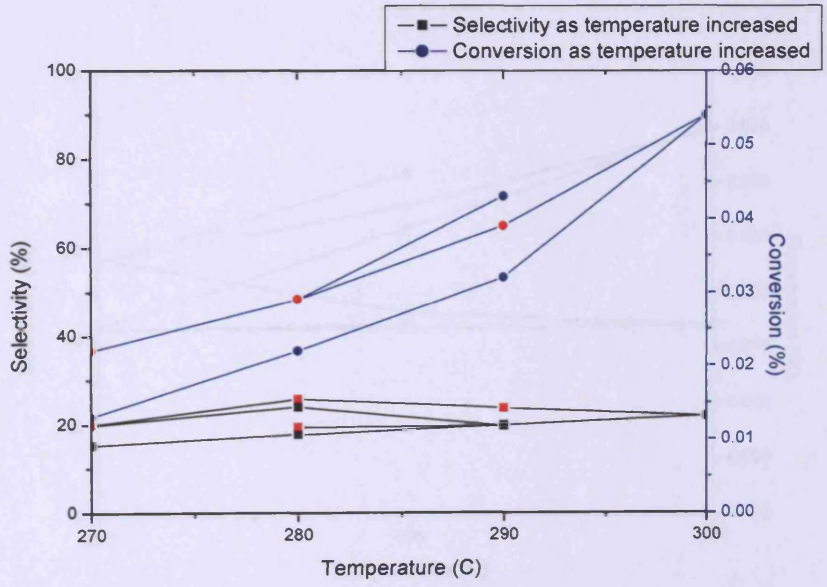

Figure 5.5. Catalytic performance for selective epoxidation of propylene between 270-300°C over 2%Ag/nano-SiO_2 catalyst pre-treated in 5% H_2/Ar for 2h. (Red points represented the catalytic activity as temperature decreased.)

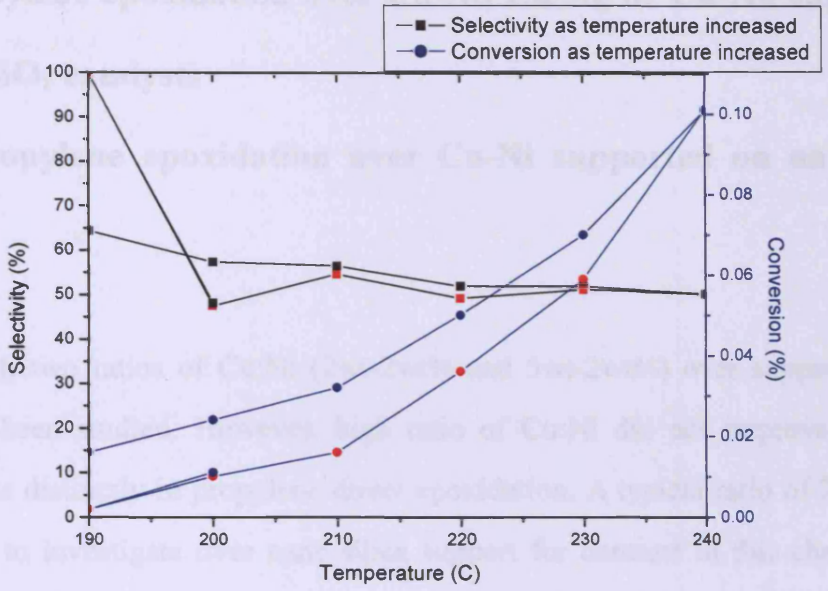

Figure 5.6. Catalytic performance for selective epoxidation of propylene between 190-240°C over 2%Cu/nano-SiO_2 catalyst pre-treated in N_2 for 2h. (Red points represented the catalytic activity as temperature decreased.)

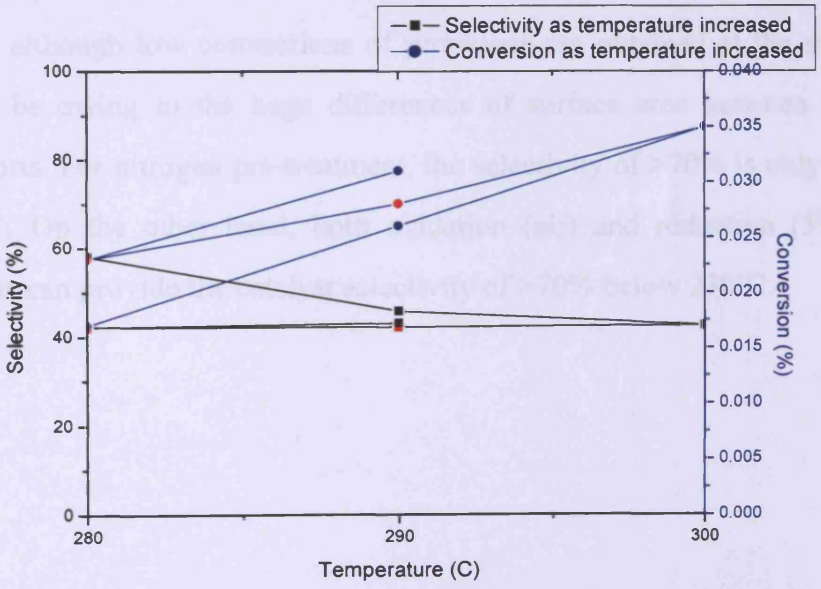

Figure 5.7. Catalytic performance for selective epoxidation of propylene between 280-300°C over 2%Ag/nano-SiO_2 catalyst pre-treated in N_2 for 2h. (Red points represented the catalytic activity as temperature decreased.)

5.3.3 Propylene epoxidation over Cu-Ni, Cu-Ag or Cu-Au supported on nano-SiO_2 catalysts

5.3.3.1 Propylene epoxidation over Cu-Ni supported on nano-SiO_2 catalysts

In Chapter 4, two ratios of Cu:Ni (2wt-2wt% and 5wt-2wt%) over support of zinc oxide have been studied. However, high ratio of Cu:Ni did not improve catalytic performances distinctly in propylene direct epoxidation. A typical ratio of 2wt-2wt% was chosen to investigate over nano-silica support for contrast in this chapter. The results of Cu-Ni supported on nano-silica and the profiles at different temperatures are shown in Tables 5.4-5.6 and Figures 5.8-5.10, in which three different pre-treatment conditions are applied.

Different from the results of the catalysts supported on zinc oxide, it is noteworthy that all three pre-treatments can offer high selectivity to PO at relatively low temperatures although low conversions of propylene are obtained at the same time, which could be owing to the huge differences of surface area between nano and regular supports. For nitrogen pre-treatment, the selectivity of >70% is only observed below 190°C. On the other hand, both oxidation (air) and reduction (5% H_2/Ar) pre-treatments can provide the catalyst selectivity of >70% below 230°C.

Table 5.4. Results of propylene epoxidation over pre-treated 2%Cu-2%Ni/nano-SiO_2 (pre-treated in 5% H_2/Ar 450°C for 2h).

Catalyst	Temp (°C)	Selectivity to PO (%)	Conversion (%)
2%Cu-2%Ni/nano-SiO_2 (pre-treated in 5% H_2/Ar 450°C for 2h)	180	100	0.005
	190	100	0.006
	200	100	0.008
	210	77.6	0.018
	220	71.6	0.030
	230	70.0	0.041
	240	66.7	0.065
	230	67.7	0.040
	220	73.9	0.020
	210	75.1	0.014
	200	100	0.006
	190	100	0.003
	200	100	0.004

Table 5.5. Results of propylene epoxidation over pre-treated 2%Cu-2%Ni/nano-SiO_2 (pre-treated in Air 450°C for 2h).

Catalyst	Temp (°C)	Selectivity to PO (%)	Conversion (%)
2%Cu-2%Ni/nano-SiO_2 (pre-treated in Air 450°C for 2h)	180	100	0.003
	190	100	0.005
	200	76.0	0.009
	210	74.7	0.016
	220	72.7	0.025
	230	70.0	0.037
	240	68.4	0.054
	230	69.4	0.031
	220	69.9	0.018
	210	70.4	0.012
	200	100	0.005
	190	100	0.004
	200	100	0.005
	190	100	0.003

Table 5.6. Results of propylene epoxidation over pre-treated 2%Cu-2%Ni/nano-SiO_2 (pre-treated in N_2 450°C for 2h).

Catalyst	Temp (°C)	Selectivity to PO (%)	Conversion (%)
2%Cu-2%Ni/nano-SiO_2 (pre-treated in N_2 450°C for 2h)	170	100	0.007
	180	78.1	0.013
	190	69.0	0.015
	200	66.2	0.023
	210	66.1	0.032
	220	64.6	0.046
	230	67.6	0.062
	240	66.6	0.086
	230	70.0	0.048
	220	63.2	0.032
	210	64.3	0.021
	200	65.1	0.013
	190	100	0.006
	180	100	0.004
	190	100	0.004
	200	62.4	0.011
	190	100	0.003

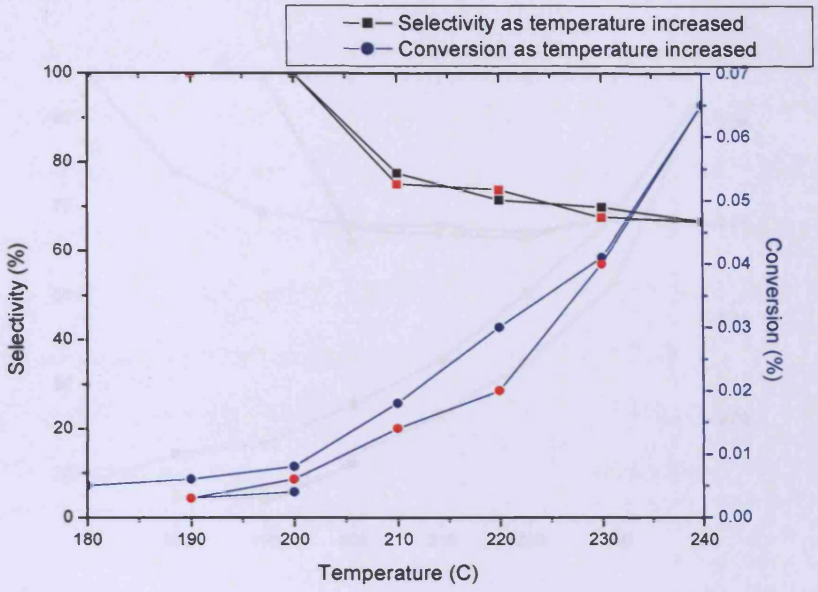

Figure 5.8. Catalytic performance for selective epoxidation of propylene between 180-240°C over 2%Cu-2%Ni/nano-SiO_2 catalyst pre-treated in 5% H_2/Ar for 2h. (Red points represented the catalytic activity as temperature decreased.)

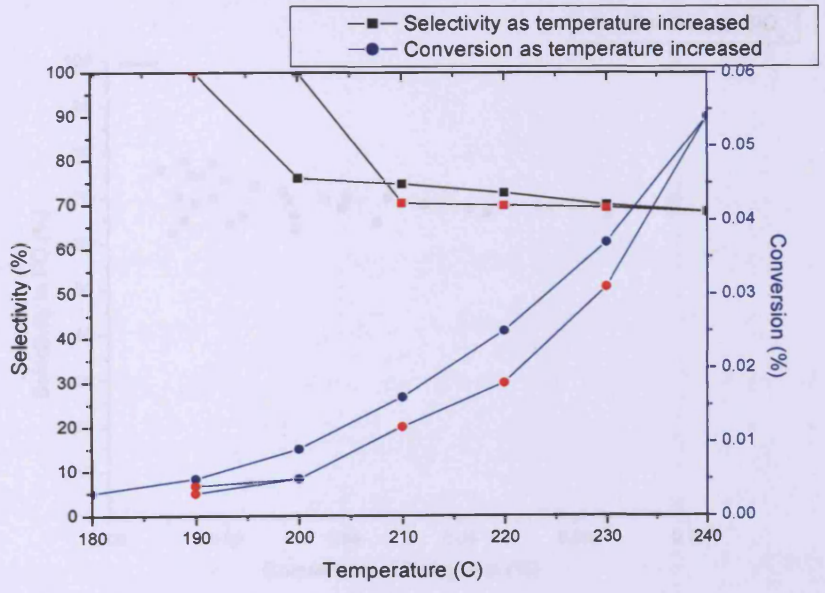

Figure 5.9. Catalytic performance for selective epoxidation of propylene between 180-240°C over 2%Cu-2%Ni/nano-SiO_2 catalyst pre-treated in air for 2h. (Red points represented the catalytic activity as temperature decreased.)

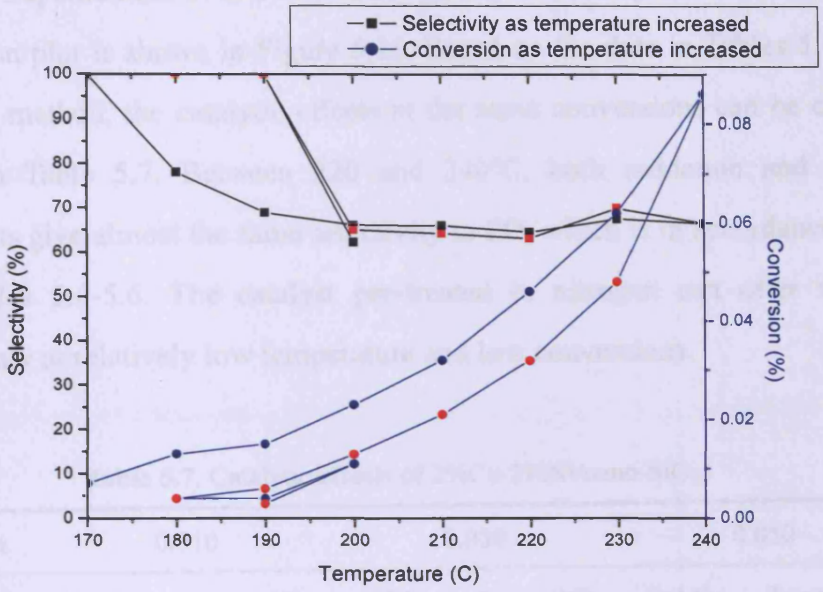

Figure 5.10. Catalytic performance for selective epoxidation of propylene between 170-240°C over 2%Cu-2%Ni/nano-SiO_2 catalyst pre-treated in N_2 for 2h. (Red points represented the catalytic activity as temperature decreased.)

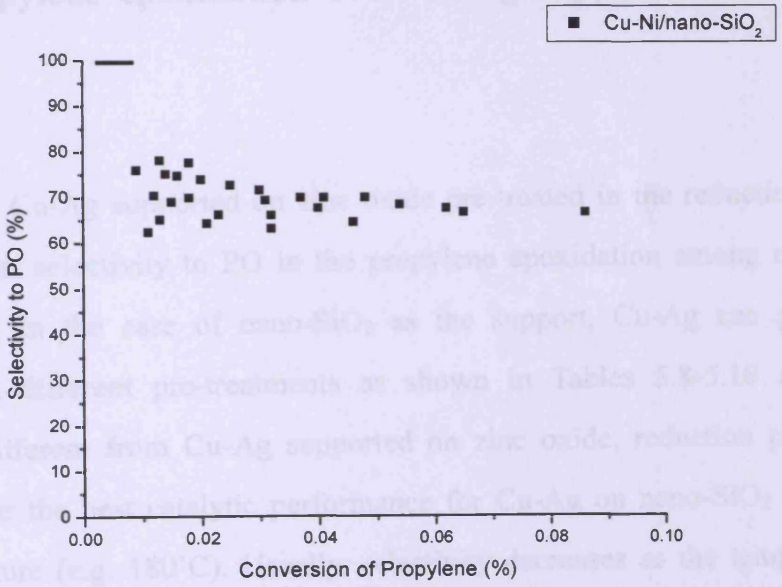

Figure 5.11. Multiple selectivity-conversion plot for propylene epoxidation to propylene oxide (PO) over Cu-Ni supported on nano-SiO_2 catalysts.

For propylene epoxidation over Cu-Ni/nano-SiO_2 system, the profile of the selectivity vs. conversion plot is shown in Figure 5.11. Based on the data in Tables 5.4-5.6 and interpolation method, the catalytic effects at the same conversions can be compared, as shown in Table 5.7. Between 220 and 240°C, both oxidation and reduction pre-treatments give almost the same selectivity to PO, which is in accordance with the data in Tables 5.4-5.6. The catalyst pre-treated in nitrogen can offer very high selectivity only at relatively low temperature and low conversions.

Table 5.7. Catalytic effects of 2%Cu-2%Ni/nano-SiO_2.

Conv %	0.010		0.030		0.050	
450°C, 2h	Sel %	Temp (°C)	Sel %	Temp (°C)	Sel %	Temp (°C)
5%H_2/Ar	95.5	202	71.6	220	68.8	234
Air	75.8	201	71.6	224	68.8	238
N_2	89.0	175	66.1	208	65.3	222

5.3.3.2 Propylene epoxidation over Cu-Ag supported on nano-SiO_2 catalysts

In Chapter 4, Cu-Ag supported on zinc oxide pre-treated in the reduction condition shows the best selectivity to PO in the propylene epoxidation among mixed metal ZnO species. In the case of nano-SiO_2 as the support, Cu-Ag can give similar selectivity in different pre-treatments as shown in Tables 5.8-5.10 and Figures 5.12-5.14. Different from Cu-Ag supported on zinc oxide, reduction pre-treatment does not offer the best catalytic performance for Cu-Ag on nano-SiO_2 at relatively low temperature (e.g. 180°C). Usually, selectivity decreases as the temperature and conversion increase. But in reduction and oxidation pre-treatments, Cu-Ag shows some abnormal data in which selectivity at some higher temperatures is higher than the one at low temperature. It is noteworthy that the profiles of selectivity to PO show the very smooth curve between 190-230°C. As the selectivity decreases slowly as the

temperature increases, there should be small errors existed among the data at different temperatures. It has also inferred that the catalyst activity can be remained for a long time since the reaction was normally carried out for over 16h. On the other hand, it has been implied that the support with high surface area plays an important role in comparison with the results of reduced Cu-Ag supported on regular silica in Table 5.11 and Figure 5.15.

Table 5.8. Results of propylene epoxidation over pre-treated 2%Cu-2%Ag/nano-SiO_2 (pre-treated in 5% H_2/Ar 450°C for 2h).

Catalyst	Temp (°C)	Selectivity to PO (%)	Conversion (%)
2%Cu-2%Ag/nano-SiO_2 (pre-treated in 5% H_2/Ar 450°C for 2h)	170	100	0.006
	180	65.8	0.018
	190	60.5	0.021
	200	58.4	0.031
	210	63.6	0.047
	220	63.8	0.069
	230	56.0	0.106
	220	60.0	0.063
	210	61.5	0.036
	200	62.3	0.024
	190	52.8	0.013
	180	100	0.004
	190	56.0	0.014
	200	61.4	0.017
	190	71.1	0.011

Table 5.9. Results of propylene epoxidation over pre-treated 2%Cu-2%Ag/nano-SiO_2 (pre-treated in Air 450°C for 2h).

Catalyst	Temp (°C)	Selectivity to PO (%)	Conversion (%)
2%Cu-2%Ag/ nano-SiO_2 (pre-treated in Air 450°C for 2h)	180	100	0.008
	190	71.4	0.015
	200	63.6	0.021
	210	59.3	0.026
	220	64.9	0.038
	230	62.0	0.055
	220	62.4	0.036
	210	55.3	0.021
	200	59.3	0.013
	190	100	0.005
	200	61.7	0.012
	190	100	0.004

Table 5.10. Results of propylene epoxidation over pre-treated 2%Cu-2%Ag/nano-SiO_2 (pre-treated in N_2 450°C for 2h)

Catalyst	Temp (°C)	Selectivity to PO (%)	Conversion (%)
2%Cu-2%Ag/nano-SiO_2 (pre-treated in N_2 450°C for 2h)	180	100	0.006
	190	74.0	0.013
	200	74.0	0.020
	210	66.2	0.032
	220	64.9	0.048
	230	58.8	0.079
	240	55.1	0.117
	230	60.5	0.063
	220	60.0	0.039
	210	64.2	0.022
	200	65.1	0.014
	190	100	0.004
	200	61.7	0.010

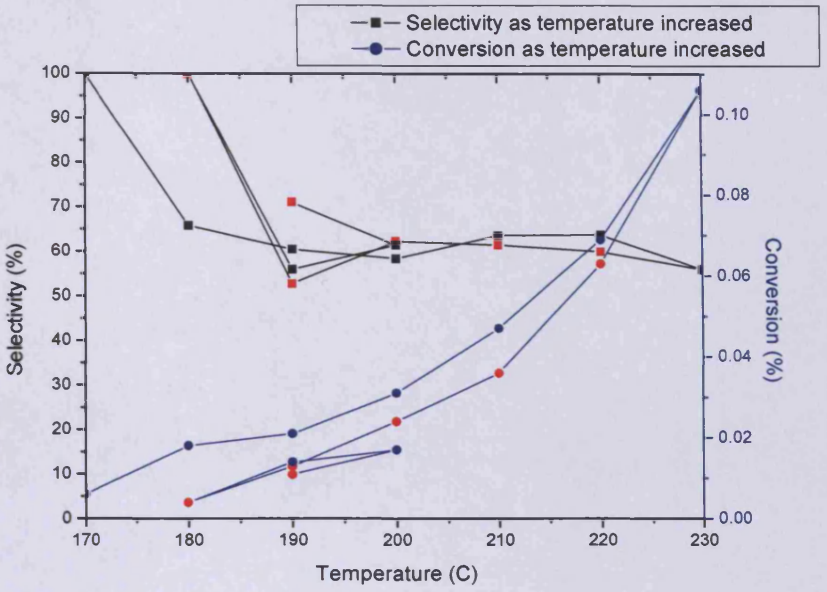

Figure 5.12. Catalytic performance for selective epoxidation of propylene between 180-230°C over 2%Cu-2%Ag/nano-SiO_2 catalyst pre-treated in 5% H_2/Ar for 2h. (Red points represented the catalytic activity as temperature decreased.)

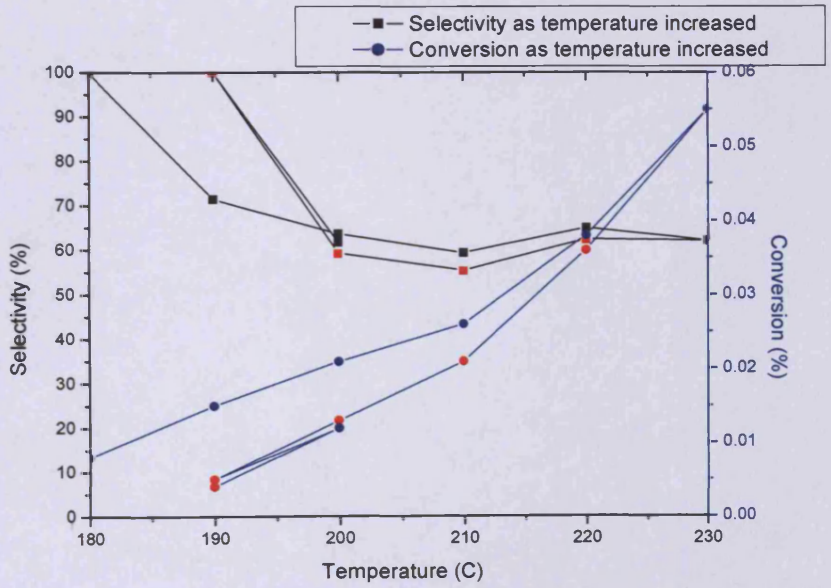

Figure 5.13. Catalytic performance for selective epoxidation of propylene between 180-230°C over 2%Cu-2%Ag/nano-SiO_2 catalyst pre-treated in Air for 2h. (Red points represented the catalytic activity as temperature decreased.)

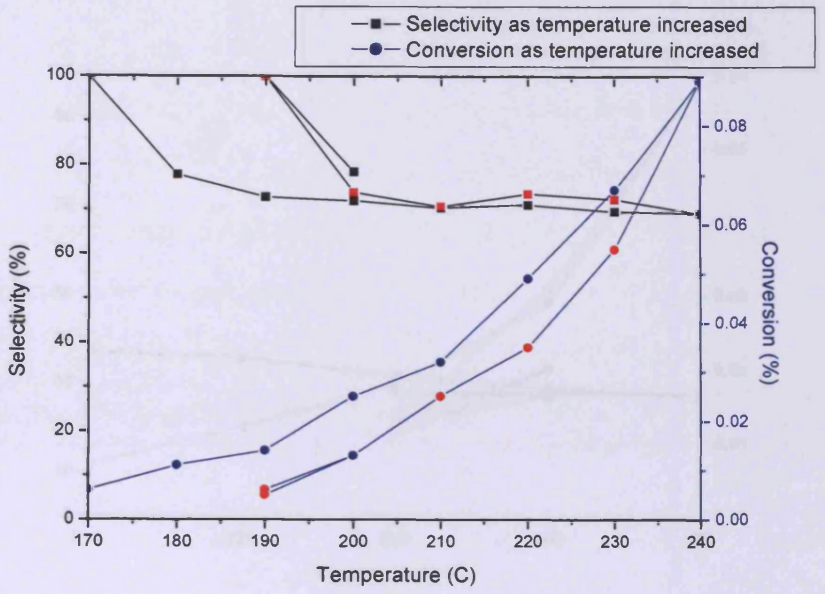

Figure 5.14. Catalytic performance for selective epoxidation of propylene between 170-240˚C over 2%Cu-2%Ag/nano-SiO_2 catalyst pre-treated in N_2 for 2h. (Red points represented the catalytic activity as temperature decreased.)

Table 5.11. Results for propylene epoxidation over Cu-Ag/SiO_2 pre-treated in 5% H_2/Ar for 2h.

Catalyst	Temp (˚C)	Selectivity to PO (%)	Conversion (%)
2%Cu-2%Ag/SiO_2 (pre-treated in 5% H_2/Ar 450˚C for 2h)	210	37.0	0.007
	220	35.8	0.012
	230	31.8	0.018
	240	29.0	0.029
	250	27.6	0.059
	240	28.1	0.031
	230	28.1	0.013
	240	27.4	0.020
	230	21.4	0.011

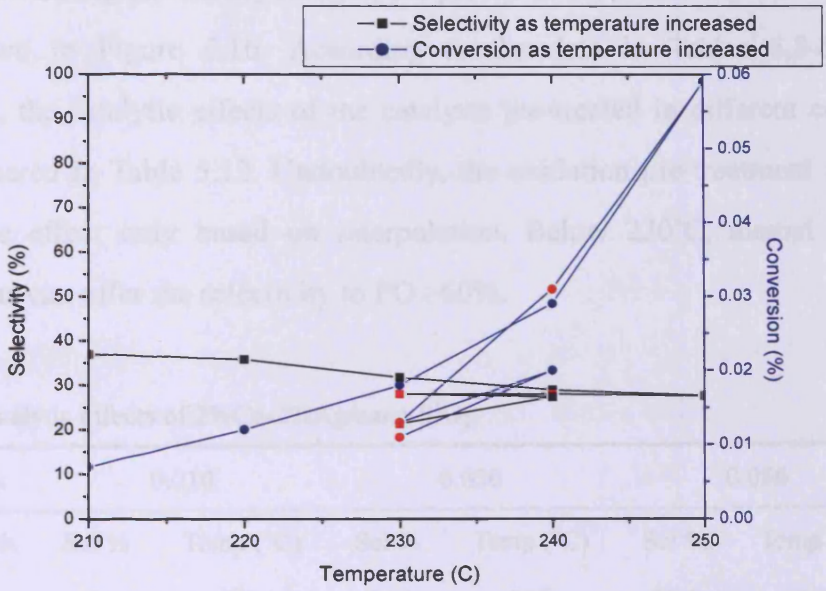

Figure 5.15. Catalytic performance for selective epoxidation of propylene between 210-250°C over 2%Cu-2%Ag/SiO_2 catalyst pre-treated in 5% H_2/Ar for 2h. (Red points represented the catalytic activity as temperature decreased.)

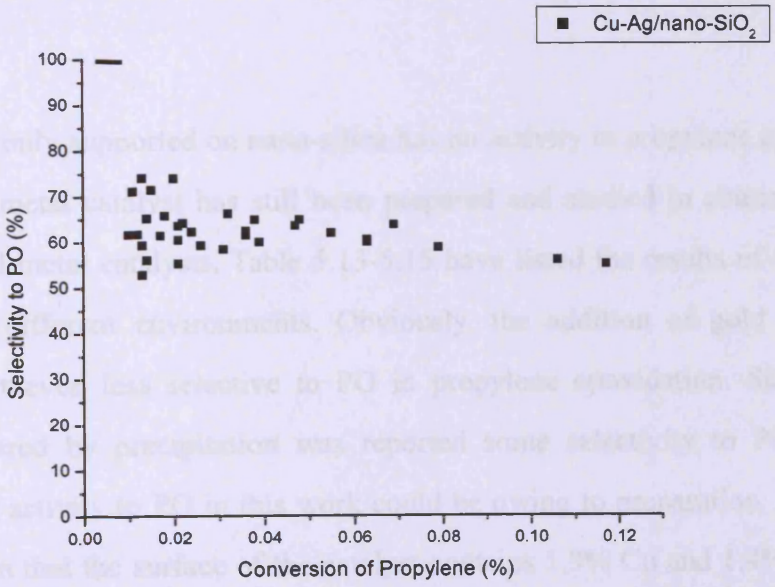

Figure 5.16. Multiple selectivity-conversion plot for propylene epoxidation to propylene oxide (PO) over Cu-Ag supported on nano-SiO_2 catalysts.

For 2wt-2wt% Cu-Ag/nano-SiO_2 catalyst, the profile of the selectivity vs. conversion plot is shown in Figure 5.16. According to the data in Tables 5.8-5.10 and interpolation, the catalytic effects of the catalysts pre-treated in different conditions can be compared in Table 5.12. Undoubtedly, the oxidation pre-treatment gives the best catalytic effect only based on interpolation. Below 220°C, almost all three pre-treatments can offer the selectivity to PO >60%.

Table 5.12. Catalytic effects of 2%Cu-2%Ag/nano-SiO_2.

Conv %	0.010		0.030		0.050	
450°C, 2h	Sel %	Temp (°C)	Sel %	Temp (°C)	Sel %	Temp (°C)
5%H_2/Ar	88.6	173	58.6	199	63.6	211
Air	91.8	183	61.2	213	62.9	227
N_2	85.2	186	67.5	208	64.5	221

5.3.3.3 Propylene epoxidation over Cu-Au supported on nano-SiO_2 catalysts

Although gold only supported on nano-silica has no activity in propylene epoxidation, Cu-Au mixed metal catalyst has still been prepared and studied in contrast to other metal or mixed metal catalysts. Table 5.13-5.15 have listed the results of the catalyst pre-treated in different environments. Obviously, the addition of gold makes the copper catalyst even less selective to PO in propylene epoxidation. Since Cu-Au catalysts prepared by precipitation was reported some selectivity to PO, the low selectivity and activity to PO in this work could be owing to preparation. SEM-EDX scan has shown that the surface of the catalyst contains 1.9% Cu and 1.4% Cl but no Au observed. After calcination in air, 2.5% Cu and 3.0% Au can be observed on the surface of the catalyst. Particularly pre-treated by 5% H_2/Ar, the surface of the catalyst looks inhomogeneous through EDX scan. For example, the weight ratio of copper ranges from 2.0% to 3.3% in some part of the surface with no gold observed,

while two other parts of the surface contain only 3.3% gold without copper and 1.9% copper together with 3.7% gold, respectively. As gold itself supported on nano-SiO_2 has no activity to PO among this temperature range, the addition of gold undoubtedly decreases the catalytic effective of copper. Basically, the impregnation method could not provide the catalyst relatively an even surface so that the catalytic performances are greatly affected. Similarly to Cu-Ag system, the selectivity to PO decreases very slowly as the temperature increases in the profiles as shown in Figures 5.17-5.19. In brief, the catalytic performances of Cu-Au supported on nano-silica are approximately equal to that of Cu-Ni on zinc oxide, which can be seen from the multiple selectivity-conversion plot of Cu-Au/nano-SiO_2 in Figure 5.20.

Table 5.13. Results of propylene epoxidation over pre-treated 2%Cu-2%Au/nano-SiO_2 (pre-treated in Air 450°C for 2h)

Catalyst	Temp (°C)	Selectivity to PO (%)	Conversion (%)
2%Cu-2%Au/nano-SiO_2 (pre-treated in Air 450°C for 2h)	200	59.8	0.009
	210	54.5	0.012
	220	43.3	0.020
	230	36.4	0.026
	240	41.4	0.037
	250	41.3	0.050
	240	42.5	0.027
	230	44.9	0.018
	220	44.5	0.013
	230	56.7	0.014
	220	54.4	0.011

Table 5.14. Results of propylene epoxidation over pre-treated 2%Cu-2%Au/nano-SiO_2 (pre-treated in 5% H_2/Ar 450°C for 2h).

Catalyst	Temp (°C)	Selectivity to PO (%)	Conversion (%)
2%Cu-2%Au/nano-SiO_2 (pre-treated in 5% H_2/Ar 450°C for 2h)	240	38.1	0.013
	250	33.6	0.023
	260	41.4	0.032
	250	51.5	0.025
	240	47.4	0.015
	230	52.4	0.011
	240	49.1	0.015
	230	59.4	0.010

Table 5.15. Results of propylene epoxidation over pre-treated 2%Cu-2%Au/nano-SiO_2 (pre-treated in N_2 450°C for 2h).

Catalyst	Temp (°C)	Selectivity to PO (%)	Conversion (%)
2%Cu-2%Au/nano-SiO_2 (pre-treated in N_2 450°C for 2h)	200	40.9	0.012
	210	37.7	0.017
	220	32.6	0.031
	230	31.8	0.040
	240	35.2	0.061
	250	36.3	0.092
	240	37.4	0.044
	230	38.6	0.021
	220	35.1	0.013
	230	44.5	0.021
	220	41.7	0.011

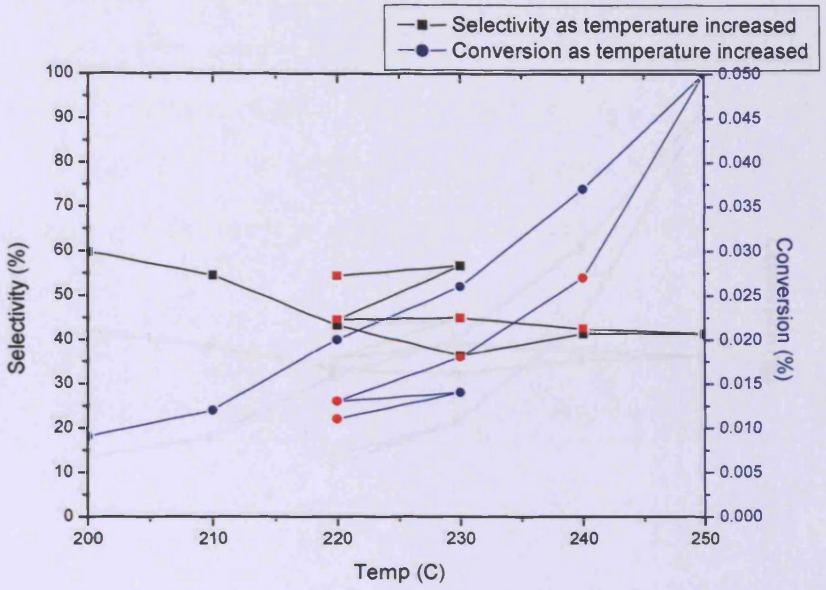

Figure 5.17. Catalytic performance for selective epoxidation of propylene between 200-250°C over 2%Cu-2%Au/nano-SiO_2 catalyst pre-treated in Air for 2h. (Red points represented the catalytic activity as temperature decreased).

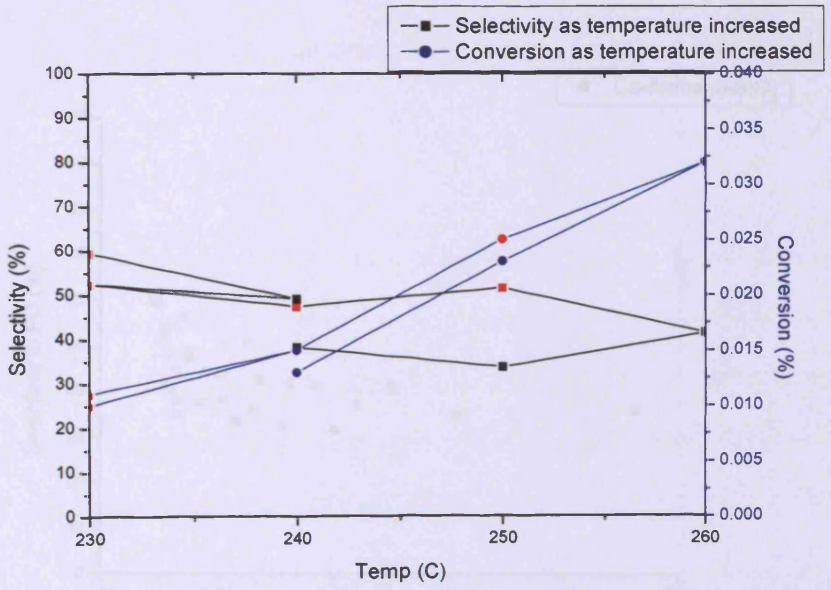

Figure 5.18. Catalytic performance for selective epoxidation of propylene between 230-260°C over 2%Cu-2%Au/nano-SiO_2 catalyst pre-treated in 5% H_2/Ar for 2h. (Red points represented the catalytic activity as temperature decreased).

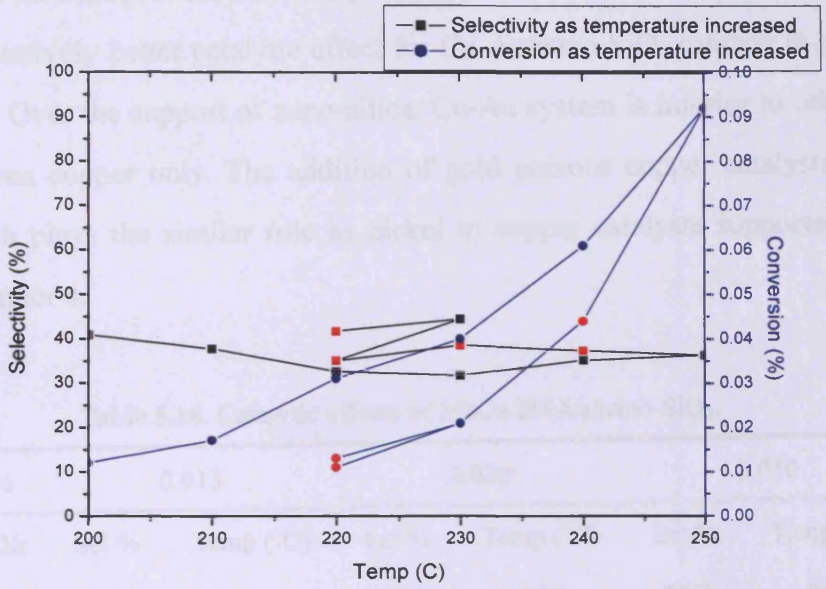

Figure 5.19. Catalytic performance for selective epoxidation of propylene between 200-250°C over 2%Cu-2%Au/nano-SiO_2 catalyst pre-treated in N_2 for 2h. (Red points represented the catalytic activity as temperature decreased).

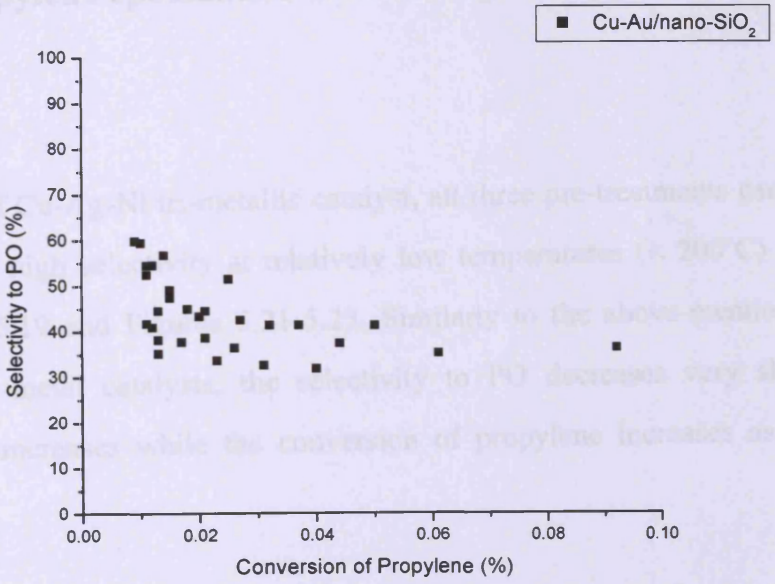

Figure 5.20. Multiple selectivity-conversion plots for propylene epoxidation to propylene oxide (PO) over Cu-Au supported on nano-SiO_2 catalysts.

According to the data produced by interpolation in Table 5.16, oxidation pre-treatment gives comparatively better catalytic effect for Cu-Au/nano-SiO_2 catalyst in propylene epoxidation. Over the support of nano-silica, Cu-Au system is inferior to other mixed metals or even copper only. The addition of gold poisons copper catalysts to some extent, which plays the similar role as nickel in copper catalysts supported on zinc oxide in Chapter 4.

Table 5.16. Catalytic effects of 2%Cu-2%Au/nano-SiO_2.

Conv %	0.013		0.020		0.030	
450°C, 2h	Sel %	Temp (°C)	Sel %	Temp (°C)	Sel %	Temp (°C)
5%H_2/Ar	38.1	240	35.0	247	39.7	258
Air	53.1	211	43.3	220	38.2	234
N_2	40.3	202	36.6	212	33.0	219

5.3.3.4 Propylene epoxidation over Cu-Ag-Ni supported on nano-SiO_2 catalysts

In the case of Cu-Ag-Ni tri-metallic catalyst, all three pre-treatments can provide the catalyst very high selectivity at relatively low temperatures (< 200°C) as shown in Tables 5.17-5.19 and Figures 5.21-5.23. Similarly to the above-mentioned data for other mixed metal catalysts, the selectivity to PO decreases very slowly as the temperature increases while the conversion of propylene increases as temperature quickly.

Table 5.17. Results of propylene epoxidation over pre-treated 2%Cu-2%Ag-2%Ni/nano-SiO_2 (pre-treated in 5% H_2/Ar 450°C for 2h).

Catalyst	Temp (°C)	Selectivity to PO (%)	Conversion (%)
2%Cu-2%Ag-2%Ni/nano-SiO_2 (pre-treated in 5% H_2/Ar 450°C for 2h)	170	100	0.004
	180	76.0	0.014
	190	72.7	0.020
	200	68.9	0.032
	210	70.5	0.048
	220	69.2	0.072
	230	66.8	0.100
	240	61.4	0.146
	230	68.0	0.079
	220	69.8	0.045
	210	69.8	0.029
	200	73.8	0.017
	190	74.9	0.009
	180	100	0.004
	190	68.9	0.008
	200	67.9	0.016
	190	75.0	0.009

Table 5.18. Results of propylene epoxidation over pre-treated 2%Cu-2%Ag-2%Ni/nano-SiO_2.

Catalyst	Temp (°C)	Selectivity to PO (%)	Conversion (%)
2%Cu-2%Ag-2%Ni/nano-SiO_2 (pre-treated in Air 450°C for 2h)	170	100	0.006
	180	77.8	0.011
	190	72.8	0.014
	200	72.0	0.025
	210	70.4	0.032
	220	71.1	0.049
	230	69.6	0.067
	240	69.1	0.089
	230	72.4	0.055
	220	73.6	0.035
	210	70.7	0.025
	200	73.9	0.013
	190	100	0.006
	180	100	0.003
	190	100	0.006
	200	78.5	0.013
	190	100	0.005

Table 5.19. Results of propylene epoxidation over pre-treated 2%Cu-2%Ag-2%Ni/nano-SiO_2 (pre-treated in N_2 450°C for 2h).

Catalyst	Temp (°C)	Selectivity to PO (%)	Conversion (%)
	180	100	0.005
	190	75.5	0.014
	200	75.7	0.023
	210	75.1	0.031
	220	73.5	0.040
	230	76.7	0.057
	240	70.4	0.078
2%Cu-2%Ag-2%Ni/nano-SiO_2	230	70.9	0.045
(pre-treated in N_2 450°C for 2h)	220	71.8	0.029
	210	72.8	0.017
	200	74.3	0.013
	190	100	0.005
	180	100	0.003
	190	100	0.005
	200	67.1	0.010
	190	100	0.005

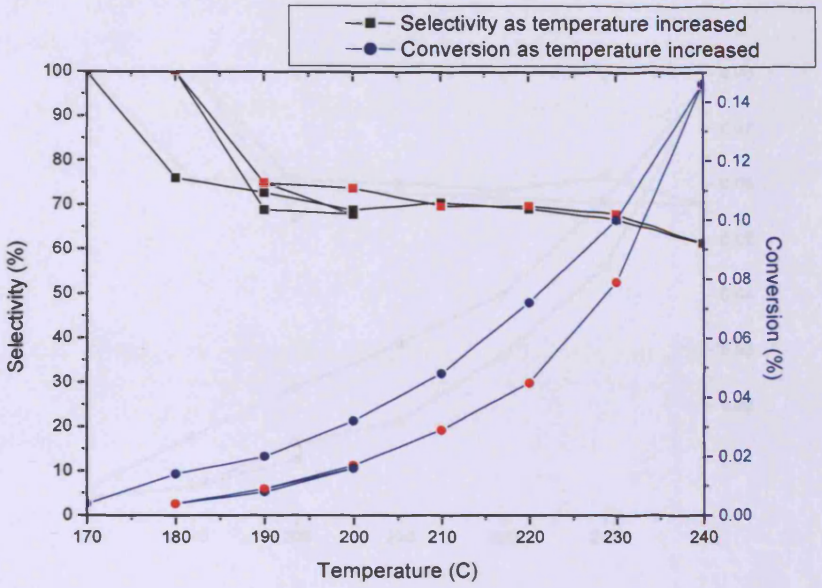

Figure 5.21. Catalytic performance for selective epoxidation of propylene between 170-240°C over 2%Cu-2%Ag-2%Ni/nano-SiO_2 catalyst pre-treated in 5% H_2/Ar for 2h. (Red points represented the catalytic activity as temperature decreased.)

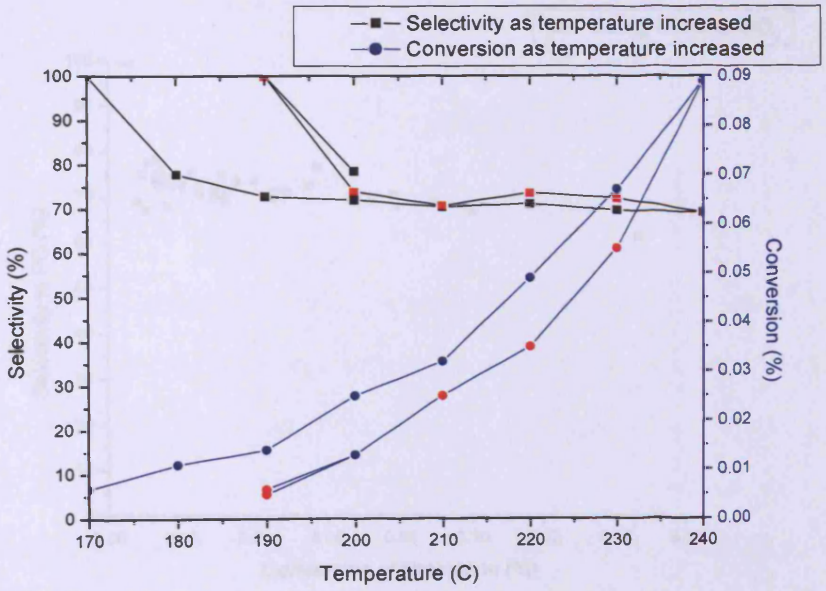

Figure 5.22. Catalytic performance for selective epoxidation of propylene between 170-240°C over 2%Cu-2%Ag-2%Ni/nano-SiO_2 catalyst pre-treated in Air for 2h. (Red points represented the catalytic activity as temperature decreased.)

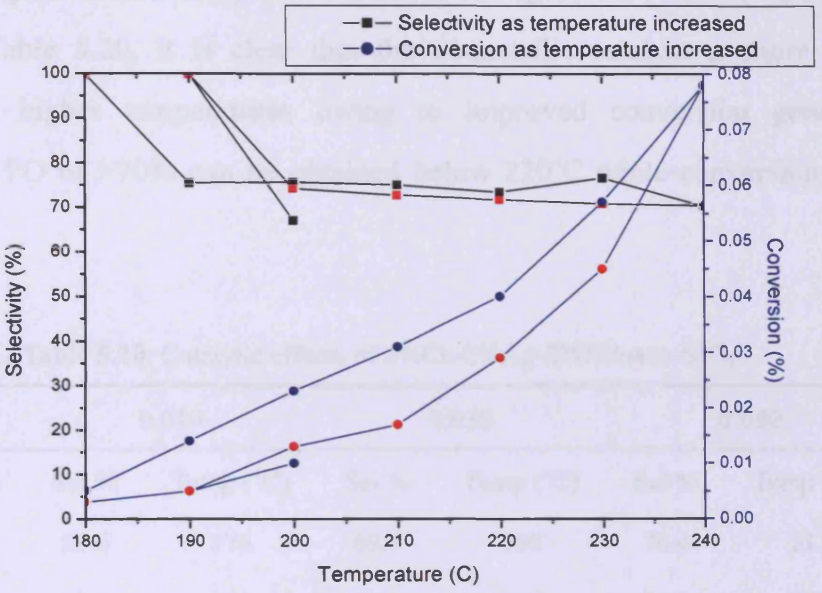

Figure 5.23. Catalytic performance for selective epoxidation of propylene between 180-240˚C over 2%Cu-2%Ag-2%Ni/nano-SiO_2 catalyst pre-treated in N_2 for 2h. (Red points represented the catalytic activity as temperature decreased.)

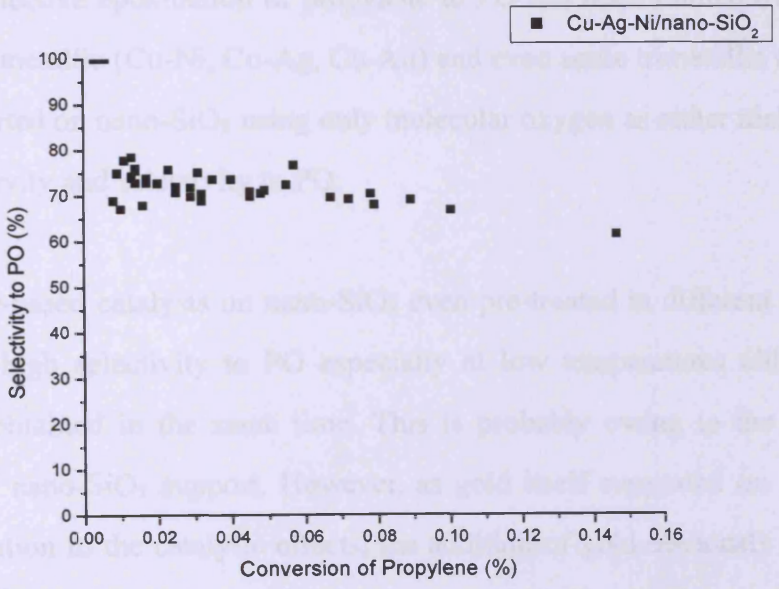

Figure 5.24. Multiple selectivity-conversion plot for propylene epoxidation to propylene oxide (PO) over Cu-Ag-Ni supported on nano-SiO_2 catalysts.

Based on the plot of selectivity *vs.* conversion in Figure 5.24 and the interpolation analysis in Table 5.20, it is clear that the tri-metallic catalyst is more effective especially at higher temperatures owing to improved conversion greatly. The selectivity to PO of >70% can be obtained below 220°C while conversion is lower than 0.05%.

Table 5.20. Catalytic effects of 2%Cu-2%Ag-2%Ni/nano-SiO_2.

Conv %	0.010		0.030		0.050	
450°C, 2h	Sel %	Temp (°C)	Sel %	Temp (°C)	Sel %	Temp (°C)
5%H_2/Ar	85.6	176	69.5	198	70.4	211
Air	82.3	178	70.9	207	71.0	221
N_2	86.4	186	75.2	209	75.4	226

5.4 Conclusions

In summary, selective epoxidation of propylene to PO has been studied over Cu and Ag catalysts, bimetallic (Cu-Ni, Cu-Ag, Cu-Au) and even some trimetallic (Cu-Ag-Ni) catalysts supported on nano-SiO_2 using only molecular oxygen as either nickel or gold only has no activity and selectivity to PO.

Most of copper-based catalysts on nano-SiO_2 even pre-treated in different conditions can give very high selectivity to PO especially at low temperatures although low conversion is obtained in the same time. This is probably owing to the very high surface area of nano-SiO_2 support. However, as gold itself supported on nano-SiO_2 has no contribution to the catalytic effects, the addition of gold obviously makes the supported copper catalyst poisoned. Unlike supported on zinc oxide, the addition of nickel has improved the catalytic performances for not only copper itself but also mixed metal catalysts in propylene epoxidation.

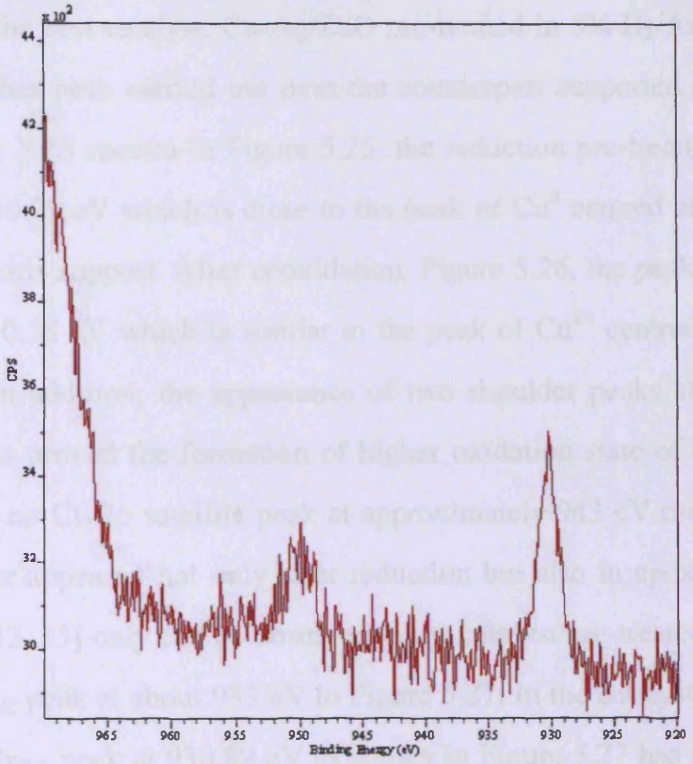

Figure 5.25. The Cu $2p_{3/2}$ XPS spectra of Cu-Ag supported on nano-SiO_2 pre-treated in 5% H_2/Ar.

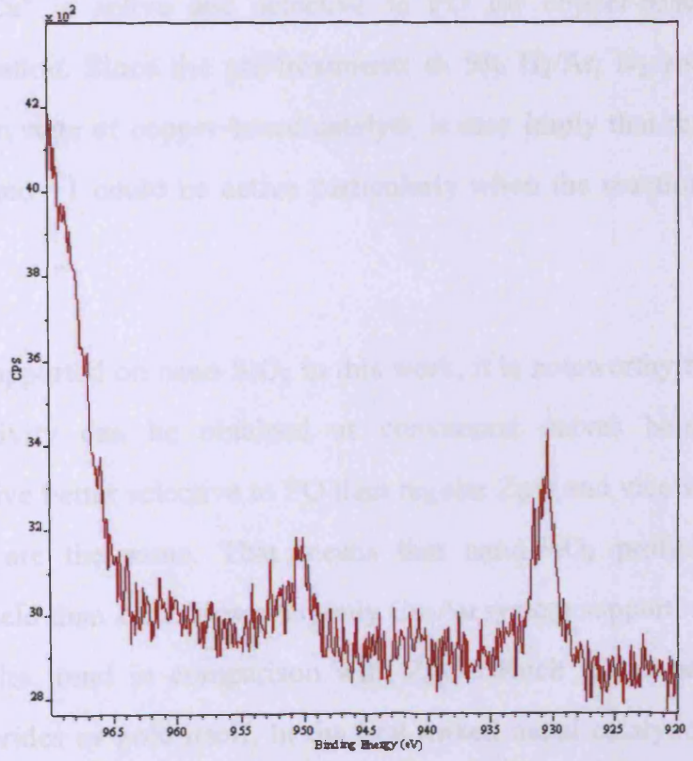

Figure 5.26. The Cu $2p_{3/2}$ XPS spectra of Cu-Ag supported on nano-SiO_2 pre-treated in 5% H_2/Ar after epoxidation.

To compare with the best catalyst, Cu-Ag/ZnO pre-treated in 5% H_2/Ar in Chapter 4, the XPS analysis has been carried out over the counterpart supported on nano-SiO_2. Based on Cu $2p_{3/2}$ XPS spectra in Figure 5.25, the reduction pre-treatment gives the peak centred at 930.21 eV which is close to the peak of Cu^0 centred at 930.18 eV in the case of zinc oxide support. After epoxidation, Figure 5.26, the peak of copper has been shifted to 930.58 eV which is similar to the peak of Cu^{1+} centred at 930.44 eV for Cu-Ag/ZnO. In addition, the appearance of two shoulder peaks at about 931.67 and 930.98 eV has proved the formation of higher oxidation state of copper ($Cu^{>0}$). However, there is no Cu 2p satellite peak at approximately 943 eV measured, which implies Cu^{2+} never appeared not only after reduction but also in epoxidation. In the meantime, Cu^{2+} [32, 33] only can be observed in the catalyst pre-treated by air, which has shown Cu $2p_{3/2}$ peak at about 933 eV in Figure 5.27. In the catalyst pre-treated by nitrogen, the Cu $2p_{3/2}$ peak at 930.89 eV as shown in Figure 5.27 has also evidenced that Cu^{1+} is the predominant component after epoxidation. Therefore, it can be concluded that Cu^0 is active and selective to PO for copper-based catalysts in propylene epoxidation. Since the pre-treatments in 5% H_2/Ar, N_2 and air represent different oxidation state of copper-based catalyst, it may imply that the Cu oxidation state between 0 and +1 could be active particularly when the reaction performed at low temperature.

In the catalysts supported on nano-SiO_2 in this work, it is noteworthy that very placid curves of selectivity can be obtained as conversion curves being kept steep. Nano-SiO_2 can give better selective to PO than regular ZnO and vice versa, if both of the conversions are the same. That means that nano-SiO_2 profits copper-based catalysts better yield than ZnO. However, only Cu-Au system supported on nano-SiO_2 represents opposite trend in comparison with ZnO, which might be owing to the influence of chlorides or gold itself. In the best mixed metal catalytic systems, both Cu-Ag and Cu-Ag-Ni, can give equivalent selectivity to PO at low conversion. But in the same range of temperature, only nano-SiO_2 can offer better yield to PO.

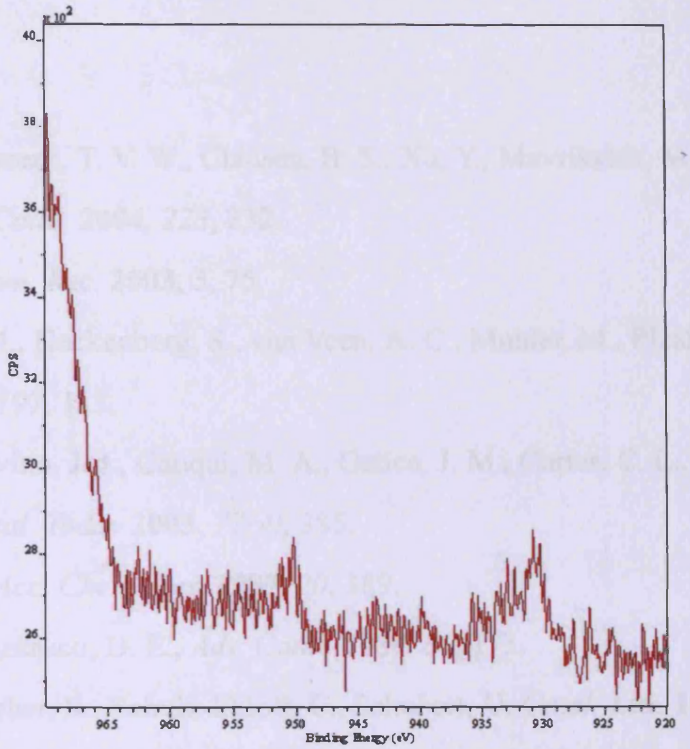

Figure 5.27. The Cu $2p_{3/2}$ XPS spectra of Cu-Ag supported on nano-SiO_2 pre-treated in air after epoxidation.

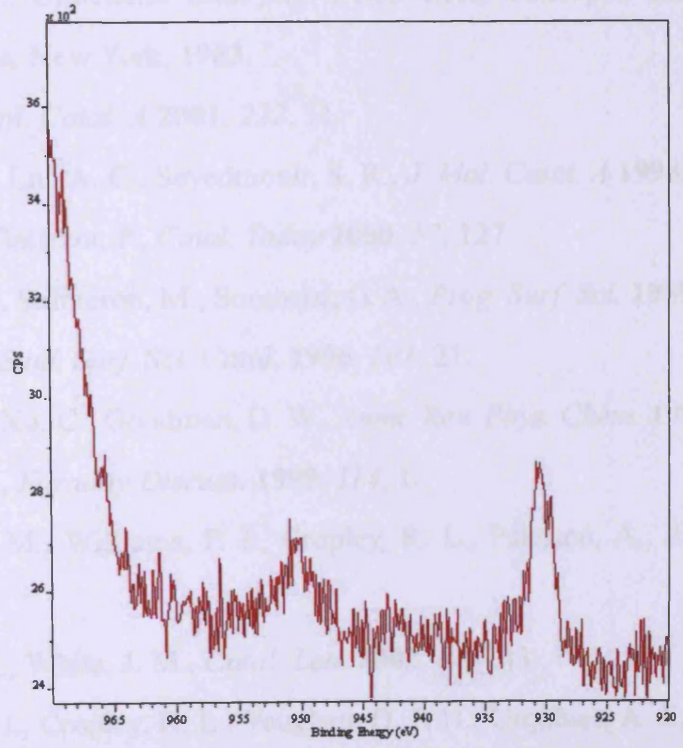

Figure 5.28. The Cu $2p_{3/2}$ XPS spectra Cu-Ag supported on nano-SiO_2 pre-treated in N_2 after epoxidation.

5.5 References

[1] Lopez, N., Janssens, T. V. W., Clausen, B. S., Xu, Y., Mavrikakis, M., Bligaard, T., Nørskov, J. K., *J. Catal.* **2004**, *223*, 232.

[2] Haruta, M. *Chem. Rec.* **2003**, *3*, 75.

[3] Schubert, M. M., Hackenberg, S., van Veen, A. C., Muhler, M., Plzak, V., Behm, R. J., *J. Catal.* **2001**, *197*, 113.

[4] Bernal, S., Calvino, J. J., Cauqui, M. A., Gatica, J. M., Cartes, C. L., Omil, J. A. P., Pintado, J. M., *Catal. Today* **2003**, *77(4)*, 385.

[5] Tauster., S. J., *Acc. Chem. Res.* **1987**, *20*, 389.

[6] Haller, G. L., Resasco, D. E., *Adv. Catal.* **1989**, *36*, 173.

[7] Hippe, C., Lamber, R., Schulz-Ekloff, G., Schubert, U. *Catal. Lett.* **1997**, *43*, 195.

[8] Hicks, R. F., Yen, Q.-J., Bell, A. T., *J. Catal.* **1984**, *89*, 498.

[9] Hayek, K., Kramer, R., Paál, Z., *Appl. Catal. A* **1997**, *162*, 1.

[10] Sinfelt, J. H., Bimetallic Catalysts: Discoveries, Concepts, and Applications, John Wiley & Sons, New York, **1983**.

[11] Ponec, V., *Appl. Catal. A* **2001**, *222*, 31.

[12] Serafin, J. G., Liu, A. C., Seyedmonir, S. R., *J. Mol. Catal. A* **1998**, *131*, 157.

[13] Besson, M., Gallezot, P., *Catal. Today* **2000**, *57*, 127.

[14] Vurens, G. H., Salmeron, M., Somorjai, G. A., *Prog. Surf. Sci.* **1989**, *32*, 333.

[15] Iwasawa, Y., *Stud. Surf. Sci. Catal.* **1996**, *101*, 21.

[16] Street, S. C., Xu, C., Goodman, D. W., *Annu. Rev. Phys. Chem.* **1997**, *48*, 43.

[17] Freund, H.-J., *Faraday Discuss.* **1999**, *114*, 1.

[18] Lambert, R. M., Williams, F. J., Cropley, R. L., Palermo, A., *J. Mol. Catal. A* **2005**, *228*, 27.

[19] Huang, W. X., White, J. M., *Catal. Lett.* **2002**, *84*, 143.

[20] Williams, F. J., Cropley, R. L., Vaughan, O. P. H., Urquhart, A. J., Tikhov, M. S., Kolczewski, C., Hermann, K., Lambert, R. M., *J. Am. Chem. Soc.* **2005**, *127*, 17007.

[21] Torres, D., Lopez, N., Illas, F., Lambert, R. M., *J. Am. Chem. Soc.* **2005**, *127*,

10774.

[22] Ranney, J. T., Bare, S. R., Gland, J. L., *Catal. Lett.* **1997**, *48*, 25.

[23] Ranney, J. T., Gland, J. L., Bare, S. R., *Surf. Sci.* **1998**, *401*, 1.

[24] Haruta, M., Date, M., *Appl. Catal. A* **2001**, *222*, 427.

[25] Zhdanov, V. P., Kasemo, B., *Surf. Sci. Rep.* **2000**, *39*, 25.

[26] Gunter, P. L. J., Niemantsverdriet, J. W., Ribeiro, F. H., Somorjai, G. A., *Catal. Rev.-Sci. Eng.* **1997**, *39*, 77.

[27] Henry, C. R., *Surf. Sci. Rep.* **1998**, *31*, 231.

[28] Baumer, M., Freund, H.-J., *Prog. Sur. Sci.* **1999**, *61*, 127.

[29] Santra, A. K., Goodman, D. W., *J. Phys.: Condens. Matter* **2003**, *15*, R31.

[30] Zhu, J. Konya, Z., Puntes, V. F., Kiricsi, I., Miao, C. X., Ager, J. W., Alivisatos, A. P., Somorjai, G. A., *Langmuir* **2003**, *19*, 4396.

[31] Rioux, R. M., Song, H., Hoefelmeyer, J. D., Yang, P., Somorjai, G. A., *J. Phys. Chem. B* **2005**, *109*, 2192.

[32] Okamoto, Y., Fukino, K., Imanaka, T., Teranishi, S., *J. Phys. Chem.* **1983**, *87*, 3740.

[33] Garbassi, F., Petrini, G., *J. Catal.* **1984**, *90*, 113.

Chapter 6.
Summary, Conclusion and Future work

6.1 Summary and conclusion

In this thesis, heterogeneous selective oxidation of *n*-butane and propylene has been investigated as the oxidation parts of ATHENA project. Based on the results, the primary conclusions can be drawn as following:

(a) The selective *n*-butane oxidation has been performed over some vanadia-species catalysts in a gas-gas periodic flow reactor. The catalytic effects have been analyzed in both aerobic and anaerobic conditions.

In aerobic condition, phase E has shown enhanced selectivity as the temperature increases in spite of very low conversion and poor yield obtained. On the other hand, VPD can give better yield than phase E in the same condition although the catalytic efficiency need be improved further. Under anaerobic condition, the formation of CO has been greatly enhanced for both phase E and VPD. Particularly for phase E, there is even no selectivity to maleic anhydride observed but carbon monoxide. This implies that a low surface concentration of the selective oxidising species is available on the surface of $VO(H_2PO_4)_2$ material. However, when excess flow air is pressed, this species is diminished in concentration.

For two different loading vanadia catalysts supported on alumina offered from Glasgow University, $1\%V/Al_2O_3$ has shown very poor selectivity and conversion to maleic anhydride while the conversion for $3.5\%V/Al_2O_3$ has been improved a lot. However, the catalytic performance of the latter is still inferior to that of phase E or VPD.

(b) The selective propylene epxodation using only molecular oxygen has been studied over a series of copper-based catalysts supported on zinc oxide and nano-silica, respectively.

A supported effect has been found on catalyst performance for selective propylene epoxidation. Among supported single metal catalysts (Cu, Ag and Au), copper is undoubtedly the best catalyst over not only zinc oxide but also nano-SiO_2. The selectivity to PO for supported copper catalysts is typically higher than 55% at temperature <200°C in spite of only low conversion obtained. In addition, it is interesting that there is completely no selectivity to PO detected for gold as it is supported on nano-SiO_2 but zinc oxide.

Among bimetallic catalysts supported on zinc oxide, Cu-Ag can offer stable performance and high selectivity to PO, *ca.* 81%, at low temperature after reduction pre-treatment, which is much better than supported copper or silver alone. Reduction pre-treatment (5% H_2/Ar) can provide Cu-Ag better catalytic performance distinctly. The XPS analysis suggests that Cu^0 plays an important role in propylene epoxidation in this process although the effect of Cu^{1+} is still unclear. The support of nano-ZnO cannot give Cu-Ag mixed metal better catalytic performance as there is not any difference on surface area between regular zinc oxide and nano counterpart. Supported nickel itself has no activity in propylene epoxidation. Furthermore, the addition of nickel poisons copper-based catalysts based on the results of not only supported Cu-Ni catalyst but also supported Cu-Ag-Ni tri-metallic catalyst. The addition of gold improves the catalytic effect of supported copper catalyst a little but the reaction temperature need be increased greatly.

For the support of nano silica, both Cu-Ni and Cu-Ag can provide stable performances after a variety of pre-treatments (e.g. reduction, oxidation or anaerobic condition). For example, supported Cu-Ni catalyst pre-treated in nitrogen can give high selectivity to PO, *ca.* 78%, at low temperature. In the case of nano silica as the

support, Cu-Ni is even better than Cu-Ag as the addition of nickel helps to stabilize the catalyst, during which the selectivity to PO decreases comparatively slowly as the temperature increases. The XPS spectra for supported Cu-Ag catalyst have also shown that Cu^0 is active for the catalyst pre-treated in reduction condition in propylene epoxidation. Cu^{1+} could be an active and selective component to PO as well since oxidation and anaerobic pre-treatments offer Cu-Ag almost the same catalytic performances. Gold itself has no activity in propylene epoxidation. Moreover, the addition of gold makes supported copper catalyst even worse, which plays the similar role as nickel in the case of zinc oxide support. For Cu-Ag-Ni tri-metallic catalyst, there is not any benefit from silver's addition at low temperature (<200°C) compare with Cu-Ni bimetallic catalyst. However, it seems that silver helps to stabilize Cu-Ni at higher temperature (>220°C), in which high selectivity to PO can be obtained with high conversion. This also implies that silver decreases the speed of deactivation for Cu-Ni and the activity of the catalyst could be remained longer. For supports between ZnO and nano-SiO_2, nano-SiO_2 undoubtedly can offer most of copper-based catalysts better yield to PO. However, as the best catalyst in this work, Cu-Ag catalytic system could not represent above-mentioned support benefit at low conversion except for equivalent selectivity to PO obtained.

According to above-mentioned results, there is a significant scope to design and optimize supported copper-based catalysts with appropriate promoters to obtain highly selective supported copper-based catalysts for selective propylene epoxidation using only molecular oxygen.

6.2 Future work

Although selective oxidation of *n*-butane to maleic anhydride (MA) over vanadium-species catalysts has been studied and applied commercially for many years, some questions remain still unclear as to how catalysts work. As most of commercial

catalysts are made up of different species or mixtures with different morphologies, it is important to study the primary components which could play the key role in selective oxidation to MA. Recently, supported vanadia catalysts have attracted increased attention in the catalysis community since the catalysts of vanadium phosphate were prepared from them. This could help to understand how catalysts work and the nature of vanadium-species catalysts in heterogeneous selective oxidation of *n*-butane.

The work in this thesis has demonstrated that supported copper-based catalysts can be applied as the promising and potential catalysts for selective propylene epoxidation under mild conditions. As silver or even gold has been studied for many years in the field of selective oxidation, copper has been proved more effective and reactive as a novel catalyst for direct epoxidation. Therefore, copper catalysts should certainly be considered as one of feasible options for propylene epoxidation in addition to traditional silver catalysts. The results in this thesis have shown supported copper catalysts or copper-based mixed metals can be very selective for direct heterogeneous epoxidation of propylene to PO using only molecular oxygen. The work has mainly involved in supported bimetallic copper-based catalysts since the catalytic performances of supported mixed metals were obviously better than supported single metals alone. Of course, the pre-treatments and the nature of the supports play some important roles in affecting the catalytic effects of the final catalysts.

Anyway, there are still some great scope and potential for developing and optimizing supported copper-based catalysts. It is worthy of further exploration in improving activity and selectivity of catalysts, optimizing conditions of reaction and pre-treatment. It will help to understand the nature of active sites and supports in catalysts and to look for the optimal combination of mixed metals. Subsequently, some studies of future work are proposed as following:

(a) Investigation of selective oxidation of *n*-butane vanadium-species catalysts with

different supports and promoters. As the catalysts prepared by different methods feature the particular morphology, the study on this aspect will help to find appropriate supports and promoters for designing and optimizing catalysts.

(b) Studies of selective oxidation of iso-butene on supported vanadia catalysts. This will contribute to compare with *n*-butane oxidation as both of them are the C-4 part of ATHENA project.

(c) Further studies on the different preparation methods for supported copper-based catalysts concerned with the selective epoxidation of propylene to PO in order to consider the effect of preparation methods on the catalytic performance of catalysts. In this thesis, the impregnation methods have been primarily applied. Other preparation methods could affect the catalysts activity and selectivity for direct propylene epoxidation using only molecular oxygen as catalysts prepared by different methods feature some specific structure and properties.

(d) Modification of the ratio between copper and the specific metal for bimetallic catalysts, especially in supported Cu-Ag and Cu-Ni catalysts. This aims to find the best ratio of Cu : metal for supported catalysts, which helps to improve activity and selectivity of catalysts for propylene epoxidation. The ratio of Cu : metal should be a significant factor to determine the catalytic effects of supported bimetallic catalysts.

(e) Further investigation of different supports and promoters. This work in the thesis has only involved in two typical supports, zinc oxide and nano-SiO_2. Other supports, such as alumina or its nano-powder and other metal oxides, are worthy of studying. In addition, a variety of promoters (metal chlorides or carbonates *etc.*) can be applied to improve the performances of catalysts. The purpose is to achieve more selective catalysts for selective epoxidation of propylene. Moreover, the investigation will provide to find compatible promoters for designing copper

catalysts which have highly selective activity toward other chemical processes.

(f) The study of the pre-treatment effect on the performance of catalysts for propylene epoxidation. In this work, supported catalysts are usually pre-treated in hydrogen/argon or air or nitrogen at 450°C for 2h. As heat treatment can affect the properties of the final catalysts such as structures, morphologies or even components on the surface, detailed studies are worthy of carrying out to give more stable and durable supported catalysts for propylene epoxidation.

(g) It is necessary to study the optimal reaction conditions for propylene epoxidation. For example, the ratio of gas blending (helium : propylene : oxygen) need be optimized further. Additionally, the reaction profiles with different GHSV should be worthy of studying. These are undoubtedly key factors for the reaction since poor selectivity can be obtained even from an excellent catalyst during inappropriate reaction conditions.

(h) Exploration on the nature of active sites in supported copper-based catalysts for propylene epoxidation. Although copper catalysts have been proved more reactive and selective than traditional catalysts, the detailed mechanism and the nature of the active sites are still unclear. Nowadays, some researchers suggested that metallic Cu could be the active phase, others proposed cationic Cu may play the key role in the reaction.

(i) Characterization of microscopic structure of the best catalysts using TEM and XPS analysis. This could help to understand the geometric and electronic structure on the surface of catalysts. Particularly, the microscopic composition can be obtained by XPS analysis which has been a very useful tool for designing catalysts with high performance and efficiency for propylene epoxidation. The relationship between reactivity and surface structure of catalysts can be found in order to improve the catalytic performances and design novel catalysts for

propylene epoxidation.

(j) Finally, as an important aspect of the future work, which factors result in limiting the selectivity as conversion increases has been attracting great attention in heterogeneous selective catalysis for many years. However, there is only limited progress achieved to date. Usually, competitive reactions such as total oxidation, rearrangement or isomerisation will occur as the conversion increases. Because this is often obtained by increasing temperature. Under higher temperatures, many by-products will come out, which results in lowering selectivity to target products. In order to resolve this issue, the kernel is to find the nature of active sites for both selective oxidation and total oxidation. In addition, another route is to design multi-component catalysts with different dopants which could block non-selective sites and promote the selective oxidation.

Appendix

The time-on-line (TOL) profiles of primary catalysts will be shown in this appendix. The profile of 2%Cu-2%Ag/ZnO has been shown in Chapter 4.

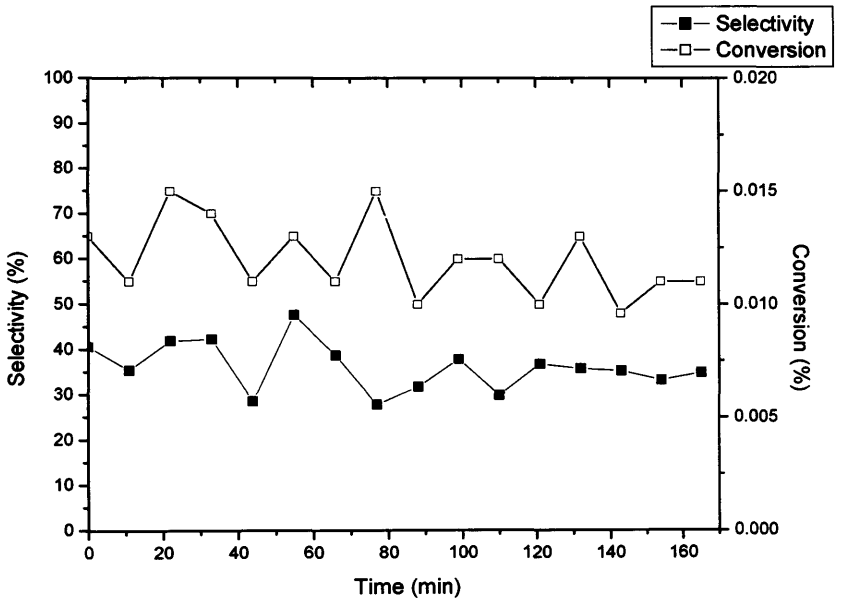

Figure 7.1. The time-on-line profile for 2%Cu-2%Ag/ZnO catalyst pre-treated in Air 450°C for 2h at 230°C.

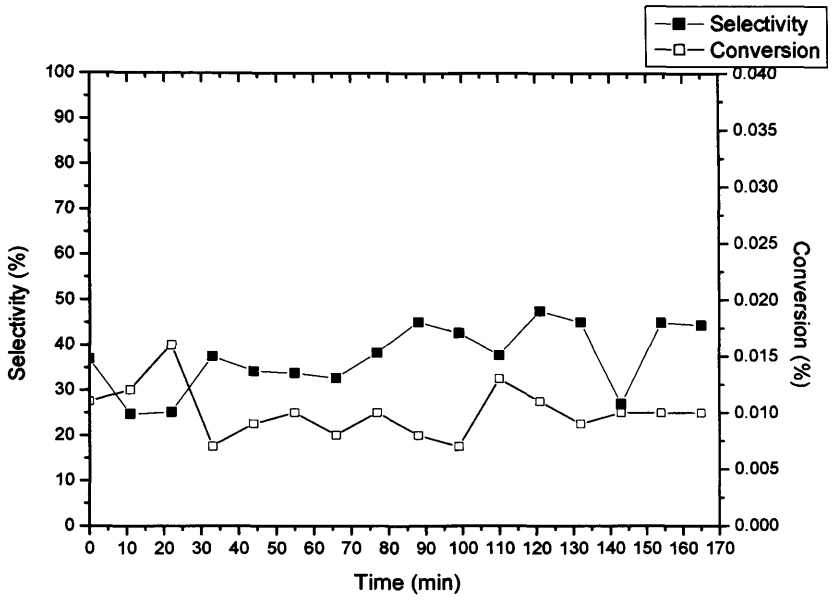

Figure 7.1. The time-on-line profile for 2%Cu-2%Ag/ZnO catalyst pre-treated in N_2 450°C for 2h at 230°C.

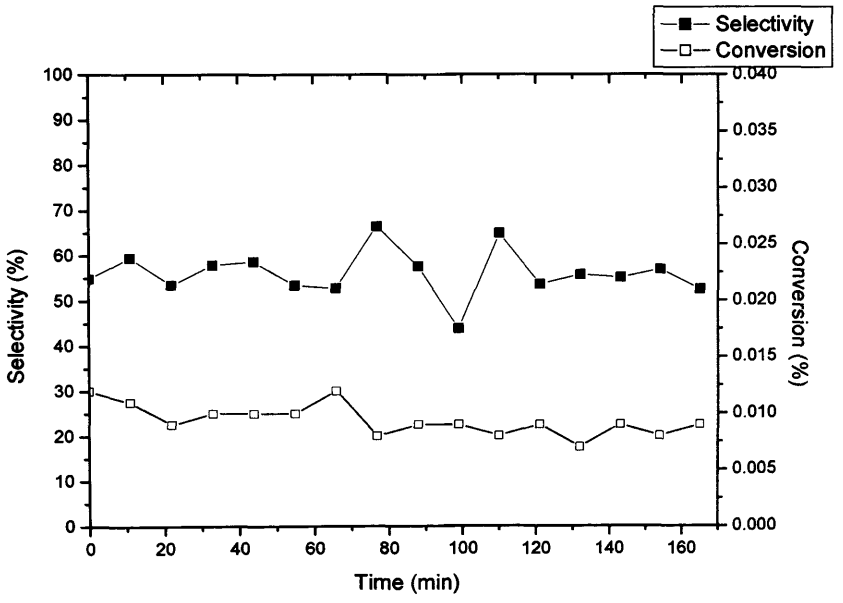

Figure 7.1. The time-on-line profile for 2%Cu-2%Au/ZnO catalyst pre-treated in 5% H_2/Ar 450°C for 2h at 230°C.

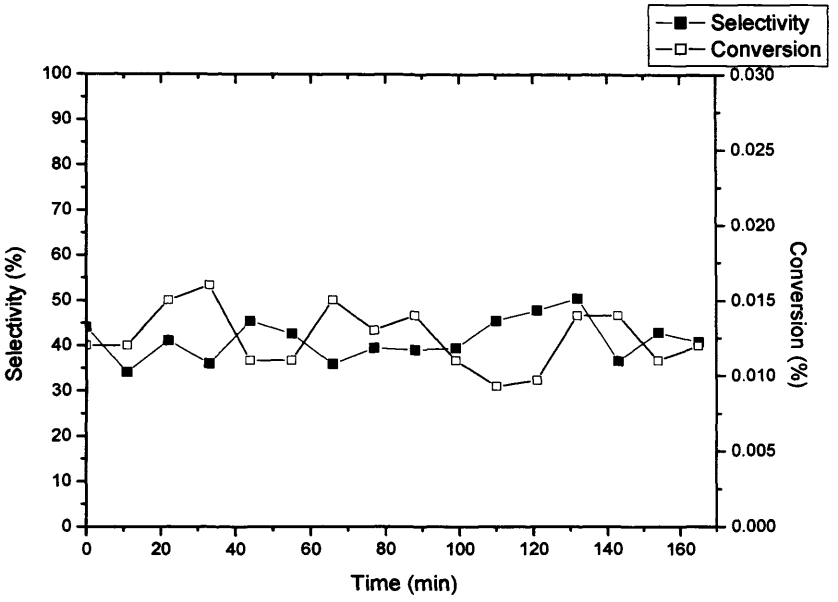

Figure 7.1. The time-on-line profile for 2%Cu-2%Ag-2%Ni/ZnO catalyst pre-treated in 5% H_2/Ar 450°C for 2h at 230°C.

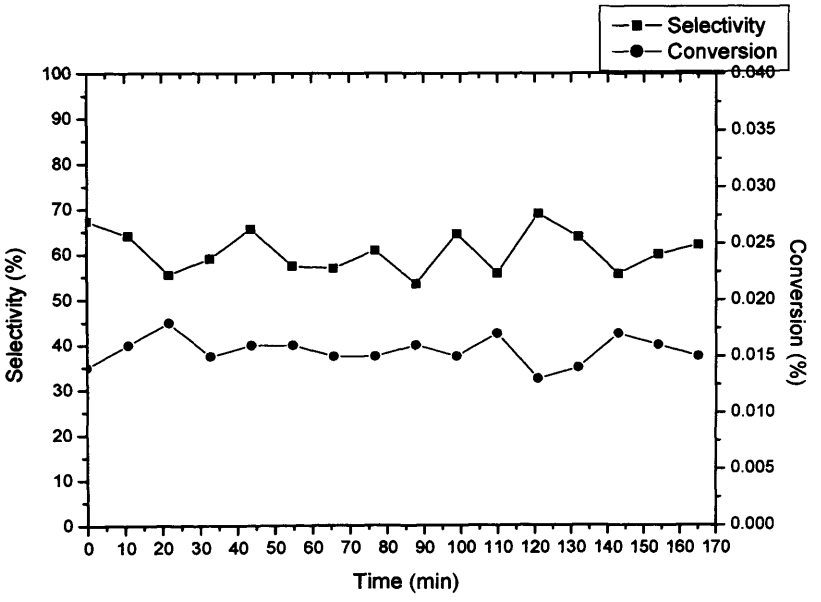

Figure 7.1. The time-on-line profile for 2%Cu/nano-SiO_2 catalyst pre-treated in 5% H_2/Ar 450°C for 2h at 210°C.

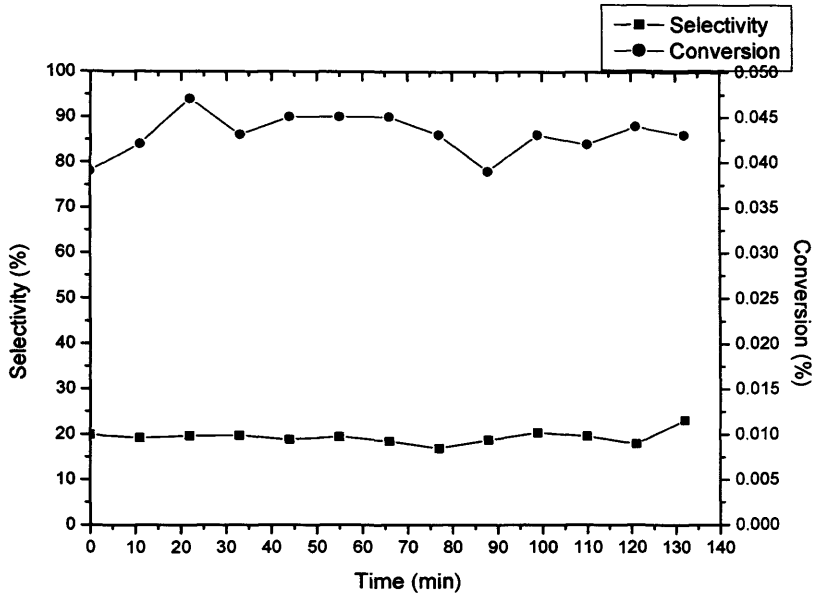

Figure 7.2. The time-on-line profile for 2%Ag/nano-SiO_2 catalyst pre-treated in 5% H_2/Ar 450°C for 2h at 290°C.

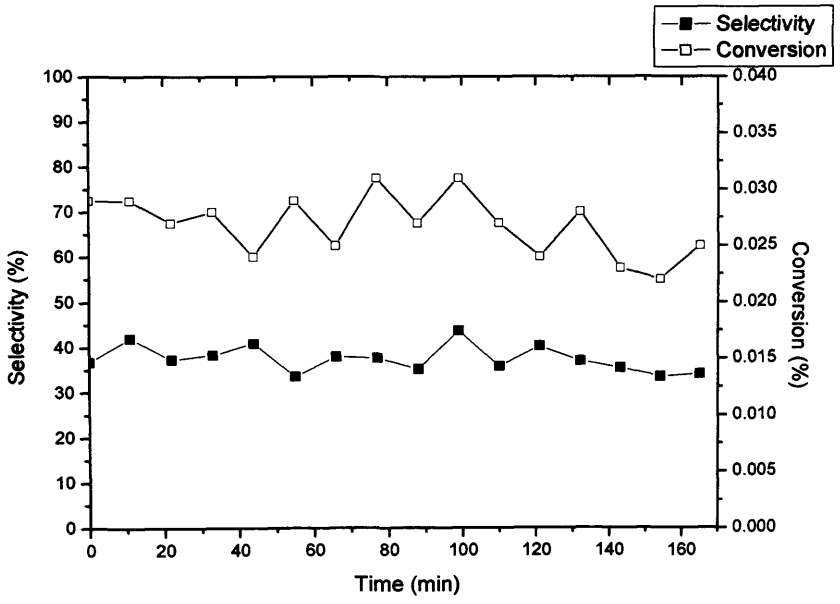

Figure 7.2. The time-on-line profile for 2%Cu-2%Ni/nano-SiO_2 catalyst pre-treated in 5% H_2/Ar 450°C for 2h at 230°C.

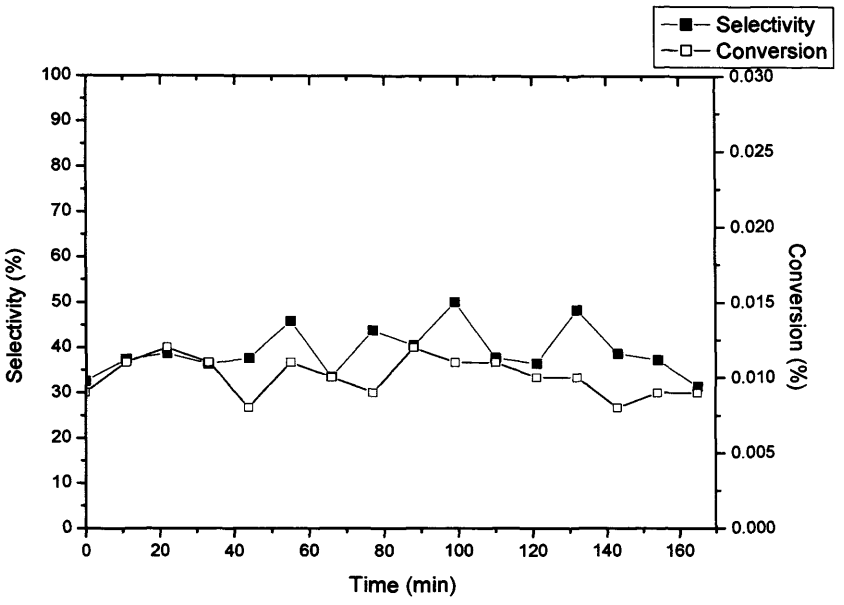

Figure 7.2. The time-on-line profile for 2%Cu-2%Ni/nano-SiO_2 catalyst pre-treated in N_2 450°C for 2h at 230°C.

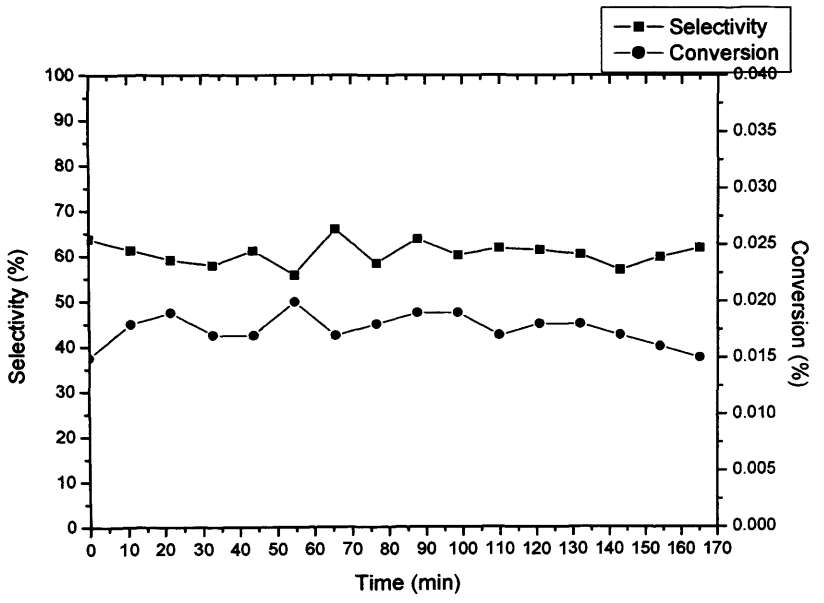

Figure 7.2. The time-on-line profile for 2%Cu-2%Ag/nano-SiO_2 catalyst pre-treated in 5% H_2/Ar 450°C for 2h at 200°C.

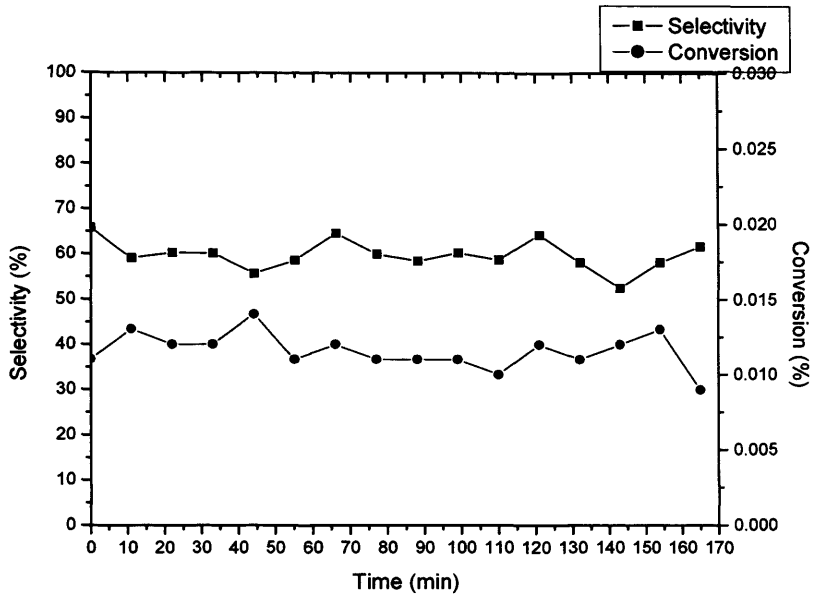

Figure 7.2. The time-on-line profile for 2%Cu-2%Ag/nano-SiO_2 catalyst pre-treated in Air 450°C for 2h at 200°C.

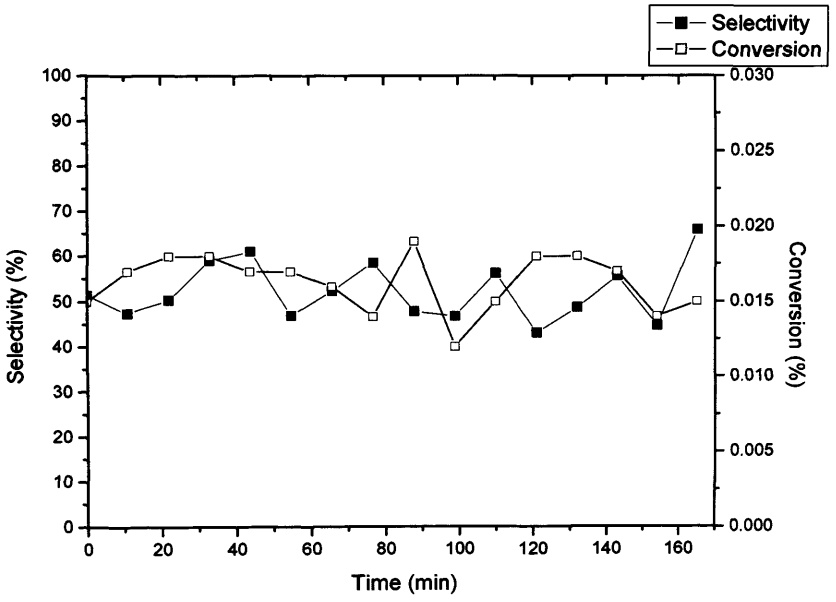

Figure 7.2. The time-on-line profile for 2%Cu-2%Au/nano-SiO_2 catalyst pre-treated in 5% H_2/Ar 450°C for 2h at 240°C.

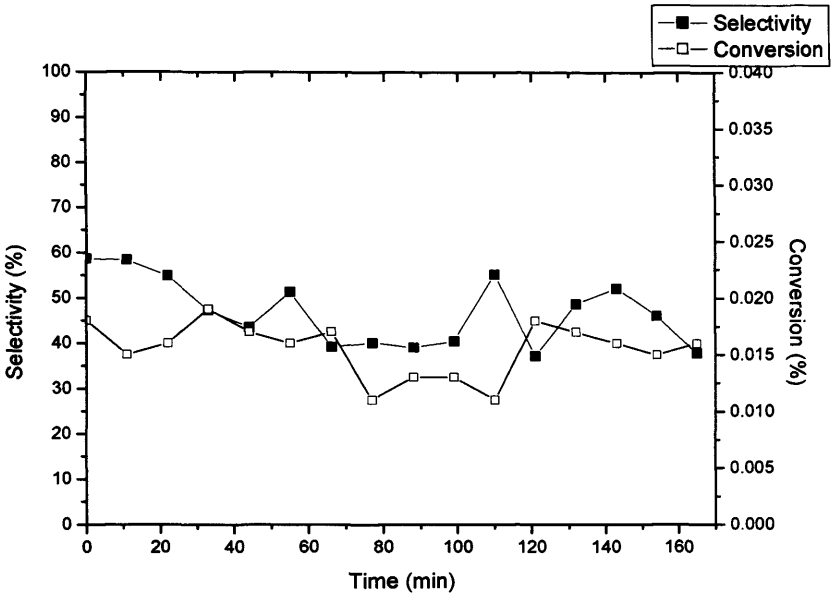

Figure 7.2. The time-on-line profile for 2%Cu-2%Au/nano-SiO_2 catalyst pre-treated in air 450°C for 2h at 230°C.

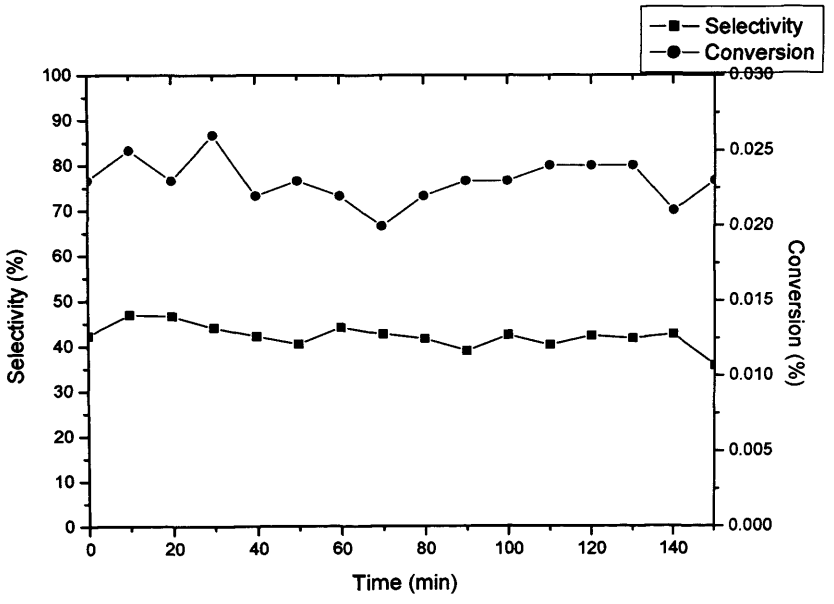

Figure 7.2. The time-on-line profile for 2%Cu-2%Au/nano-SiO_2 catalyst pre-treated in N_2 450°C for 2h at 230°C.